2009

SYNTHESIS AND EVALUATION OF PROUTEOLYSIS TAURGETING CHIMERAS (PROTACs): A POTENTIAL CHEMICAL GENETIC APPROACH TO BREAST CANCER THERAPY

Kedra C. Cyrus
University of Kentucky, kccyru2@uky.edu

ABSTRACT OF DISSERTATION

Kedra C. Cyrus

The Graduate School

University of Kentucky

2009

SYNTHESIS AND EVALUATION OF PROTEOLYSIS TARGETING CHIMERAS (PROTACs): A POTENTIAL CHEMICAL GENETIC APPROACH TO BREAST CANCER THERAPY

ABSTRACT OF DISSERTATION

A dissertation submitted in partial fulfillment of
the requirements for the degree of Doctor of Philosophy in the
College of Pharmacy at the University of Kentucky

By

Kedra C. Cyrus

Lexington, Kentucky

Director: Dr. Kyung Bo Kim, Associate Professor of Pharmaceutical Sciences

Lexington, Kentucky

2009

ABSTRACT OF DISSERTATION

SYNTHESIS AND EVALUATION OF PROTEOLYSIS TARGETING CHIMERAS (PROTACs): A POTENTIAL CHEMICAL GENETIC APPROACH TO BREAST CANCER THERAPY

The use of small molecules to probe the function of proteins is referred to as chemical genetics. The Proteolysis Targeting Chimera (PROTAC) is a chemical genetic tool that contains the ligand for a target protein of interest and the recognition motif for an E3 ubiquitin ligase attached by a linker. The PROTAC is capable of binding to and recruiting specific target proteins to the intracellular degradation system, the ubiquitin proteasome system (UPS). While the approach has had success it has not been optimized to be used on a broader scale.

Optimization efforts focused on elucidating the ideal linker length between the ligand and the E3-ligase recognition motif, the preferred location for attachment of the linker to the two moieties, and the possibility for a dimeric PROTAC comprised of two ligands. An estrogen receptor (ER)-targeting PROTAC was chosen as a model for optimization attempts as the ER is known to have pathological significance in breast cancer. Optimization of the PROTAC technology will not only provide a novel tool to probe ER biology, but may also offer a novel approach to breast cancer therapies. The ER targeting PROTAC constitute the 17β-estradiol (E2), as the ligand for ER and a pentapeptide derived from HIF-1α as the E3-ligase recognition motif, joined by a linker.

Following the successful synthesis and evaluation of a number of PROTACs, it was revealed that an optimum ER-targeting monomeric PROTAC (KC-3) has a spacer of 16 atoms between the E2 and HIF-1α pentapeptide. The spacer is attached at the C-7α position on E2 and at the N-terminus of the HIF-1α pentapeptide. It was also established that the PROTAC is capable of targeting the ER for degradation in a proteasome and E3-ligase dependent manner, which translated to a decrease in the proliferation of MCF-7 cells with an IC_{50} similar to that of tamoxifen. KC-3, in comparison with E2, displayed lower agonistic activity on an ER-regulated downstream target, the progesterone receptor (PR). A dimeric PROTAC more effectively binds and degrades the ER in a proteasome dependent manner, suggesting that the dimeric ligand approach may be applied to the design of other PROTACs.

KEYWORDS: PROTAC, Chemical-genetics, Estrogen-receptor, breast-cancer, ubiquitin proteasome system.

Kedra Cyrus

October 19, 2009

SYNTHESIS AND EVALUATION OF PROTEOLYSIS TARGETING CHIMERAS (PROTACs): A POTENTIAL CHEMICAL GENETIC APPROACH TO BREAST CANCER THERAPY

By

Kedra C. Cyrus

Dr. Kyung Bo Kim

Director of Dissertation

Dr. Robert Yokel

Director of Graduate Studies

October 19, 2009

RULES FOR THE USE OF DISSERTATION

Unpublished dissertations submitted for the Doctor's degree and deposited in the University of Kentucky Library are as a rule open for inspection, but are to be used only with due regard to the rights of the authors. Bibliographical references may be noted, but quotations or summaries of the parts may be published only with the permission of the author, and with the usual scholarly acknowledgments.

Extensive copying or publication of the dissertation in whole or in part also requires the consent of the Dean of the Graduate School of the University of Kentucky.

A library that borrows this dissertation for use by its patrons is expected to secure the signature of each user.

Name Date

DISSERTATION

Kedra C. Cyrus

The Graduate School

University of Kentucky

2009

SYNTHESIS AND EVALUATION OF PROTEOLYSIS TARGETING CHIMERAS (PROTACs): A POTENTIAL CHEMICAL GENETIC APPROACH TO BREAST CANCER THERAPY

DISSERTATION

A dissertation submitted in partial fulfillment of
the requirements for the degree of Doctor of Philosophy in the
College of Pharmacy at the University of Kentucky

By

Kedra C. Cyrus

Lexington, Kentucky

Director: Dr. Kyung Bo Kim, Associate Professor of Pharmaceutical Sciences

Lexington, Kentucky

2009

ACKNOWLEDGEMENTS

This dissertation would not have been possible without the support and encouragement from a number of people. To my advisor Dr. Kyung Bo Kim I express my sincere gratitude for your guidance and especially your patience throughout my graduate studies. I appreciate your sound advice over the years. To my committee members Dr. Rolf Craven, Dr. Todd Porter, Dr. Jurgen Rohr and Dr. Dan Tai, thank you for your feedback on my project throughout the years. Special thanks to Dr. Spielmann for agreeing to serve as my outside examiner for my defense.

I would like to thank the many laboratories who collaborated on this project: Dr. Kathy Sakamoto, UCLA and Dr. Ray Deshaies, Caltech, Dr. Carrie Klinge - UofL, Dr. Wooin Lee - UK, Dr. Eun-Young Choi and Dr. Hollie Sawanson - UK.

Special thanks to all my colleagues, former and current: Marie Wehenkel, words cannot express my gratitude to you for your friendship and your time and effort spent in assisting me with the biological data; I am forever in your debt. Hyosung Lee, your friendship and assistance throughout the years have been invaluable; Dr. Abby Ho, your friendship and support have been tremendous; Sung Hee Park, my Korean sister, thanks for your friendship and support; Samantha Mangold, my 'little sister', thanks for your support; Hyeong Jun Han, Jung Ok Ban, Yang Eon Kim, thanks for your assistance. Good friends I've met on this journey, Leah Allen, Miranda Beam and Yolanda Williams, thanks for your encouragement.

Finally to my family and friends, I could not have made it without your support; my grandmother Cecilia and aunt Roslyn, your prayers lifted me up during difficult times. My mom Claudia, Brother Mark, Charlette, Mandy, Jules, Anne, Shelton, Alice, Tona and Lanker thanks for believing in and encouraging me every step of the way. To my family and friends in Grenada, thanks for your support. Thanks to my nieces and nephews, you are my biggest inspiration.

TABLE OF CONTENTS

LIST OF TABLES

LIST OF FIGURES

LIST OF SCHEMES

CHAPTER 1: OVERVIEW

Traditionally, the roles of proteins in cells have been elucidated using classical genetic approaches; while this system has provided powerful tools for investigating protein functions, there are several limitations to the classical method (reviewed in chapter 2). Thus, a complimentary strategy termed "chemical genetics" has been developed, which may shed light in areas where "classical genetics" has constraints. Chemical genetics employs small molecules to interrogate the roles of proteins. The use of small molecules confers high spatial and temporal control that is difficult to obtain by classical genetic approaches. A major advantage of chemical genetic tools over classical genetic methods is that chemical genetic tools can be directly translated into new therapeutic agents. Thus, a number of approaches have been developed to identify small molecules that modulate specific protein functions.

Recently, a novel small molecule approach termed Proteolysis Targeting Chimeras (PROTACs) has been developed by exploiting an intracellular protein degradation system, the ubiquitin-proteasome system (UPS). Since the pioneering work by the Crews and Deshaies laboratories [1], the PROTAC technology has been developed for a number of target proteins [2, 3, 4, 5, 6, 7, 8, 9], but it has not yet been optimized as a tool to be used on a broad scale. This dissertation details an attempt to elucidate an effective PROTAC design strategy. The knowledge gained from this research will provide a blueprint for the future development of PROTACs targeting a variety of proteins and offer some insights into the potential of PROTACs as therapeutic agents. The PROTAC is comprised of a ligand specific for a target protein of interest linked to an E3 ligase recognition motif (Figure 1.1). Once bound to the target protein the E3 recognition motif is identified and the target protein is ubiquinated and ultimately degraded by the UPS. The work set forth in this dissertation utilizes the PROTAC approach to develop a unique molecular probe of ER biology and to potentially develop novel therapeutic agents for treatment of breast cancer.

A large subset of breast cancers over- expresses the estrogen receptor (ER) and is classified as ER-positive. Due to the high levels of ER in this class of breast cancer, therapies (antiestrogens, aromatase inhibitors) aimed at blocking the interaction of ER with its natural ligand, 17β-estradiol (E2), have frequently been employed [10, 11].

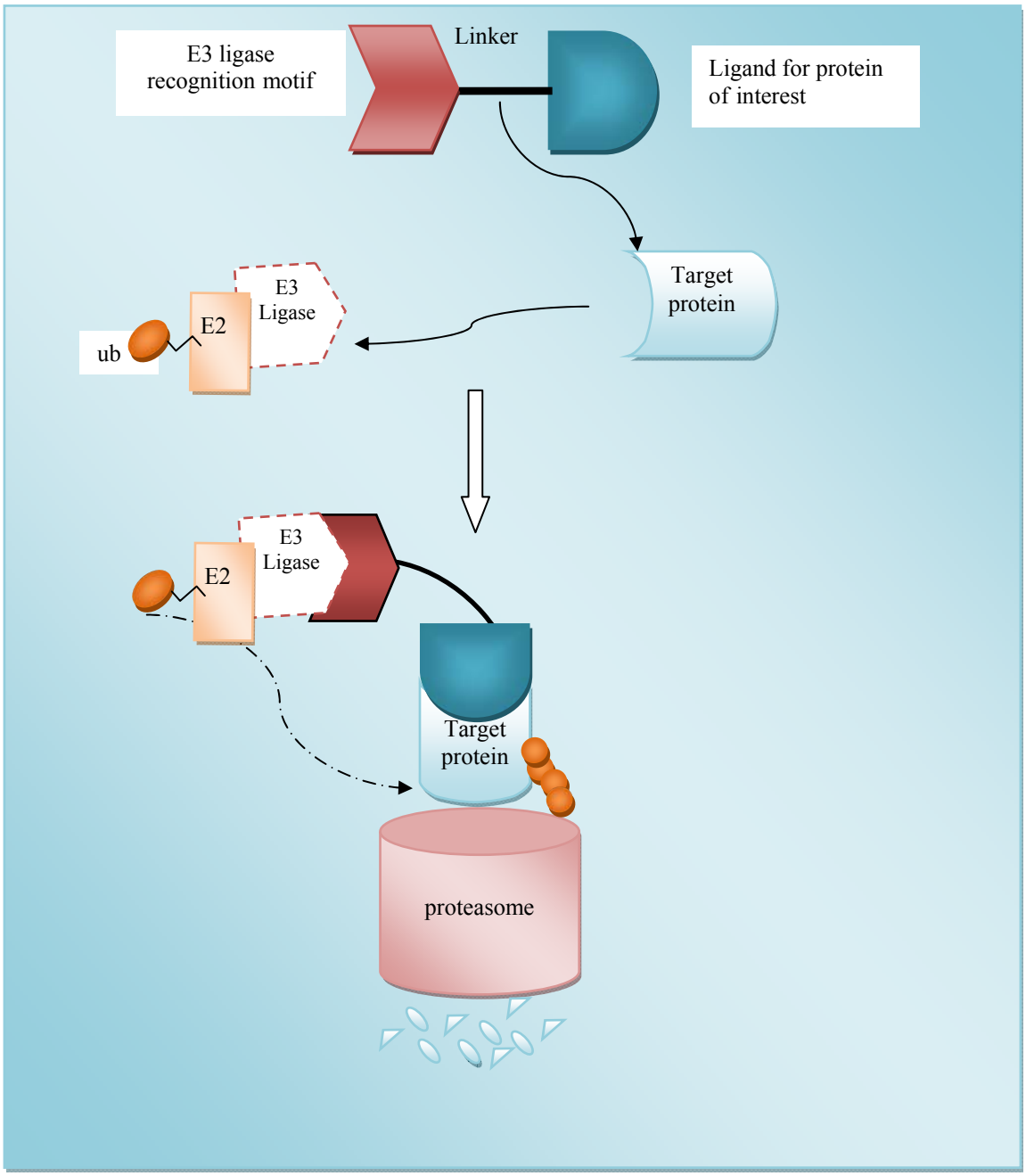

Figure 1.1 The PROTAC

Prolonged antiestrogen treatment however, results in the development of resistance to these therapies [12]. One principal concern related to resistance is the fact that most tumors maintain expression of functional ERs. However, these ERs are often aberrantly regulated; for example, unusual phosphorylation, which causes antagonists to act as

agonists [12, 13, 14]. Thus, mere perturbation of ER's interaction with its ligand is not sufficient, and a strategy that selectively knocks-out the ER will be useful for the treatment of breast cancer. As such, development of an effective ER-PROTAC may provide a novel breast cancer treatment strategy.

Goal:

The goal of this project is to develop an effective PROTAC design strategy as well as efficient ER-degrading PROTACs.

Specific aims:

Specific aim 1: Synthesis of PROTACs that target the ER

The first aim of this study is the synthesis of a number of PROTACs. In earlier designs of an ER-PROTAC the attachment of the linker was via an ester linkage. Initial (unpublished) data indicated that the linkage was susceptible, *in vivo,* to esterase activity. Therefore, the first attempt at optimization is to replace the ester linkage with a stable linkage, such as a C-C linkage, by changing the location of the attachment of the linker on 17β-estradiol. The bulk of the optimization work will be focused on the length of the linker between the two moieties of the PROTAC to provide an adequate distance between the E3 ligase and target protein for optimum ubiquitination. To increase the binding opportunity with the target protein, a dimeric ligand PROTAC having two estradiols will also be introduced.

Specific aim 2: Determine optimal PROTACs based on their ability to degrade ER in a proteasome-dependent manner

Following the successful synthesis of PROTACs, their ability to specifically target the ER for degradation will be evaluated in MCF-7 ER-positive cells. Western blotting techniques as well as immunofluorescence will be employed to look at the ER status after treatment with PROTACs. The IC_{50} for each compound will also be determined.

Specific aim 3: Evaluate optimal PROTACs effect on ER regulated genes

Based on the information gathered from the initial ER screening the optimal PROTACs will be tested for the ability to affect downstream targets of ER.

CHAPTER 2: BACKGROUND

2.1 Chemical genetic approach

2.1.1 Introduction

Perturbation of protein function is essential in understanding the role of a particular protein in the etiology of a specific disease. Presently, two different approaches can be applied to study the function of a protein of interest. One method, termed "classical genetics" involves the genetic manipulation of the target protein's genes with subsequent observation of phenotypic changes. The other approach involves the use of small molecules to achieve essentially the same result and is termed "chemical genetics." In essence, regulation of protein can occur at three different points; at the genetic stage, post-transcriptional stage and at the post-translational stage [15].

2.2 Classical Genetics

Modifications involving the removal or activation of genes for a protein of interest are referred to as the "genetic" or "classical genetic" approach [16]. Such manipulations allow for the observation of phenotypic differences between wild-type and altered proteins and ultimately identification of a functional role of the protein in the diseased state. Classical genetics can be divided into two approaches, forward and reverse.

Forward genetics starts with the random mutation (chemical or radiation) of the DNA of a wild-type cell/organism, and following mutation the phenotypes of the mutants and wild-types are compared. Once a phenotype (growth, behavior or morphological change) is chosen, gene mapping is performed to identify the gene responsible [17, 18, 19, 20]. Basically, forward genetics function on an "effect to cause" basis [18, 21, 22]. On the other hand, reverse genetics deals with the targeted deletion of a particular gene, observing phenotypic differences when compared to wild-type and eventually delineating the role of that specific gene [23]. Reverse genetics owes its evolution to the many progresses in molecular biology techniques [17, 23]. However, one of the major limitations encountered

in applying the classical genetic strategy is that of lethality. Deletion of certain genes can be fatal to the organism under investigation due to the fact that a particular gene may be required for developmental purposes [24]. To overcome these problems new strategies were implemented such as conditional knock-out/knock-in and siRNA strategies.

The use of conditional alleles has provided a level of temporal control within the field of classical genetics. The gene of interest can be turned on or off at a particular time based on certain conditions. Initial attempts to achieve temporal control made use of single transgenes that were stimulated by heavy metals, temperature, interferon and steroids [24]. However, these methods proved unreliable as there were unrelated effects related to the induction or low basal activity in the absence of induction [24, 25].

Eventually a dual transgenic system was adopted that relies on the association of two different transgenes, an "effector" and a "target". The dual transgenic system is classified based on the activity of the "effector". In one case the effector is responsible for transcriptional transactivation of the "target" transgene while in the other case, the effector is DNA recombinase. DNA recombinase is site specific, and its action results in rearrangement of the target gene resulting in the subsequent activation or deactivation of the gene. Among the two most commonly used and established dual systems are the Tetracycline regulated (*TetR*) and *Cre/loxp* systems representing the transactivation and the site specific DNA recombinase systems, respectively [25].

As with conditional knock-out, small interfering RNA (siRNA) technology has had a great impact on studies of protein function. Protein silencing by siRNA involves double-stranded siRNA having average sizes of around 22 nucleotides [26]. There is two-nucleotide overhang at the 3'-end, that is specifically recognized by the RNA-induced silencing complex (RISC) and a 5'-end that is phorsphorylated [27, 28]. Following 5'-end phosphorylation, the siRNA forms a complex with RISC that ultimately leads to the release of one strand (passenger strand). The resulting complex consists of the other strand (guide strand) and RISC. This complex is capable of binding and cleaving complimentary mRNA and silencing its expression [26].

Despite the obvious advantages of the siRNA strategy there are a few limitations. Among these is the lack of complete knock-down of the protein of interest as compared to a genetic knockout; additionally, this method only blocks new protein synthesis and

thus, has no effect on the current protein pool [15]. Added to the above limitations are the lack of temporal control, some reported off-target effects as well as limited in vivo uses of siRNA [15, 17].

2.3 Chemical Genetics

The constraints of classical genetic approaches pointed to a need for alternative methods that can control protein function in areas where traditional methods may not be viable. Chemical genetics is a complimentary tool to classical genetics and affords control of protein function at the post-translational level. Chemical genetics is defined as the use of small molecules to disturb the function of protein with high temporal and quantitative control [16, 29]. Like classical genetics, chemical genetics approaches can be classified as forward and reverse.

Forward chemical genetics employs small molecules to look for phenotypic changes in the biological system under examination, and ultimately leads to the revelation of the protein that is being affected by the small molecule [29]. In the same way classical genetics uses random mutagenesis in its forward approach, chemical genetics uses small molecule libraries and screens for certain phenotypic changes [18]. Conversely, reverse chemical genetics targets small molecules towards a protein of interest and once the interaction is confirmed, the effect of the small molecule against the target is deduced [18, 29, 30].

2.3.1 Advantages of chemical genetics

Chemical genetics has a number of advantages compared to classical genetics. Among the many advantages, it is most important to note the high spatial and temporal control provided by this strategy [29, 31]. Removal or addition of the small molecule can be time controlled even in situations where a process is occurring on a short time scale [32]. This conditional control is only rarely available in classical genetics and when employed often has off-target effects [23]. Moreover, chemical genetics allows for the possibility of a "multi-knockout" scenario by merely adding small molecules specific for different

targets of interest, a scenario that is not readily accomplished using classical genetic methods [33, 34].

Classical genetic approaches, in essence, remove the entire protein product resulting in total loss of function or, in the case of a critical gene deletion, no possible characterization of the gene due to lethality [32]. This total loss of protein by the classical genetic method makes it difficult to decipher effects that are due to the deletion or effects that occur due to a precise function of the protein [20, 35]. Lethality can be avoided using the chemical genetic approach by adjusting the dose to sublethal levels, ensuring a partial knock-out phenotype [36].

With chemical genetics, since the small molecule directly affects the protein under study, it can be applied to probe one function of a multifunctional protein [37]. This selectivity of function has proven significant in the cases of kinases. Kinases have been shown to have different roles owing to their enzymatic and protein scaffold activities. The use of small molecule kinase inhibitor allows for blockage of the phospho-transfer activity and leaves the protein scaffold activity untouched allowing for the categorization of distinct activities which would be lost in the case of gene deletion [38]. Tubacin provides another example of selectivity of function by a small molecule approach. This small molecule selectivity inhibits the tubulin deacetylase activity of histone deactylase 6 while sparing the histone deacetylase activity [39, 40].

Knight et al, [41] showed an additional advantage of a small molecule approach: looking at the specificity of small molecules for certain isoforms of the phosphoinositide 3-kinases (PI3K) and then deciphering the roles of the isoforms in insulin signaling. A small molecule approach may also be effective in studying protein-protein interaction. Recently, an inhibitor that binds tumor necrosis factor (TNF-α) and causes dissociation of one of the members of the trimer was shown to cause inactivation of TNF-α signaling [42].

Perhaps one of the most attractive aspects of chemical genetics is its ability to simultaneously identify proteins that are “druggable” and develop small molecules that target the protein as drug candidates [32]. As it relates to drug development, within the field of chemical genetics there are two major requirements. First, the target has to play a

decisive role in the progression of the disease. Second, the target protein's role has to be amendable to modulation by a small molecule [43].

2.3.2 Chemical genetic libraries

In order to conduct chemical genetic studies the first criteria is the formation of a small molecule chemical library. A chemical genetic library may take on a number of different forms ranging from natural product, natural product-like, tagged libraries, to annotated chemical libraries [18]. Following is a brief summary of some of the library types employed in chemical genetic studies:

Natural product libraries - as the name implies these libraries are constructed from natural sources like plants, sponges and soil [20]. The limitation of a natural product library is that isolation and purification of active compounds is laborious and time-consuming; even after successful isolation there is the added difficulty of structure determination [44, 45, 46, 47]. Despite these limitations, natural products have lent a great deal to chemical genetics efforts. Some of the better known natural products used in chemical genetics and their targets are rapamycin, which is an immunosuppressant, trichostatin an HDAC inhibitor and FK506 which binds FKBP12.

Natural product-like libraries – these libraries comprise small molecules whose structure significantly resembles their natural product counterparts [48]. Because natural products are considered "privileged" structures, meaning they contain structural motifs that can interface with unrelated targets. Natural products are also considered "biologically validated" and as such offer a great starting point for the creation of libraries that should have biological activity [49, 50, 51]. These libraries can be constructed in order to generate derivatives of the natural product [46, 52, 53, 54, 55] or to expand the utility of a molecule to seek out unknown properties [56].

Tagged libraries – compounds in these libraries must incorporate a tag in the molecule and these tags should confer some function to the molecule. Some of the functions rendered by tags are: fluorescence, purification, identification, cell-permeability and immobilization [57]. Among the better-known tags being utilized in chemical genetics is the green fluorescence protein (GFP). Another tag that is in use is polyamide nucleic acid (PNA) tags, which specifically bind to certain sequences on DNA. The first

successful use of PNA-tag small molecules was used in the exploration for inhibitors of cathepsin L [58].

Diversity oriented synthesis (DOS) – The goal of such a library is to synthetically mimic the diversity observed among natural products. In this sense, a library is complied of many different types of structures without regard to any particular biological target [59]. Among the common methods applied in constructing such a library is the "split-pool/one-bead-one compound" method [45]. The split-pool method involves the linking of substrates having a desired core structure to beads which are then split into different reaction vessels and other reactants are added. Once mixed, the beads are pooled and split again repeating the procedure until all desired components are added [45, 59, 60, 61].

Focused library – In contrast to a DOS library, a focused library builds compounds intended to bind to a particular target [44]. A "rational" design is favorable when there is a known ligand for a particular protein of interest, as in the case of receptors and enzymes [29].

2.3.3 Screening

Regardless of the type of library constructed, the next step in any chemical genetic study is screening; as mentioned previously, screening can be under the banner of forward or reverse chemical genetic approaches. When dealing with large compound libraries high-throughput screening (HTS) is the standard procedure as it has the ability to investigate large numbers of compounds in a short time frame. Single cell systems like yeast/bacterial, human and mouse cells [62].

2.3.4 *Forward genetic screening/ phenotype-based screening*

Akin to the forward classical genetic methods, this methodology aims to find targets that are affected when a collection of small molecules are applied to a test system. The effects of the small molecule on a target can be ascertained by looking at phenotypic read-outs. Read-outs may include "markers", which measure the abundance of specific proteins as a readout of a global cellular phenotypic effects; functional assays, which measures cellular activities including those associated with cell division, metabolism and

apoptosis; or microscopic analysis, which looks at the physical nature of the cell or any localization events of a particular marker" [19, 62]. Perhaps one of the best-known compounds to be identified in a phenotype-based screen is FK506, an immunosuppressant, identified by researchers in Japan in a screen of natural products active against interleukin 2 (IL-2) [63, 64]. Later the targets of FK506 were shown to be FKBP12 and calcenurin [65, 66].

One common method employed in phenotypic screening is the cytoblot. Cytoblot assay is a high throughput assay that is capable of measuring DNA synthesis and posttranslational activities such as phosphorylation. This assay was pioneered in the Schreiber laboratory [67]. The assay includes the techniques of western blot and the enzyme linked immunosorbent assay (ELISA). In short, whole cells are fixed and detected with a specific primary antibody, followed by exposure to horseradish peroxidase (HRP)-linked secondary antibody, quantity of product present is detected via chemiluminescence [67]. One of the first compound-target interactions to be elucidated via cytoblot was the monostrol-motor protein interaction. It was shown that monostrol affected a motor protein necessary for spindle bipolarity, but had no effect on tublin [68].

Other common techniques employed in forward genetic screens involve the use of reporter gene assays such as luciferase and automated microscopy [18, 19].

2.3.5 Reverse genetic screening

This type of screening looks at the effects of small molecules on the identified target of interest. The limitation of the reverse genetic screen is that only a few protein targets have known small molecule partners [67]. Nonetheless, in the few cases where a reverse genetic approach is feasible it offers tremendous insights into the functions of proteins. According to Thorpe, this is the method widely used in pharmaceutical companies, where small molecule effectors for proteins of interest are selectively sought [69]. There are several techniques employed in reverse genetic screening; however, for the purpose of this dissertation only the Proteolysis Targeting Chimeric (PROTAC) approach will be discussed in detail.

2.3.6 Proteolysis Targeting Chimeras (PROTACs)

The PROTAC approach is a reverse chemical genetic approach pioneered by the Crews and Deshaies laboratories [1]. While most reverse chemical genetic methods perturb protein function simply by binding the target, the PROTAC approach induces a chemical knock-out of the target protein. The PROTAC is a chimera having a small molecule ligand of a target protein at one end and an E3 ligase recognition motif at the other end. Thus, the PROTAC is designed to recruit target protein to E3 ubiquitin ligase for polyubiquitination and subsequent degradation by the 26S proteasome (Figure 1.1).

The first PROTAC developed by Sakamoto et al. provided proof of concept for the utility of the technology. Specifically, they developed a PROTAC composed of the ligand ovalicin, an angiogenesis inhibitor that binds covalently to methionine aminopeptidase-2 (MetAP-2), at one end and the IκBα-derived E3 recognition motif at the other end. The IκBα derived peptide ligand is specifically recognized by a Skp1-Cullin-F box (SCF) E3 ligase, $SCF^{\beta\text{-}TRCP}$ [1]. This study showed that the PROTAC can recruit otherwise non-proteasome related, MetAP-2, to the E3 ligase where it is ubiquitinated and ultimately degraded by the ubiquitin proteasome pathway [1].

Parallel to the success of PROTACs *in vitro*, many practical issues were raised regarding the general utility of the approach. They included concerns as to whether PROTAC would work in cells, be able to target other proteins especially those related to disease progression, and target proteins without requiring covalent attachment [70]. To address such questions, PROTACs targeting the estrogen and androgen receptor, (ER) and (AR) respectively, were developed [70]. These PROTACs contained the same phosphopeptide derived from IκBα that is specifically recognized by $SCF^{\beta\text{-}TRCP}$ [70]. The study proved that the PROTACs were capable of targeting therapeutically relevant proteins, in cells without requiring a covalent attachment to the target. However, the use of the phosphopeptide renders the PROTACs impermeable to cells and therefore microinjection had to be performed in order to deliver the PROTACs to cells [70].

The cell permeability issues that arose from the use of the phosphopeptide were overcome by the development of PROTACs that contain a recognition motif derived from HIF-1α. The HIF-1α is specifically recognized by the von Hippel Lindau (pVHL) E3 ligase complex [6, 7, 8]. Zhang et al. first employed the HIF-1α : pVHL specific

interaction to target both ER and MetAP-2 (in this study the term small molecule proteolysis inducer [SMPI] was used instead of PROTAC) [8]. Furthermore, they showed that a pentapeptide derived from HIF-1α is sufficient for recognition by pVHL [2, 7]. Similarly, Schneekloth et al. designed PROTACs having the HIF1-α derived hepta or octapeptides that target FKBP12 and AR. In this study, they added a polyarginine tail to further enhance cell permeability [6]. Using the HIF-1α: pVHL system, additional PROTACs that target the arylhydrocarbon receptor (AHR) [3, 9], the ER and AR [4] have been developed.

2.4 The Ubiquitin-Proteasome System (UPS)

The PROTAC approach exploits an intracellular protein degradation system, the ubiquitin-proteasome system (UPS). The UPS is responsible for the selective and specific degradation of most proteins in eukaryotic cells, including the degradation of misfolded and many signaling proteins. Destruction of proteins via the UPS is a highly selective process and involves two distinct and consecutive steps. The first step is the covalent attachment of multi-ubiquitin to a target protein. The second step is the degradation of the ubiquitin tagged protein by the 26S proteasome.

2.4.1 *Ubiquitination process*

Ubiquitin (Ub) is a highly conserved 76-amino acid polypeptide present in all eukaryotic cells which is used to tag proteins for destruction by the UPS. The process of protein ubiquitination involves the actions of three different enzymes referred to as E1 (activating enzyme), E2 (conjugating enzyme) and E3 (ligase) (Figure 2.2). It is interesting to note that ubiquitinated proteins are not always targeted for degradation by the proteasome. For example, certain proteins are tagged with one or a few ubiquitins and then undergo endocytosis via the lysosomal pathway. Lysine 29 (K29) is believed to be responsible for the lysosomal degradation [71, 72]. Chain formation on lysine 63 (K63) does not appear to be proteolytic and may be associated with DNA repair activities, among others [72]. Nevertheless, for proteins that are fated for destruction, a highly selective series of enzymatic events have to occur. First, the C-terminal glycine residue

(Gly76) on Ub is activated by the E1 activating enzyme in an ATP dependent manner. Until recently it was believed that only one E1 existed, but the latest reports seem to suggest that there may be additional E1s [73, 74]. The activation reaction involves the formation of a Ub-adenylate with the release of pyrophosphate (PPi) from ATP. The activated Ub is then transferred to a cysteine residue on the E1 with the concomitant liberation of AMP [75, 76, 77]. The result of this reaction is the formation of a high energy E1-thiol-ester-Ub intermediate that is then transferred to an E2 conjugating enzyme (Figure 2.2) [75, 76, 77].

In comparison to the E1 enzyme, there are known to be a number of E2s. As many as eleven have been reported in the yeast genome and that number is thought to be greater in higher organisms [78]. The E2s are referred to as the Ub carrier proteins or Ub conjugating enzymes as they accept the activated Ub from E1 and facilitates its attachment to the target protein in conjunction with E3s (Figure 2.2). The E2s may serve as a bridge between the target protein and an E3 or may transfer the Ub to an E3, which will subsequently tag the protein.

The E3s are responsible for the specific recognition of a particular substrate and can be either a protein or a protein-complex [79]. The E3 reaction involves two events, the Ub signal dependent binding of the E3 to substrate and the covalent attachment of Ub to the target protein [78]. Two of the most widely studied classes of E3s are the HECT (Homologous to the E6-AP C-Terminus) [80] domain E3s and the RING (Really Interesting New Gene) finger domain E3s.

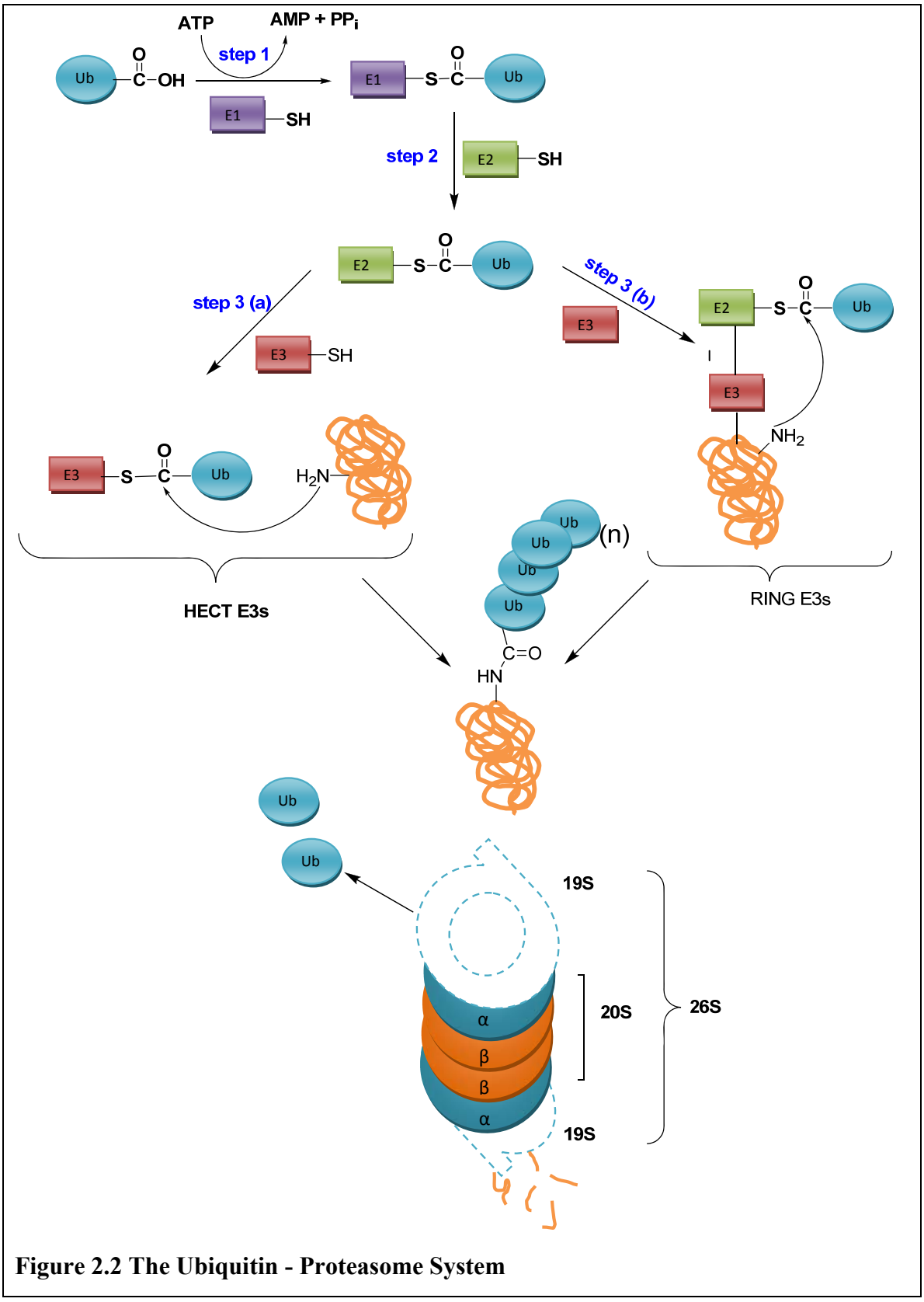

Figure 2.2 The Ubiquitin - Proteasome System

The HECT domain E3s has a conserved cysteine residue to which Ub from the E2 is transferred, forming another high energy thiol ester bond [81]. These E3s then transfer the activated ubiquitins to a lysine residue, often lysine-48 (K48), on the substrate. A member of the HECT E3 family is NEDD4 that targets the sodium channel in the kidney epithelium [82]. Unlike HECT E3s, the RING finger family of E3s acts as a bridge between the substrate and E2. They do so by binding to both the E2 and the substrate thereby, bringing the two within a proximity where the E2 is able to directly transfer Ub to the K48 residue of the substrate [83]. RING E3s are monomers or homodimers containing both the RING finger domain and the substrate recognition site in one molecule. Examples include mdm2, which targets p53 [84, 85] and parkin, which targets synaptic vesicle-associated protein, CDCrel-1 [86, 87]. A number of RING E3s are part of larger multisubunit complexes such as the SCF complex, which is involved in the degradation of IkB [88], the APC (Anaphase Promoting Complex, responsible for degrading cell cycle regulators [89] and the VBC (von-Hippel Lindau(VHL)-Elongins B and C)-Cul2-Rbx1 E3 ligase complex associated with the degradation of Hypoxia Inducible Factor (HIF)-1α [90, 91, 92].

2.4.2 VBC-Cul2-Rbx1 E3 ligase complex and HIF-1α

The unique interaction of HIF-1α with the VBC E3 ligase has been well characterized. HIF is important for normal development and plays a pivotal role in pathophysiological responses to low oxygen (hypoxic) conditions, as well as in tumor growth and angiogenesis [93]. HIF is a heterodimer consisting of α and β subunits that binds to DNA under hypoxic conditions. The β subunits are constitutively expressed whereas the alpha subunit is highly regulated. Under normal oxygen (normoxia) conditions, the alpha subunits are rapidly targeted for polyubiquitination by pVHL and subsequently degraded by the proteasome.

pVHL is a tumor suppressor protein whose mutation is associated with the development of VHL disease, a hereditary cancer characterized by the presence of highly vascularized tumors [94]. pVHL binds to a specific region on HIF-1α known as the oxygen-dependent degradation domain (ODD) [95, 96]. There are two distinct regions that

can operate independently of each other: one at the C-terminal (C-ODD) and the other at the N-terminal (N-ODD) [97, 98]. The interaction of pVHL at these domains is regulated by the hydroxylation on specific proline residues within the ODD proline 402 (Pro 402) in the N-ODD and proline 564 (Pro 564) in the C-ODD [95, 99]. Experiments conducted using various peptide lengths within the ODD indicated that the C-ODD region in HIF-1α is important for the binding of pVHL, while the N-ODD region only increases binding slightly [100]. Further, mutation studies demonstrated that there is a highly conserved motif containing a proline residue (Pro-564) and this motif is critical for the interaction with pVHL. Later, it was shown that hydroxylation of the proline initiates the ubiquitination and degradation of HIF-1α [99]. In the present studies, this interaction has been exploited in designing PROTACs that target the ER for proteasomal degradation.

2.4.3 The Proteasomes

The 26S proteasome is a hollow cylindrical-shaped mega structure (2.4 MDa) containing a 20S subunit referred to as the catalytic core and the 19S regulatory subunit [101] (Figure 2.2). There are two types of proteasomes, the regular (or constitutive) proteasome and the cytokine-inducible immunoproteasome. The immunoproteasome is thought to be associated with the generation of MHC class I antigens [102].

The 20S catalytic subunit consists of two sets of heptameric α and β subunits arranged as four stacked rings. The two outer rings are each made up of seven α subunits while the two inner rings each contain seven β subunits [103]. Three of the β subunits, β1, β2 and β5, are catalytically active and their proteolytic activities are unique [79]. β1 displays caspase-like (C-L) activity, cleaving after acidic residues, β2 cleaves after basic residues (trypsin-like activity, T-L) and β5 cleaves after bulky hydrophobic residues (chymotrypsin-like activity, CT-L) [104]. In response to γ-interferon signaling these β subunits are replaced with three alternative subunits: β1 replaced with β1i/LMP2, β2 with β2i/MECL-1/LMP10 and β replaced with β5i/LMP7 [105] to form the immunoproteasome.

As it relates to the function of the α subunits, it has been shown that the N-termini of the α subunits block entry of protein substrates to the proteolytic cavity thus acting as a gate to prevent unwanted degradation [106]. The 20S proteasome only becomes accessible

upon the binding of the 19S regulatory subunit. The 19S regulatory particle consists of a 9-protein lid for polyubiquitin binding, and a 10-protein base that interacts specifically with the α ring. The 19S base binds to and displaces the N-terminal of the α subunits [107], wheras the 19S-lid regulatory particle is involved in the recognition, binding and deubiquitination of polyubiquitinated substrates [108, 109, 110, 111]. The 19S-base contains several ATPases and deubiquitinases [112]. Once the substrate enters the catalytic core it is degraded into smaller peptides.

2.5 Estrogen receptors (ER) and Breast Cancer

2.5.1 Estrogen receptor (ER)

The estrogen receptors (ER) belong to the family of nuclear receptors, which is one of the largest classes of proteins having over 70 known members. The ER is more specifically referred to as a steroid hormone nuclear transcription factor. Currently, two types of estrogen receptors exists ERα and ERβ. The ER (ERα) was cloned in 1986 [113] approximately 40 years after Jensen indicated the possible role of a receptor that specifically binds 17β-estradiol (E2) [10, 11, 114]. The second receptor ERβ was cloned in 1996 [115].

The ER contains a number of functional domains [116, 117, 118, 119] as depicted in Figure 2.3. There is an N-terminal A/B domain that is not well conserved among the steroid receptors. Within the A/B domain is a transactivation function (AF-1) responsible for ligand-independent transcriptional activation. The C domain comprises the DNA binding domain, which is the most highly conserved domain within the nuclear receptor family. The DBD is responsible for the high specificity, high affinity binding of the ERs to their estrogen responsive elements (EREs) [120, 121, 122]. Within the DBD there are two zinc finger motifs. While there are a number of similarities among zinc fingers within the nuclear receptor family, mutagenesis studies indicate that one of the zinc fingers lends specificity to the individual receptors by binding to specific residues in the major groove of DNA; the other zinc finger works to stabilize the aforementioned interaction [123, 124]. In

addition to the DNA binding domain the C domain also contains a dimerization functionality as well as a nuclear localization signal [121, 125, 126].

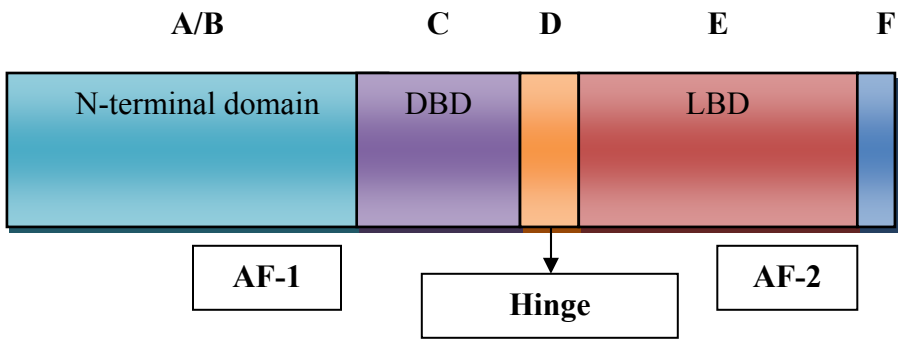

Figure 2.3 The functional domains of the estrogen receptor (ER): DBD- DNA binding domain, LBD- ligand binding domain, AF-1, 2 (transcription activation function 1 and 2).

The D domain is a non-conserved, hydrophilic domain that acts a hinge between the DBD and the ligand binding domain (LBD). This domain may direct the DNA-binding activities of the receptor while the hinge region may also play a role as an anchor for co-repressor proteins [10, 122, 127, 128]. The ligand binding domain (LBD) is located in the C-terminal E region which contains a hydrophobic pocket formed as a result of 12α helices; the hydrophobic pocket is important for ligand binding [128, 129, 130]. The LBD is less well conserved in comparison to the DBD. Within the E region there is also a ligand-dependent dimerization function, a ligand-dependent nuclear localization signal, heat shock protein 90 (HSP90) binding utility and another activation function (AF-2), which is ligand-dependent [128, 130]. The F region at the C terminal domain is involved in a number of activities including the selection of agonists or agonists, crosstalk between other signaling pathways, regulation of proteasomal degradation and possible blockade of dimerization [131, 132, 133, 134].

It must be noted that while the DBD of ERα and ERβ are almost identical (95% amino acid identity), and their LBDs are moderately identical, approximately 56%, while they differ markedly in their AF-1 (around 21% amino acid identity) [135, 136]; the AF-1 of ERβ seems to be inconsequential in regulating reporter gene expression [137]. Additionally the hinge and the F region are not conserved among the receptors [138]. The ERs also differ in their tissue distribution. ERα is predominantly expressed in the breast, vagina and uterus while ERβ is more highly expressed in the gastrointestinal system, central nervous system, lungs, cardiovascular system, immune system and bone, but is not highly expressed in breast tissues [135]. In certain breast cancers, the ERα is over expressed; therefore these cancers are termed ER-positive or hormone sensitive.

2.5.2 Mechanisms of action of ERs

The estrogen receptor is a member of the ligand activated transcription factor family. In response to ligand binding, the ER binds to EREs, initiating transcription of target genes [139, 140]. The cellular localization of the unliganded ER has been controversial and it seems that the location of the ER plays a role in ER actions. It is thought that the unliganded ER predominately resides in the nucleus, but there is also a pool of ERs located in the cytoplasm and at the membranes [139, 141, 142, 143].

Genomic actions of ER

In the "classical or genomic" mechanism, E2 diffuses through the membrane and binds to ER, resulting in a conformational change of the ER that allows it to dissociate from chaperones, dimerize and bind to the ERE on the target gene's promoter. Once bound to the ERE, AF-1 and AF-2 are responsible for recruiting co-activators from the p160 family, steroid receptor co-activators 1, 2 and 3 (SRC1,2,3). Other factors responsible for chromatin remodeling, that interact with the general transcription machinery in order to initiate transcription of the target genes are also recruited [144]. Some of the genes transcribed via the ER genomic action include, trefoil factor (pS2/TFF1) and vascular endothelial growth factor (VEGF) [145].

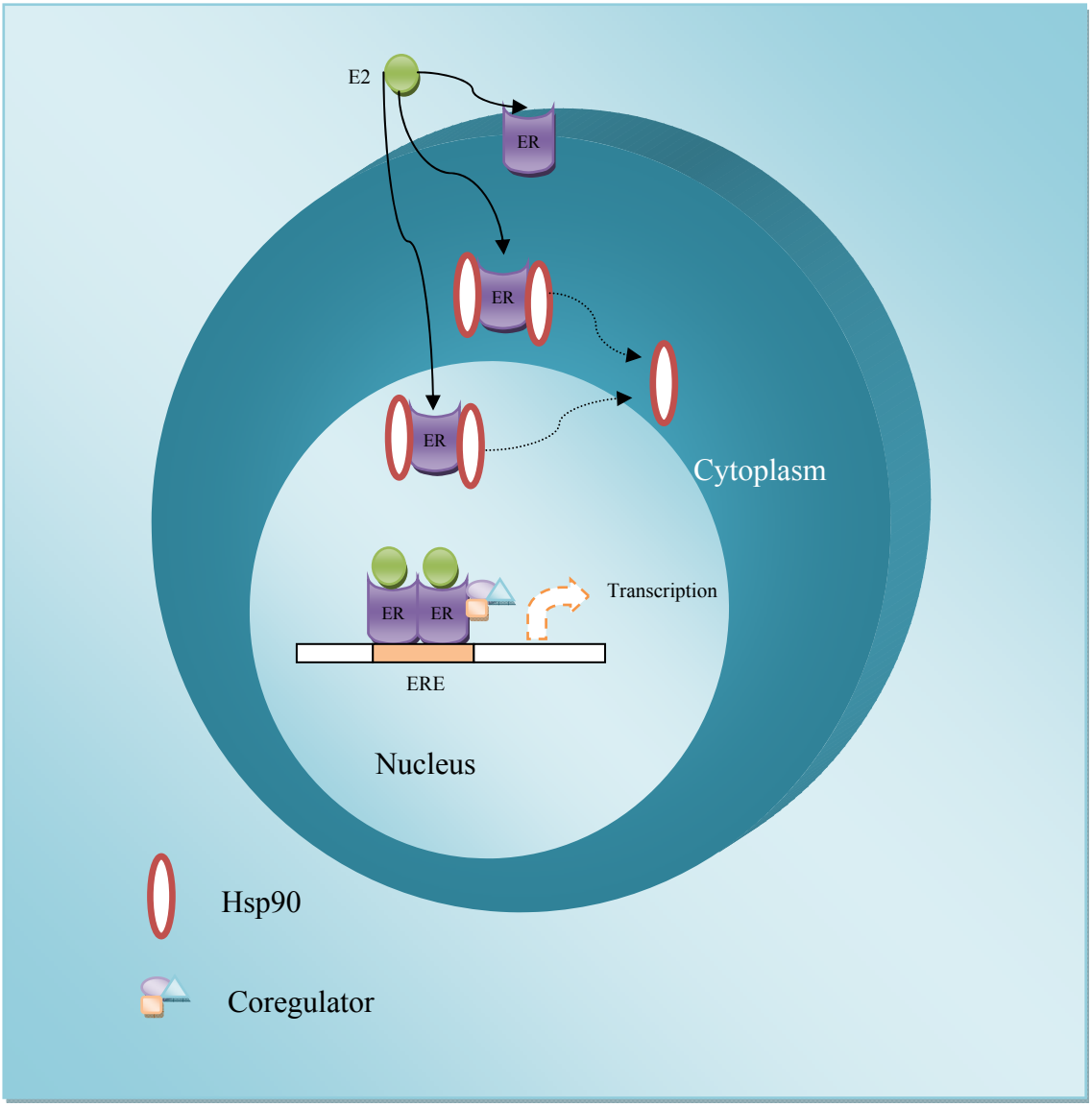

Figure 2.4 Mechanism of ER actions

Nongenomic actions

ERs can also act independently of ERE binding. This non-genomic action of the ER occurs via protein-protein interactions with other transcription factors. Approximately 35% of target genes are transcribed in this manner [145]. For example, ER action through AP-1 activation is responsible for the transcription of such genes as insulin growth factor-1 (IGF-1), cyclin D1 and collagenase [145, 146, 147]. Opposite effects at AP-1 sites have been

indicated for ERβ [148, 149]. ER also interacts via a non-classical mechanism with ER-specific protein-1 or stimulating protein-1 (SP-1) to mediate transcription of target genes [145, 150]. Interaction at SP-1 sites involves the complex binding to GC- rich regions within the promoters of target genes enabling transcription of such genes as retinoic acid receptor 1α (RXRα), insulin growth factor binding protein -4, low-density lipoprotein (LDL) receptor and cathepsin [151, 152, 153].

Non-genomic actions

Membrane or cytoplasmic ERs are also believed to be responsible for the rapid non-classical/ non-genomic actions of ER. In this case, ligand binding to these receptor pools result in the activation of a number of signaling pathways. One such example is the mitogen activated protein kinase pathway (MAPK) [154, 155]. Estrogen bound membrane ER has also been shown to activate the insulin-like growth factor receptor-1(IGF-1R) and epidermal growth factor receptor (EGFR) cell signaling cascades [12, 156].

2.5.3 ER-positive breast cancer and treatment

Breast cancer is the second leading cause of cancer death among women in industrialized countries. According to the 2009 cancer statistics an estimated 192, 370 women will be diagnosed with breast cancer and over 40, 000 will die from the disease [157]. Approximately 70% of breast cancer diagnosed is ER-positive. The length of exposure to estrogen has been shown to play a role in increasing the chance of developing breast cancer. Most of the genes that are upregulated by the ER are involved in proliferation and as such have a direct effect on the progression of breast cancer [158]. Thus, current breast cancer therapies aim to inhibit the action of the ER by blocking the production of E2 (eg. aromatase inhibitors) [159, 160] or blocking the binding of estrogen to the ER (eg. antiestrogens) [161, 162, 163, 164, 165, 166] .

One of the oldest and most widely used antiestrogen is tamoxifen (Figure 2.5). Tamoxifen is classified as a selective estrogen receptor modulator (SERM) having antagonist activity in the breast, but agonist activity in the uterus and bone [167, 168]. It has been shown that the binding of tamoxifen to the ER leads to a conformational change that

is different from E2 binding [12]. Specifically, the binding of tamoxifen within the ER's binding pocket results in a conformational change that results in the pocket not being sealed properly. This conformational change deters the binding of coactivators resulting in the inactivation of AF-2 function. The inhibition of AF-2 function prevents transcription of genes that are dependent of AF-2-ER functionality [169]. The breast tissue is reliant on AF-2-ER mediated gene transcription, whereas the uterus is reliant on the ER-AF-1 function; this is why tamoxifen acts as an antagonist in breast, but as an agonist in the uterus, where the AF-2 function is not important [170, 171].

Tamoxifen, by virtue of its SERM nature, has been linked to an increase in the chances of developing endometrial cancer [172]. The main problem with Tamoxifen and other antiestrogenic compounds, as well as aromatase inhibitors [173], is the eventual development of resistance after prolonged use. Close to 100% of patients with metastatic disease and about 40% of patients receiving adjuvant therapy succumb to resistance and eventually die from the disease [12]. There have been several mechanisms proposed for the development of resistance to these therapies including, increased ER-HER2 crosstalk [174, 175]; elevated levels of EGF, responsible for mediating autocrine growth pathways in resistant cells [176] as well as increased phosphorylation of Ser 118 on the ER [13]. Phosphorylation at Ser 305 has recently been implicated in the causation of resistance as well [14]. It is important to note that loss of ER may not be a factor in development of resistance as both tamoxifen-resistant and primary breast tumors retain high levels of ER and is affected by pure antagonists [176, 177].

Another antiestrogen, termed a pure antagonist, is Faslodex® (ICI182,780). At the time of its discovery, ICI182,780 displayed no estrogenic activity and was developed as an alternative second line therapy to treat patients that were no longer affected by tamoxifen treatment [178]. While its mode of action is not clearly understood, ICI182,780 seem to cause a down regulation of the ER [179]. Recent studies seem to suggest that ICI182,780 may not be a pure antagonist after all, as it displays agonist activity in Hippocampal Neurons [180]. While the effect is a positive one, there might be other yet undiscovered agonistic activities of this drug that may have negative impacts.

Given the role of ER in the progression of breast cancer, alternative methods are needed to delineate unknown roles or unknown targets that may be associated with the

ER. Thus, the employment of a PROTAC that selectively knocks-down the ER is proposed as a novel probe to elucidate ER biology. In addition the PROTAC strategy may provide a new therapeutic candidate for treating ER-positive breast cancers.

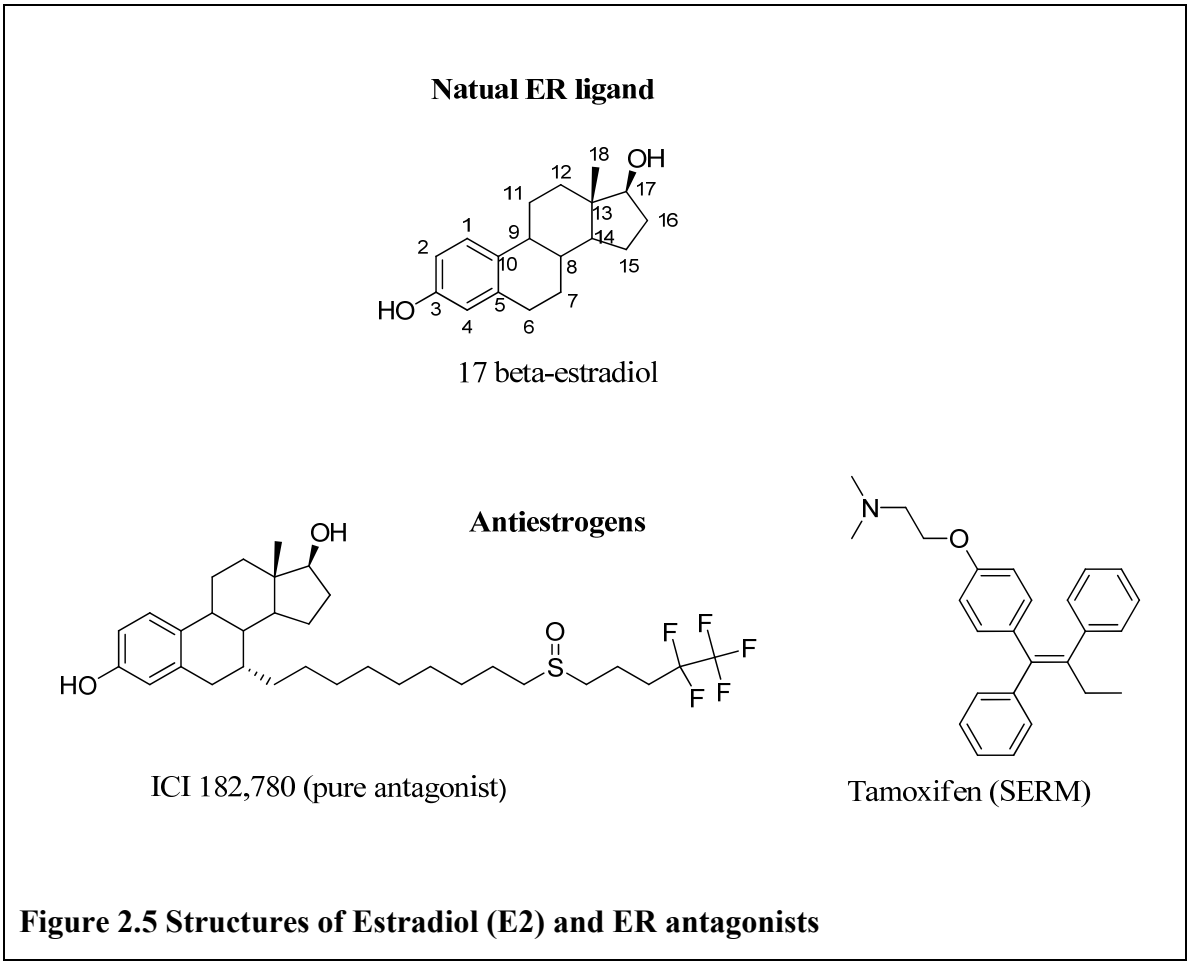

Figure 2.5 Structures of Estradiol (E2) and ER antagonists

CHAPTER 3: CHEMISTRY- SYNTHESES OF PROTACs

3.1 Introduction

While the PROTAC technology has been developed to target proteins for degradation and may be a valuable tool to investigate protein functions, a detailed PROTAC optimization strategy has never been explored. As such, the main objective of this project is to optimize the PROTAC technology for broad applications. The ER targeting PROTAC was used as the model in this optimization effort since the first generation of cell permeable PROTACs were developed based on ER-targeting strategy. In addition, the ER is the main therapeutic target for breast cancer therapy and optimization of a PROTAC that specifically targets the ER may pave the way to develop a novel ER antagonist that acts differently from any other ER antagonists clinically available. The information gathered from this optimization study may also be useful for the design of PROTACs that target other proteins.

The first generation ER targeting PROTAC (Figure 3.1) involved the attachment of a linker at the O-17 position on E2, the natural ligand of the ER (Figure 3.1). The successful development of the first ER targeting PROTAC provided proof of concept for targeting the ER by this approach; however, while this PROTAC was able to cause degradation of the ER *in vitro,* the ester linkage proved to be problematic in initial *in vivo* studies. The linkage was apparently cleaved off as a result of intracellular esterase activity resulting in tumor growth (unpublished data).

In this current study, three main areas were focused on to improve the PROTAC: First, in order to address the issue of linker cleavage, the ester linkage was replaced with a carbon-carbon linkage through the C-16 and C-7 positions of E2 (Figure 3.1). Second, PROTACs were synthesized with varying lengths, in order to determine an optimal distance between E3 ubiquitin ligase (pVHL) and the protein of interest (ER). Third, a dimeric PROTAC having two estradiols at both ends of the pVHL recognition motif was developed in order to increase the chances of recruiting the ER for ubiquitination and ultimately degradation.

In this chapter the synthetic routes, reaction details and structural analysis of intermediates leading up to and including PROTAC synthesis are presented.

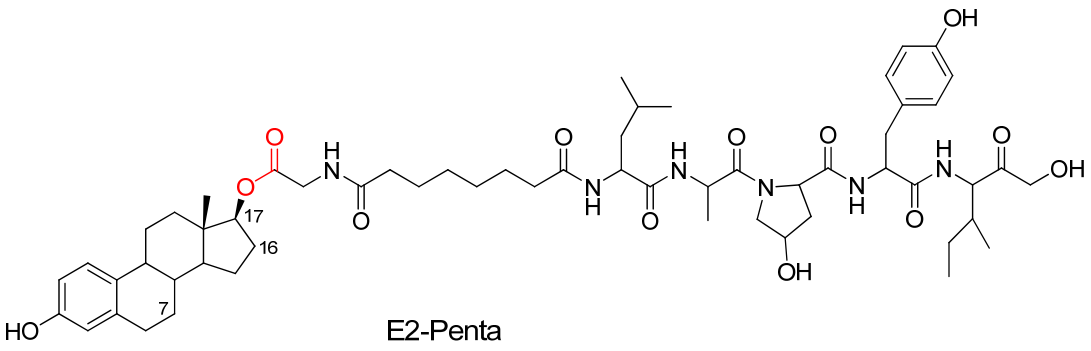

Figure 3.1 Structure of the original ER-PROTAC (E2-Penta): highlighting the O-17 ester linkage and the C-16 and C-7 locations for C-C bond formation.

General: Unless otherwise noted, all reactions were carried out under nitrogen or argon in freshly distilled solvents, oven-dried glassware. Reagent grade solvents were used. Tetrahydrofuran (THF) was distilled from sodium/benzophenone. Methylene chloride (CH_2Cl_2) was distilled from calcium hydride. Anhydrous diethyl ether was purchased from Fisher and used without further distillation. All other reagents were purchased from Sigma-Aldrich and used without further purification. Peptides were purchased from Advanced Chem Tech (Louisville, KY). Reactions were monitored by TLC using E. Merck 60F254 pre-coated silica gel plates. Flash column chromatography was performed using E. Merck silica gel 60 (particle size 0.040-0.063mm). ^{1}H NMR spectra were recorded on a Varian 300MHz or 500MHz spectrometers. Mass spectral analyses were carried out by the University of Kentucky Mass Spectrometry Facility.

3.2 pVHL recognition motif derived from HIF-1α

One of the components of the PROTAC is the degradation signal derived from the HIF-1α protein. The amino acid sequence recognized by pVHL consists of an (ODD) containing the highly conserved sequence (Met-Leu-Ala-Pro-Tyr-Ile-Pro-Met). In

previous work it was shown that a pentapeptide derived from HIF-1α ODD domain is sufficient to be recognized by pVHL [7].

The pentapeptide was synthesized following conventional peptide synthesis approaches. Briefly, for pentapeptide-1, the synthesis began with the coupling of a C-terminal protected isoleucine to a tyrosine protected at both its N-terminal and its hydroxyl with Fmoc (9-fluorenyl-methoxy-carbonyl) and tertiary-butyl (t-Bu) respectively, the coupling reagents HBTU (2-(1H-Benzotriazol-1-yl)-1,1,3,3-Tetramethyluronium hexafluorophosphate) and HOBt (N-Hydroxybenzotriazole), along with DIPEA (*N*,*N*-Diisopropylethylamine) as a base in CH_2Cl_2. Following successful coupling, the Fmoc group was removed with 20% piperidine in DMF (N,N-Dimethyl formamide) and the process was repeated with the remaining Fmoc-protected amino acids to give pentapeptide-1 (Figure 3.2). t-Bu protecting group on tyrosine was either removed prior to or after full assembly of the PROTAC. A mutant pentapeptide (pentapeptide-2, Figure 3.2) containing nor-leucine in place of the hydroxyproline residue was also synthesized following a similar procedure described above; this will serve as a negative control for pentapeptide-2. In order to study whether linker attachment to the C- or N-terminus of the pentapeptide is important for PROTAC activity, an additional pentapeptide that was protected at the N-terminal with a benzyloxycarbonyl (cbz/Z) group and a free carboxylic acid at its C-terminus was also synthesized (Figure 3.2).

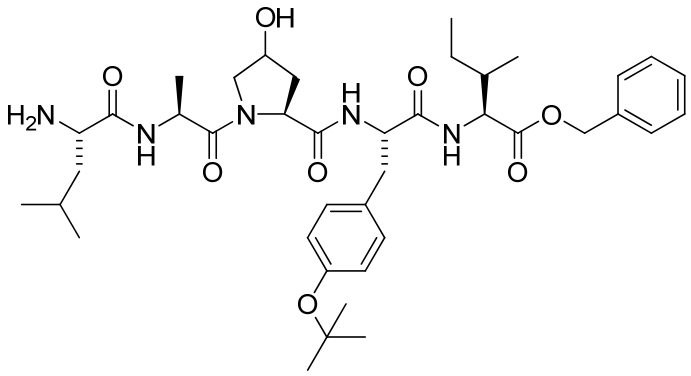

Pentapeptide-1 (C-terminus protected)

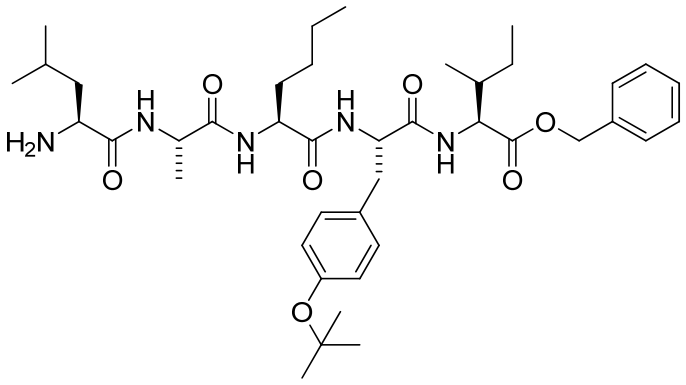

Pentapeptide-2 (Negative control)

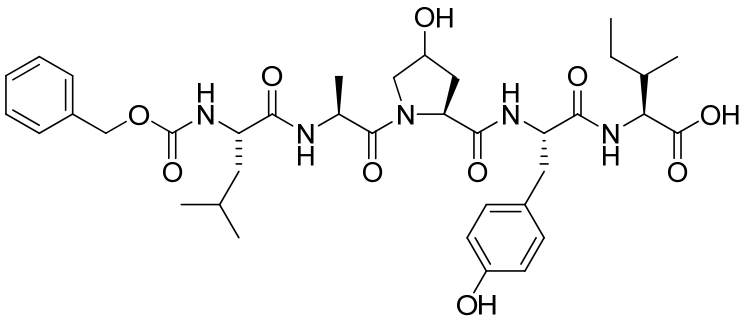

Pentapeptide-3 (N-terminus protected)

Figure 3.2: Structures of pentapeptide-1 to 3

3.3 Synthesis of C-16α PROTACs

One of the primary goals of this project was to synthesize a PROTAC that had a less labile linkage by eliminating the ester linkage and adding hydrolytically stable C-C bond. The task was to find a place on E2 that will allow for attachment of the linker without disrupting the E2- ER interaction significantly. Another critical issue with the original ER-targeting PROTAC was the loss of the 17-OH which was used attach the linker. It has been reported that the OH is important for the binding activity of E2 to ER [181]; therefore, any modification that can spare the hydroxyls is most desirable in designing an ER targeting compound based on the E2. Derivatization at the C-16α position on E2 has been previously reported in the construction of a Geldanamycin tagged E2 compound that maintained good E2-ER interaction [182].

In order to attach the pentapeptide to the C-16α position and extend the length of the linker attaching the two different moieties a "handle" had to be placed on the E2 that would allow for further extension. A scheme, (Scheme 3.1), similar to the one reported in [182, 183] was followed for synthesis of a "free amine handle" attached to the C-16α position of E2. The scheme allowed for the formation of the desired α-alkylation at the C-16 position, a stereochemistry that is important for the high binding affinity to the ER [184]. The handle, can be further extended via amide bond formation.

Scheme 3.1- Synthesis of C-16α handle

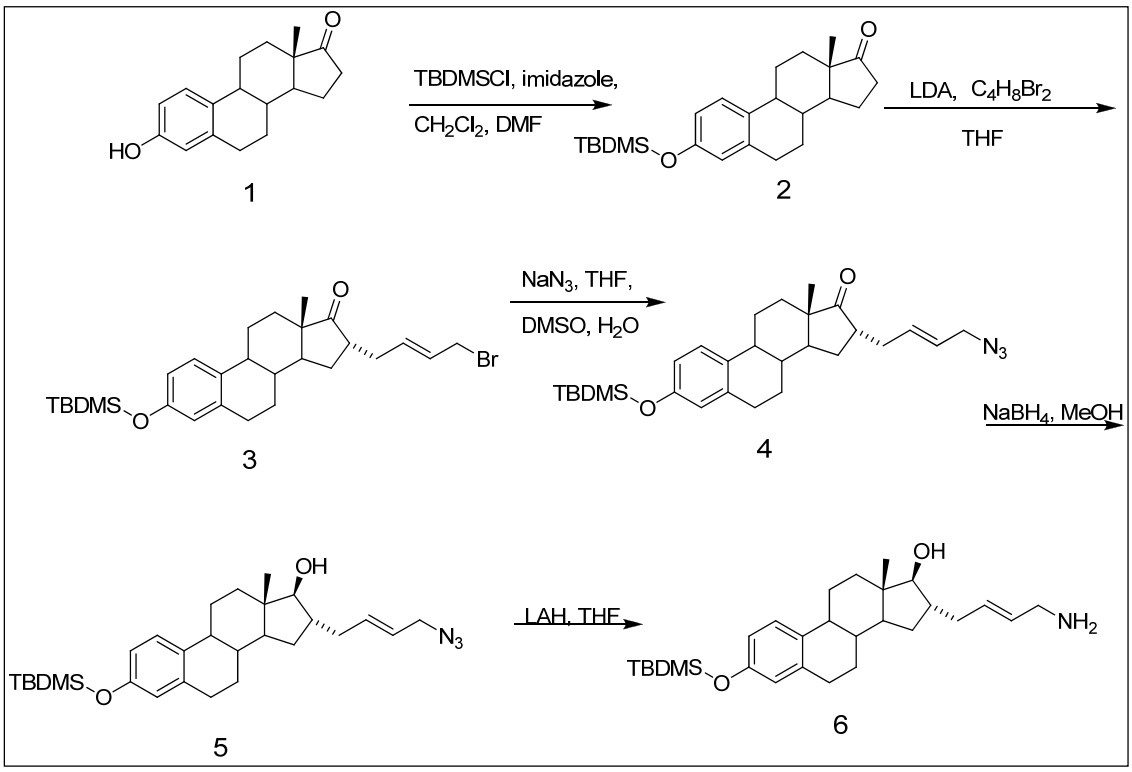

Synthesis of C-16α PROTACs K-1 and K-2

Following the successful synthesis of the free amine handle the length was further extended using glycine, and an eight carbon linker, disuccinimidyl suberate (DSS). The pentapeptide was then attached to give the fully assembled protected PROTACs, after deprotection of protecting groups the C-16 PROTACs were isolated as K-1 and K-2 (Scheme 3.2).

Scheme 3.2 synthesis of C-16α PROTACs K-1 and K-2

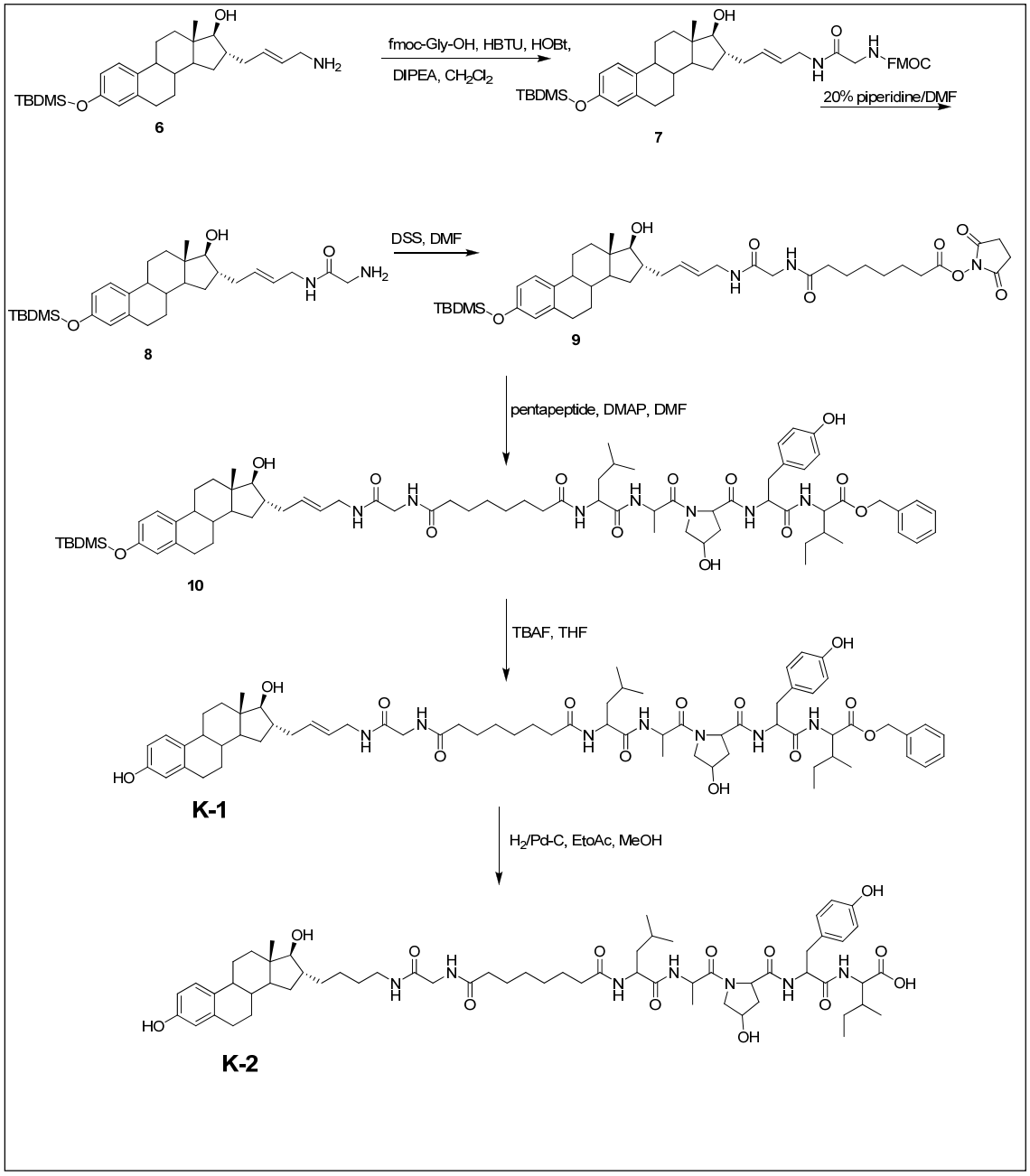

Reaction details and NMR data for the synthesis of C-16α PROTAC's handle

Compound 2: Estrone **(1)** (4.00 g, 0.0148 mol) and imidazole (3.00 g, 0.044 mol) were dissolved in 40 mL (CH_2Cl_2) and 15 ml DMF. tert-Butyldimethylsilyl chloride (TBDMS-Cl) (6.70g, 0.044mol) was added, and the solution was stirred at room temperature, after 2 hours the solution was filtered through filter paper and solvent removed, the residue was dissolved in CH_2Cl_2 and column chromatography was performed using (5:1 hexanes:ethyl acetate (Hex:EtOAc)) to yield a white solid (5.62 g, 99%).

^{1}H NMR ($CDCl_3$, 500 MHz): δ 0.19 (s, 6H), 0.91 (s, 3 H), 0.98 (s, 9H), 2.84-2.87 (m, 2H), 6.57 (d, 2.5 Hz, 1 H), 6.62 (dd, *J* = 8.5, 2.5 Hz, 1 H), 7.13(d, *J* = 8 Hz, 1H)

Compound 3: Under nitrogen, dry THF (6 mL) was added to a flask containing **(2)** (400.0 mg, 1.04 mmol) and the solution was cooled to 0 °C. Lithium diisopropylamide (LDA) (0.80 mL, 1.45 mmol) was then added (drop-wise) and the solution was stirred for an additional 0.5 h at 0 °C. The reaction was then cooled to -20 °C using an external bath (sodium chloride (NaCl), ice), and electrophile (1,4 dibromo-2-butene) (440.0 mg, 2.08 mmol, in 1 mL of THF) was added (drop-wise). The reaction mixture was stirred at -20 °C for an additional 4 hrs, water was then added and mixture was extracted with three 50 ml portions of EtOAc. The organic phase was washed with brine and dried over sodium sulfate (Na_2SO_4). Following filtration and solvent removal, the residue was dissolved in CH_2Cl_2 and column chromatography was performed using (10: l Hex: EtOAc) to give a thick yellow oil. Reaction was repeated 4 times with the same amounts to yield **(3)** (1.2 g, 45%).

^{1}H NMR ($CDCl_3$, 500 MHz): δ 0.19 (s, 6 H), 0.96 (s, 3 H), 0.98 (s, 9 H), 2.82-2.85 (m, 2 H), 3.95 (d, *J* = 6.6 Hz, 2 H), 5.74 – 5.78 (m, 2 H), 6.57 (d, *J* = 3 Hz, 1 H), 6.63 (dd, *J* = 8.5, 2.5 Hz, 1H), 7.12 (d, 1 H, *J* = 8.5 Hz, 1 H).

Compound 4: Sodium azide (NaN_3) (520 mg, 7.64 mmol) was added to a flask containing **(3)** (960 mg, 1.91 mmol) and the contents were dissolved in THF (25ml), 2 ml of water and 2 ml DMSO. The mixture was stirred at room temperature for 2 hrs after

which, water was added and extraction performed with EtOAc. The organic phase was washed with brine and dried over (Na_2SO_4). Following filtration and solvent removal, residue was dissolved in CH_2Cl_2 and column chromatography was performed (10: 1 Hex: EtOAc) to give **(4)** as a pale yellow oil (889 mg, 96 %).

^{1}H NMR ($CDCl_3$, 300MHz): δ 0.19 (s, 6 H), 0.96 (s, 3 H), 0.98 (s, 9 H), 2.83 (m, 2H), 3.73 (d, *J* = 6.3 Hz, 2 H), 5.47-5.80 (m, 2 H), 6.56 (d, *J* = 2.4 Hz, 1H), 6.62 (dd, *J* = 8.3, 2.4 Hz, 1 H), 7.11 (d, *J* = 8.5 Hz, 1 H).

Compound 5: Methanol (MeOH) was added to **(4)** (510 mg, 1.06 mmol) and cooled to 0 °C, after 10 min sodium borohydride ($NaBH_4$) (120 mg, 3.19 mmol) was added and reaction stirred for an additional 2.25 hrs. MeOH was removed under reduced pressure, water was added and EtOAc was used for extraction. The organic fraction was washed with brine and dried over (Na_2SO_4). Product was isolated as a white solid (250 mg, 49%) following column chromatography (10: 1 Hex: EtOAc). * *Attempts to simultaneously reduce the azide and ketone using LAH were unsuccessful; therefore sequential reduction steps were employed: $NABH_4$- ketone reduction and LAH-azide reduction.*

^{1}H NMR ($CDCl_3$, 300MHz) δ 0.19 (s, 6H), 0.82 (s, 3 H), 0.99 (s, 9H), 2.80 (m, 2 H), 3.33 (d, *J* = 7.8 Hz, 1H), 3.74 (d, J = 6.6 Hz, 2H), 5.56-5.88 (m, 2 H), 6.55 (d, *J* = 2.7 Hz, 1 H), 6.62 (dd, *J* = 8.5, 2.5 Hz, 1 H), 7.12 (d, *J* = 8.1 Hz, 1H).

Compound 6: (5) (250 mg, 0.52 mmol) was dissolved in dry THF (15ml) and then cooled to approximately -10°C. Excess lithium aluminum hydride (LAH), (100 mg, 2.60 mmol) was slowly added and the reaction was stirred for 2 hours. Reaction was then extracted with CH_2Cl_2 dried over Na_2SO_4 and purified via column chromatography (95:5 CH_2Cl_2: MeOH), **(6),** (159mg, 67%) was obtained as white solid.

^{1}H NMR ($CDCl_3$, 300 MHz) δ 0.19 (s, 6H), 0.82 (s, 3 H), 0.98 (s, 9H), 2.78 - 2.80 (m, 2 H), 3.21-3.28 (m, 3 H) 5.58-5.63 (m, 2 H), 6.55 (d, *J* = 2 Hz, 1 H), 6.61 (dd, *J* = 8.1, 2.4 Hz, 1 H), 7.12 (d, *J* = 8.1 Hz, 1H).

Reaction details NMR AND Mass spectrometry data for the synthesis of C-16α PROTACs K-1 and K-2

Compound 7: Fmoc-Gly-OH (107mg, 0.360mmo1), HBTU (170 mg, 0.45 mmol) and HOBt (69 mg, 0.45 mmol) was added to a flask containing the free amine **(6)** (136 mg, 0.30 mmol). The reagents were dissolved in CH_2Cl_2 and excess DIPEA (310µl) was added. The reaction was stirred at room temperature overnight. Column chromatography was performed using (1:1 Hex: EtoAC) to yield **(7)**, (105 mg, 47%) as a clear oil.

^{1}H NMR ($CDCl_3$ 500 MHz) δ 0.19 (s, 6H), 0.79 (s, 3H), 0.98 (s, 9H), 2.78 – 2.81 (m, 2H), 2.82 (s, 4H), 3.25 (d, *J* = 7 Hz, 1H), 3.77-3.89 (m, 4H), 4.23 (t, *J* = 6.7 Hz, 1H), 4.43 (d, *J* = 7 Hz, 2H), 5.47 - 5.70 (m, 2H), 6.27 (t, *J* = 5.4 Hz, 1H), 6.55 (d, *J* = 2.4 Hz, 1H), 6.62 (dd, *J* = 8.5, 2.4, 2.7 Hz, 1 H), 7.11 (d, *J* = 8.5 Hz, 1H),7.30 – 7.33 (m, 2H), 7.39 – 7.42 (m, 2H), 7.60 (d, *J* = 7.5 Hz, 2H), 7.77 (d, *J* = 7.5 Hz, 2H)

Compound 8: 20% piperidine in DMF (1.5 ml) was added to **(7)** (105mg, 0.143mmol) and the reaction was stirred at room temperature for 40 mins. Solvents were removed under high vacuum and column chromatography was performed using (95:5 CH_2Cl_2: MeOH) to remove by products. The column was washed with MeOH to isolate **(8)** (49mg, 67%) as a white solid. Free amine confirmed by Kaiser test.

Compound 9: Disuccinimidyl suberate (DSS) (70.0 mg, 0.191 mmol) was added to a flask containing **(8)** (49mg, 0.095mmol) and the contents were dissolved in DMF (2.5 ml) and stirred at room temperature overnight. DMF was removed under high vacuum and (95:5 CH_2Cl_2: MeOH) was used to purify the product via column chromatography. **(9)** (27mg, 38%) was isolated as an oil.

^{1}H NMR ($CDCl_3$ 300 MHz) δ 0.18 (s, 6H), 0.80 (s, 3H), 0.97 (s, 9H), 2.61 (t, *J* = 7.2 Hz, 2H), 2.78 – 2.84 (m, 6H), 3.27 (d, *J* = 7.2 Hz, 1H), 3.75-3.81 (m, 2H), 3.90 (d, *J* = 5.4 Hz, 2H), 5.44 - 5.70 (m, 2H), 6.33 (t, *J* = 5.4 Hz, 1H), 6.48 (t, J = 4.8 Hz, 1H), 6.55 (d, *J* = 2.4 Hz, 1H), 6.62 (dd, *J* = 8.5, 2.7, 2.4 Hz, 1 H), 7.11 (d, *J* = 8.5 Hz, 1H)

Compound 10: Pentapeptide-1(no t-Bu), (26.0 mg, 0.035 mmol) was added to **(9)** (27.0 mg, 0.035 mmol), dissolved in DMF (2 ml) and stirred under N_2 overnight at room temperature. Following removal of DMF under high vacuum, (95:5 CH_2Cl_2: MeOH) was used to purify product as a white solid (22.5 mg, 47%).

^{1}H NMR ($CDCl_3$ 500 MHz) δ 0.18 (s, 6H), 0.79 (s, 3H), 0.80-0.84 (m, 6H), 0.89-0.93 (m, 6H), 0.97 (s, 9H), 2.78 – 2.81 (m, 2H), 3.11 (dd *J* = 7, 3 Hz, 2H), 3.26 (d, *J* = 7 Hz, 1H), 3.55 (dd, *J* = 10.7, 2.7 Hz, 1H), 3.70-3.81 (m, 4H), 3.85 (d, *J* = 6 Hz, 2H), 4.36 – 4.55 (m, 6H), 4.60 (t, J = 7 Hz, 1H), 5.13 (s, 2H), 5.45 - 5.49 (m, 1H), 5.66 – 5.69 (m, 1H), 6.54 (d, *J* = 2.5 Hz, 1H), 6.60 (dd, *J* = 8.5, 2.5, Hz, 1 H), 6.87 (d, J = 8.5 Hz, 2H), 6.95 (d, *J* = 8.5 Hz, 1H), 7.09 (d, *J* = 8.5 Hz, 2H), 7.13 (d, *J* = 6.5 Hz, 1H), 7.30 – 7.38 (m, 6H), 7.39 (d, *J* = 7 Hz, 1H), 7.55 (d, *J* = 7.5 Hz, 1H)

K-1: To obtain K-1 the TBDMS protecting group was removed. THF (1ml) was added to **(10)** (22.5 mg, 0.016 mmol), followed by tertiary butyl ammonium fluoride in THF (TBAF) (14 µl, 0.048 mmol) and reaction was stirred at room temperature for 20 mins. Column chromatography was performed using (95:5 CH_2Cl_2: MeOH) initially and then increasing MeOH concentrations to isolate **K-1** (20.6 mg, 100%) as a white solid.

^{1}H NMR ($CDCl_3$ 300 MHz) δ: 0.79 (s, 3H), 0.80-0.84 (m, 6H), 0.89-0.93 (m, 6H), 2.78 – 2.81 (m, 2H), 3.11 (dd *J* = 7, 3 Hz, 2H), 3.26 (d, *J* = 7 Hz, 1H), 3.55 (dd, *J* = 10.7, 2.7 Hz, 1H), 3.75-3.86 (m, 4H), 4.39 – 4.57 (m, 6H), 5.13 (d, *J* = 5 Hz, 2H), 5.45 - 5.50 (m, 1H), 5.61 – 5.70 (m, 1H), 5.56 (d, *J* = 2.5, Hz, 1 H), 6.62 (dd, J = 8.5, 2.5 Hz, 1H), 6.76 (d, *J* = 8.5 Hz, 2H), 7.02 (d, J = 8.5 Hz, 2H), 7.11 (d, *J* = 8.5 Hz, 2H), 7.22 (d, *J* = 8.5 Hz, 1H), 7.35 (s, 4H), 7.46 (d, *J* = 7.8 Hz, 1H), 7.51 (d, *J* = 6.6 Hz, 1H). MS (MALDI, DHB) *m/z* 1219 (M+H, calcd for $C_{68}H_{95}N_7O_{13}$ requires 1217.70)

K-2: To obtain K-2 an additional deprotection step was required to remove the benzyl protecting group from isoleucine. **K-1**, (16.6 mg, 0.0125 mmol) was dissolved in EtOAc and MeOH 1:1 ratio (2 ml) and to this was added 15% palladium on charcoal. Hydrogen was bubbled through the reaction mixture for 20 mins. The mixture was filtered through

celite, concentrated under reduced pressure and dried under high vacuum to yield 16 mg of product, white solid. Product from hydrogenolysis (16 mg, 0.013 mmol) was dissolved in THF and TBAF in THF (0.039µl) was added. The mixture was stirred at room temperature for 20 mins. Column chromatography was performed using CH_2Cl_2: MeOH (95:5) initially and then increasing MeOH concentrations to isolate K-2 (14.0 mg, 89%) as a yellow solid. MS (MALDI, DHB) *m/z* 1131 (M+H, calcd for $C_{61}H_{91}N_7O_{13}$ requires 1129.67)

Figure 3.3: Mass spectrum for K-2

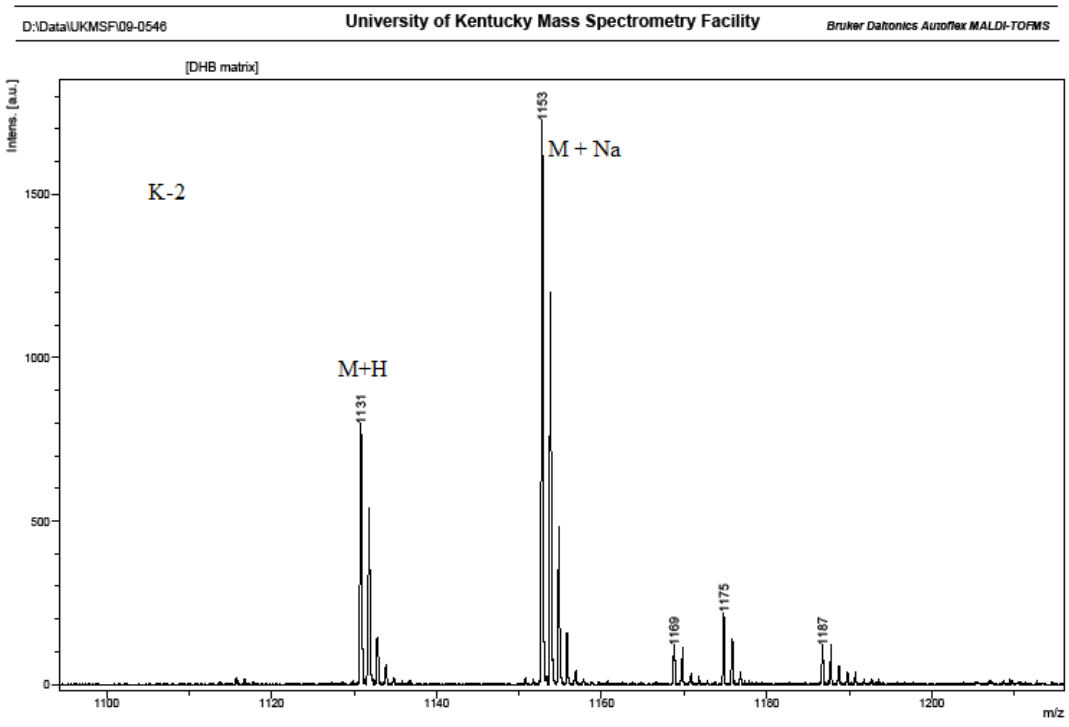

3.4 C-7α PROTACs syntheses /optimization of linker length

Our initial results from the screening done with the C-16 PROTACs indicated that the C-16 PROTAC was not better at degrading the ER than the original E2-penta

PROTAC **(Figure 3.4)**. Another observation from Figure 3.4 was that the K-1 PROTAC, having the benzyl group was more effective in degrading the ER than K-2 lacking the benzyl protection group. Therefore, with the belief that benzyl protection may play a role in the activity of the PROTAC, the O-17/E2-penta was re-synthesized to include the benzyl protecting group. All four compounds were analyzed for their ability to degrade the ER. As displayed in **Figure 3.5**, the benzyl protected PROTACs showed a greater ability to degrade the ER than unprotected PROTACs. However, the O-17 PROTACs induced more ER degradation than any of the C-16α PROTACs.

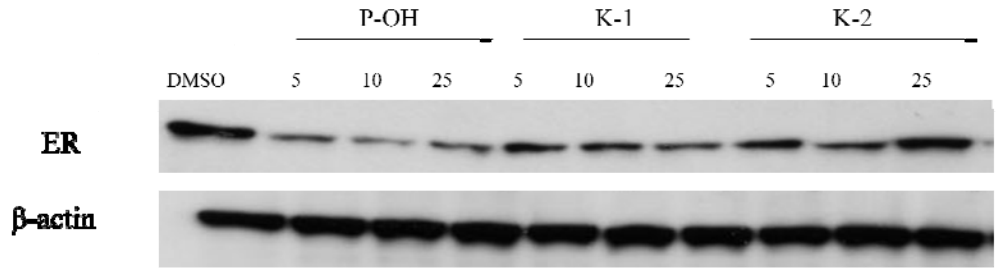

Figure 3.4 Evaluation of C-16 and O-17 PROTACs on ER degradation. MCF-7 cells were treated with PROTACs at the indicated concentrations (μM) or with DMSO for 48hrs. Cells were then lysed and analyzed via western blot using anti ERα antibody. β-actin was used as a loading control. P-OH (E2-penta/O-17 PROTAC), K-1 and K-2 (benzyl protected and deprotected C-16 PROTACs, respectively).

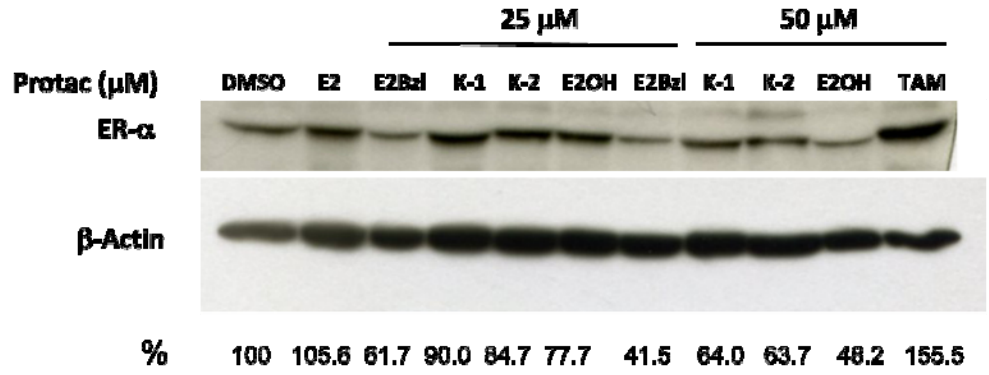

Figure 3.5 Comparisons of C-16α and O-17/E2- Penta PROTACs. MCF-7 cells were treated with PROTACs at the indicated concentrations or with DMSO, E2 (10 nM) and tamoxifen (TAM 5 µM) for 48hrs. Cells were lysed and analyzed via western blot using anti ERα antibody. The intensities of the bands were quantified (%) using volumetric densitometry (Quantity One, Bio-Rad). The ERα values were normalized to β-actin and DMSO was arbitrarily assigned a value of 100% for comparison purposes. The benzyl protected PROTACs were better at degrading the ER than unprotected. K-1 (C-16 PROTAC- protected C-terminus), K-2 (C-16 PROTAC - unprotected C-terminus), P-bzl (E2-penta/O-17 PROTAC- benzyl protected C-terminus), P-OH (E2-penta/O-17 PROTAC - unprotected C-terminus).

These results indicated that the C-16 position on E2 may not be ideal for the development of PROTACs, and as such a more appropriate derivatization site on E2 was sought. It has been shown that derivatization at the C-7α position on estradiol results in the maintenance of high ER-E2 binding affinity. For example, the ER antagonist ICI182,780 which has demonstrated high binding affinity for the ER is a C-7α derivative [185, 186, 187, 188]. Based on the above data, the C-7α position on E2 was explored as a possible location for further optimization of the PROTAC. The initial assessment of the C-16 PROTACs also indicated a possible role for benzyl protection at the C-terminus of the penatpeptide; therefore, the C-7 PROTACs contained a benzyl group at the C-terminus of the pentapeptide as well.

Synthesis of C-7 PROTACs handle (free NH_2)

As was the case for the C-16 derivatives the first step in designing C-7α based PROTACs was the synthesis of a short primary amine "handle" attached at the C-7α position on estradiol which will be further extended to produce PROTACs of varying lengths. The procedures that were used to synthesize the C-7α handle were similar to that previously reported [189, 190, 191, 192].

Scheme 3.3 Synthesis of C-7 PROTAC's "handle" (free amine)

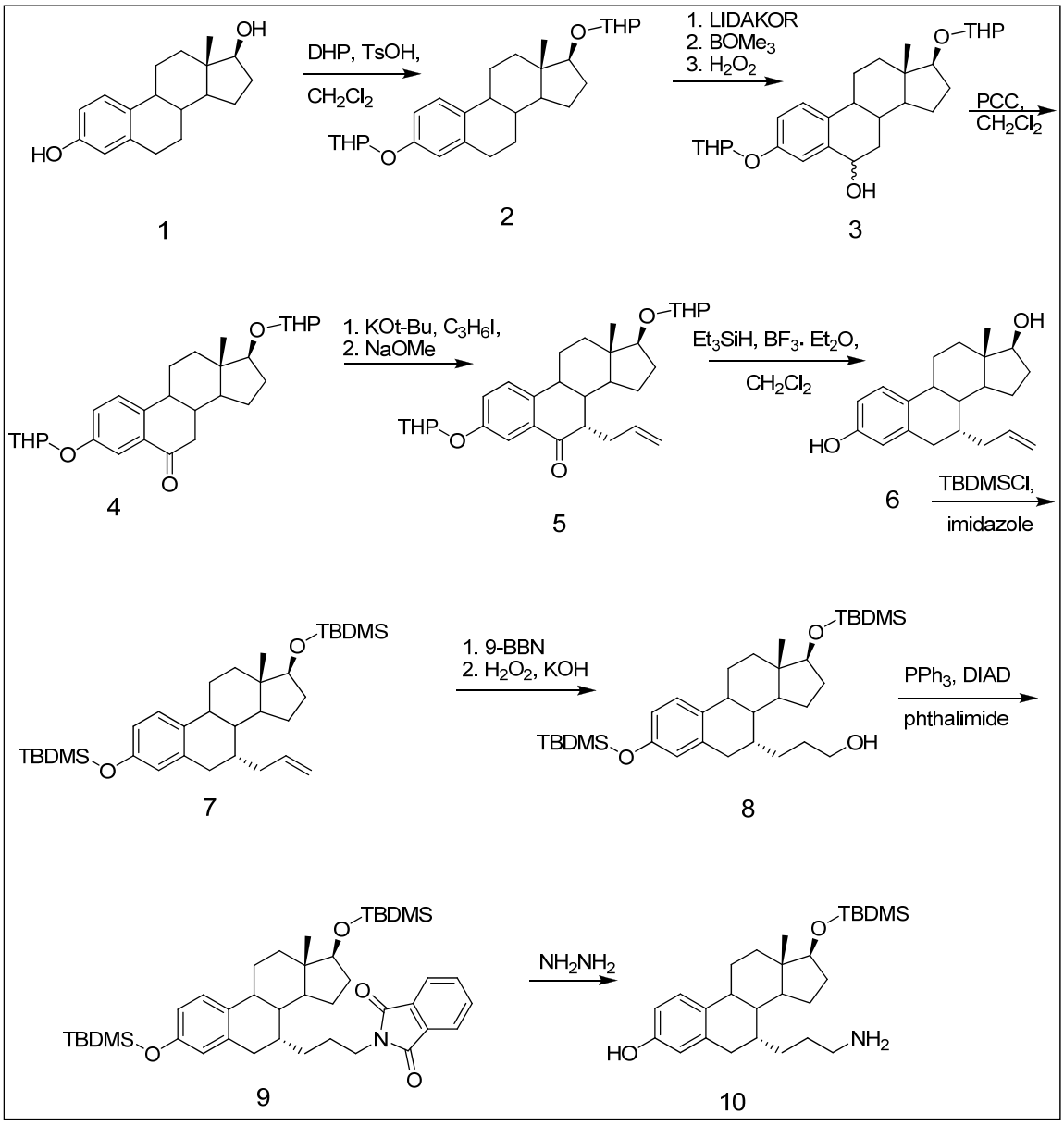

Reaction details and NMR and MS data for the synthesis of C-7 PROTACs free -amine handle

Compound 2: Estradiol, (8.00 g, 29.4 mmol) was dissolved in CH_2Cl_2 (100 ml) and p-toluene sulfonic acid (TsOH), (56 mg, 0.29 mmol) was added, followed by Dihydropyran (DHP) (13.3 ml, 146.8 mmol) The mixture was stirred at room temperature, after 2 hours water was added and product was extracted with ether. Column chromatography was performed to isolate THP protected products as a clear oil (12 g, 94%).

^{1}H NMR ($CDCl_3$, 500 MHz): δ 0.79, 0.81 (2s, 3H), 2.83-2.87 (m, 2H), 3.47-3.52 (m, 1H), 3.57-3.61 (m, 1H), 3.72 (t, J = 8.5 Hz, 1H), 3.89-3.97 (m, 2H), 4.64 - 4.65 (m, 1H), 5.38 - 5.39 (m, 1H), 6.78 (d, J = 2.5 Hz, 1H), 6.84 (dd, J = 8.5, 2.5 Hz, 1H), 7.22 (d, J = 8 Hz, 1H)

Compound 3: To a -78 °C solution of 2.5 M n-butyl lithium (*n*-BuLi) in hexanes, (30 mL, 75.0 mmol) dissolved in THF (50 mL), was added diisopropylamine (10.5 mL, 75.0 mmol), followed by 1 M potassium *t*-butoxide (KO*t*-Bu), (75.0 mL, 75.0 mmol) (a yellow color change was observed with addition of KO*t*-Bu). After 5 min, a solution of **(2),** (4.18 g, 9.49 mmol) dissolved in THF (20 mL) was added resulting in a dark red color reaction mixture which was stirred for 1.5 hours at -78 °C under N_2. The dry ice/acetone bath was replaced with an ice bath and trimethylborate ($B(OCH_3)_3$) (20 mL, 171.0 mmol) was slowly added. The reaction was stirred for an additional 2 hours at 0° C (reaction became turbid upon adition of ($B(OCH_3)_3$)). 35% hydrogen peroxide (H_2O_2) (25 mL) was then added and the reaction was stirred for 1 hour at room temperature, after which time it was cooled to 0 °C, and 10% sodium thiosulfate ($Na_2S_2O_3$) (100 mL) was added. Product was extracted using EtOAc, dried over Na_2SO_4 and solvents were ecaporated. The crude mixture was dissolved in CH_2Cl_2 and flash chromatography was performed (3:1, Hex:EtOAc) to afford the 6-OH compound as a pale yellow foam (2.86 g, 66%).

^{1}H NMR ($CDCl_3$, 500 MHz): δ 0.79, 0.81 (2s, 3H), 3.45-3.49 (m, 1H), 3.56 - 3.59 (m, 1H), 3.68 – 3.73 (m, 1H), 3.87-3.93 (m, 2H), 4.63 - 4.67 (m, 1H), 4.78 – 4.81 (m, 1H),

5.40 - 5.43 (m, 1H), 6.92 (2dd, *J* = 8.5, 2.5 Hz, 1H), 7.17, 7.18 (2d, *J* = 8 Hz, 1H), 7.26 (d, *J* = 2.5 Hz, 1H).

Compound 4: The 6-OH compound, (2.86 g, 6.26 mmol) was dissolved in CH_2Cl_2 (30 mL) and cooled to 0 °C, pyridinium chlorochromate (PCC) (2.7 g, 12.5 mmol) was then added in portions within 15 min. After stirring for 15 min at 0 °C, the mixture was warmed to room temperature and stirred for an additional 2 hours. The reaction was diluted with ether (50 mL) and then filtered through Florisil to remove the chromium salts. The solvent was evaporated and the residue was purified via flash chromatography (3:1, Hex: EtOAc) to yield **(4)** as a white foam (2.28 g, 80%).
^{1}H NMR ($CDCl_3$, 500 MHz): δ 0.81, 0.82 (2s, 3H), 2.73 (dd, J = 16.5, 3.5 Hz, 1H), 3.47 – 3.52 (m, 1H), 3.58 – 3.62 (m, 1H), 3.73, 3.75 (2t, J = 8.5 Hz, 1H), 3.86-3.94 (m, 2H), 4.63 - 4.69 (m, 1H), 5.46 – 5.48 (m, 1H), 7.21 – 7.26 (2dd, *J* = 8.5, 3 Hz, 1H), 7.33, 7.34 (2d, *J* = 8.5 Hz, 1H), 7.71, 7.72 (2d, *J* = 3 Hz, 1H).

Compound 5: The Ketone, **(4),** (1.91 g, 4.20 mmol) was dissolved in THF and cooled to 0° C, then 1M KO*t*-Bu (4.6 ml, 4.60 mmol) was added and mixture was stirred at 0 °C for 30 min and then cooled to -78°C. Allyl iodide (383 μL, 4.60 mmol) was then added (drop-wise) to the solution and after 10 min the reaction was quenched with water and warmed to room temperature. The solvents were removed, redissolved in ether, and then passed through a plug of silica (7-β product). After evaporation of solvents, the residue (7-β product) was dissolved in MeOH (25 mL), and to this was added several small pieces of sodium. The mixture was stirred for an additional 2 hours at room temperature, then quenched with water, the MeOH was evaporated, and the product was extracted from with ether. The solvents were evaporated and the residue was purified by flash chromatography (5:1 Hex:EtOAc) to give **(5)**, the 7-α product as a white foam (272 mg, 13%), recovered **(4)** 896 mg, corrected yield 25%. (7-α product- confirmed by NOESY, diagonistic NOE between H_7 and H_8). This process was repeated two more times with recovered starting material to provide a total (575 mg, overall uncorrected 28%, corrected 36%).

^{1}H NMR ($CDCl_3$, 500 MHz): δ 0.80, 0.82 (2s, 3H), 3.47 – 3.52 (m, 1H), 3.60 – 3.62 (m, 1H), 3.74, 3.77 (2t, *J* = 8.5 Hz, 1H), 3.87-3.94 (m, 2H), 4.63 - 4.69 (m, 1H), 4.92 – 5.00 (m, 1H), 5.45 – 5.48 (m, 1H), 5.74 – 5.82 (m, 1H), 7.22 (2dd, *J* = 8.5, 2.5 Hz, 1H), 7.32, 7.34 (2d, *J* = 8.5 Hz, 1H), 7.69 (d, *J* = 2 Hz, 1H).

Assignment of 7α-sterochemistry to compound ***(5)*** *by NOESY 2D NMR (scanned image).*

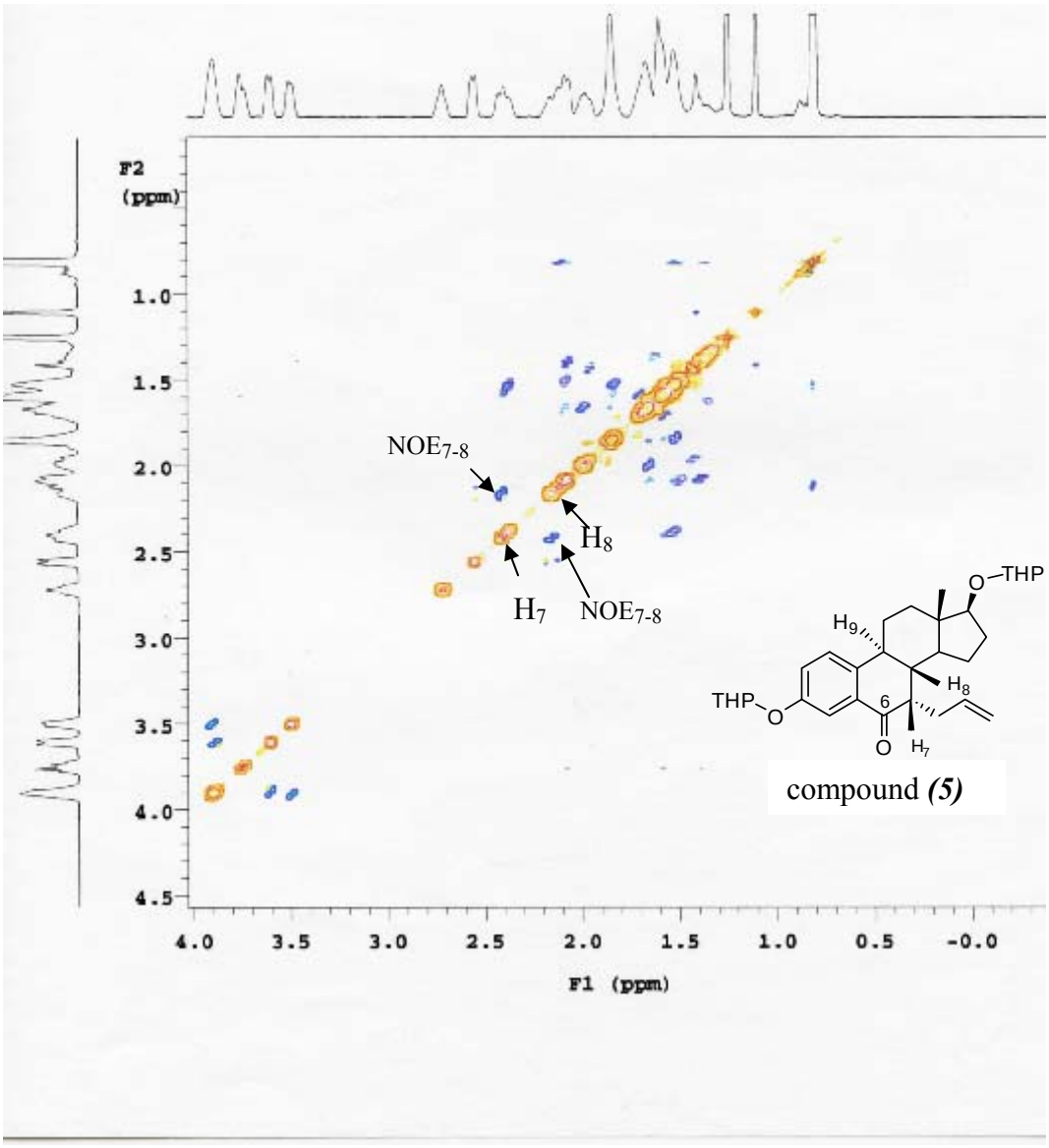

Compound 6: Triethylsilane (Et_3SiH), (4.37 ml) was added to a solution of **(5)** (205 mg, 0.41 mmol) in CH_2Cl_2 and the mixture was cooled to 0 °C. Boron trifluoride diethyletherate ($BF_3.Et_2O$) (15 ml) was added (drop-wise) and the mixture was warmed

to room temp and stirred overnight (greenish-yellow color change). Reaction mixture was then carefully hydrolyzed with 10% K_2CO_3 (72 ml) and filtered through a buccner funnel. The filtrate was extracted with CH_2Cl_2, dried over Na_2SO_4 and flash chromatography was performed (1:1, Hex:EtOAc) to yield a white solid (116 mg, 90%).
^{1}H NMR ($CDCl_3$, 500 MHz): δ 0.79 (s, 3H), 2.72 (d, *J* = 16 Hz, 1H), 2.83 (dd, *J* = 17, 5.5 Hz, 1H), 3.77 (t, *J* = 8.5 Hz, 1H), 4.91 - 5.00 (m, 1H), 5.74 – 5.82 (m, 1H), 6.54 (d, *J* = 3 Hz, 1H), 6.64 (dd, *J* = 8.5, 2.5 Hz, 1H), 7.15 (d, *J* = 8.5 Hz, 1H).

Compound 7: Imidazole, (303 mg, 4.45 mmol) was dissolved in CH_2Cl_2 and DMF (10 ml and 2 mL respectively) and was cooled to 0 °C for about ten mins. TBDMSCl (335 mg, 2.23 mmol) was then added and the mixture was warmed to room temperature. A solution of **(6)**, (116 mg, 0.37 mmol in 3 ml DMF) was added to the mixture and stirred overnight at room temeprature. CH_2Cl_2 and DMF was evaporated and 0.1% K_2CO_3 (30 mL) was added. The crude product was extracted with CH_2Cl_2 and passed through a short column (3:1 Hex:EtOAc) to yield **(7)** as a yellow oil (170 mg, 85%).
^{1}H NMR ($CDCl_3$, 500 MHz): δ 0.03 (s, 3H), 0.04 (s, 3H), 0.18 (s, 6 H), 0.75 (s, 3H), 0.89 (s, 9H), 0.97 (s, 9H), 2.70 (d, *J* = 16 Hz, 1H), 2.83 (dd, *J* = 17, 5.5 Hz, 1H), 3.65 (t, *J* = 8.5 Hz, 1H), 4.88 – 4.98 (m, 1H), 5.74 – 5.82 (m, 1H), 6.52 (d, *J* = 2.5 Hz, 1H), 6.61 (dd, *J* = 8.5, 2.5 Hz, 1H), 7.11 (d, *J* = 8.5 Hz, 1H).

Compound 8: A 0.5 M solution of 9-boro-bicyclononane (9-BBN) in THF (3.14 mL, 1.57 mmol) was added to a solution of steroid **(7)** (170 mg, 0.31 mmol) already dissolved in THF (10 mL). After stirring overnight at room temperature the reaction was cooled to 0 °C and quenched with 3 M potassium hydroxide (KOH), (2 mL), after 5 min 35% H_2O_2 (2 mL) was added and the reaction was stirred for an addidional 3 h. Saturated NaHCO3 was added and the mixture was extracted with CH_2Cl_2. The residue was purified by flash chromatography (5:1 Hex:EtOAc) to provide **(8)** as a viscous oil (116 mg, 66%).
^{1}H NMR ($CDCl_3$, 300 MHz): δ 0.02 (s, 3H), 0.03 (s, 3H), 0.19 (s, 6 H), 0.74 (s, 3H), 0.89 (s, 9H), 0.97 (s, 9H), 2.68 (d, *J* = 16 Hz, 1H), 2.88 (dd, *J* = 16.7, 5.5 Hz, 1H), 3.58 – 3.60

(m, 2H), 3.65 (t, *J* = 8.5 Hz, 1H), 6.53 (d, *J* = 2.5 Hz, 1H), 6.61 (dd, *J* = 8.5, 2.5 Hz, 1H), 7.11 (d, *J* = 8.5 Hz, 1H).

Compound 9: To a cooled solution (0 °C) of triphenyl phosphine (PPh3) (97 mg, 0.415 mmol) and THF (5 mL), was added Diisopropyl azo-dicarboxylate (DIAD) (dropwise) (77 µl, 0.415 mmol). A white precipitate of the ylide was observed, and the reaction was stirred for 40 min at 0 °C. A solution of **(8)**, (116 mg, 0.207 mmol) and phthalimide (58 mg, 0.415 mmol) in THF (2 mL) was then added to the ylide. The reaction was stirred for 1 h at 0 °C and then at room temperature overnight. The solvent was evaporated *in vacuo*, and the residue was purified via flash chromatography (5:1 Hex:EtOAc) to give (9) as a white foam (118 mg, 83%).

^{1}H NMR ($CDCl_3$, 500 MHz): δ 0.03 (s, 3H), 0.04 (s, 3H), 0.18 (s, 6 H), 0.74 (s, 3H), 0.89 (s, 9H), 0.99 (s, 9H), 2.67 (d, *J* = 16.5 Hz, 1H), 2.87 (dd, *J* = 17, 5 Hz, 1H), 3.55 – 3.68 (m, 3H), 6.52 (d, J = 2.5 Hz, 1H), 6.60 (dd, *J* = 8.5, 2.5 Hz, 1H), 7.11 (d, *J* = 8.5 Hz, 1H), 7.69 – 7.72 (m, 2H), 7.81 – 7.83 (m, 2H).

Compound 10: Anhydrous hydrazine (800 μl) was added to a solution of **(9),** (118 mg, 0.171 mmol) dissolved in DME (1.6 mL) and ethanol (1.6 mL). The mixture was refluxed for 2 h, during which time a slightly brown precipitate formed on the sides of the flask and the solution turned slightly green. The reaction was cooled, and 5% NaOH (1.6 mL) was added, dissolving the precipitate. After 30 min, water was added, and the solution was extracted with CH_2Cl_2, dried over Na_2SO_4. The solvent was evaporated in vacuo, and the residue was purified via flash chromatography (95:5, CH_2Cl_2: MeOH) to give 10 as a white foam solid (56.7 mg, 76%). The TBDMS group at the 3-OH position is lost during this reaction.

^{1}H NMR ($CDCl_3$, 500 MHz): δ 0.02 (s, 3H), 0.03 (s, 3H), 0.74 (s, 3H), 0.89 (s, 9H), 2.68 (d, *J* = 16.5 Hz, 1H), 2.88 (dd, *J* = 17, 5 Hz, 1H), 3.65 (t, J = 8.5 Hz, 1H), 6.50 (d, *J* = 2.5 Hz, 1H), 6.59 (dd, *J* = 8.5, 2.5 Hz, 1H), 7.11 (d, *J* = 8.5 Hz, 1H)

Optimization of linker length of C-7 PROTACs

Successful synthesis of the free amine handle at the C-7α position allowed us to vary the linker length via amide bond formation. To this end, we prepared PROTACs with varying linker lengths. In addition, two other PROTACs, one lacking the critical hydroxyl-proline residue (NC) and another attached at the C-terminal of the HIF-1α derived pentapeptide (KC-6), were prepared. The schemes and detailed reaction conditions for the synthesis of C-7 PROTACs are outlined below:

Scheme 3.4 Synthesis of KC-1 (9-atom linker)

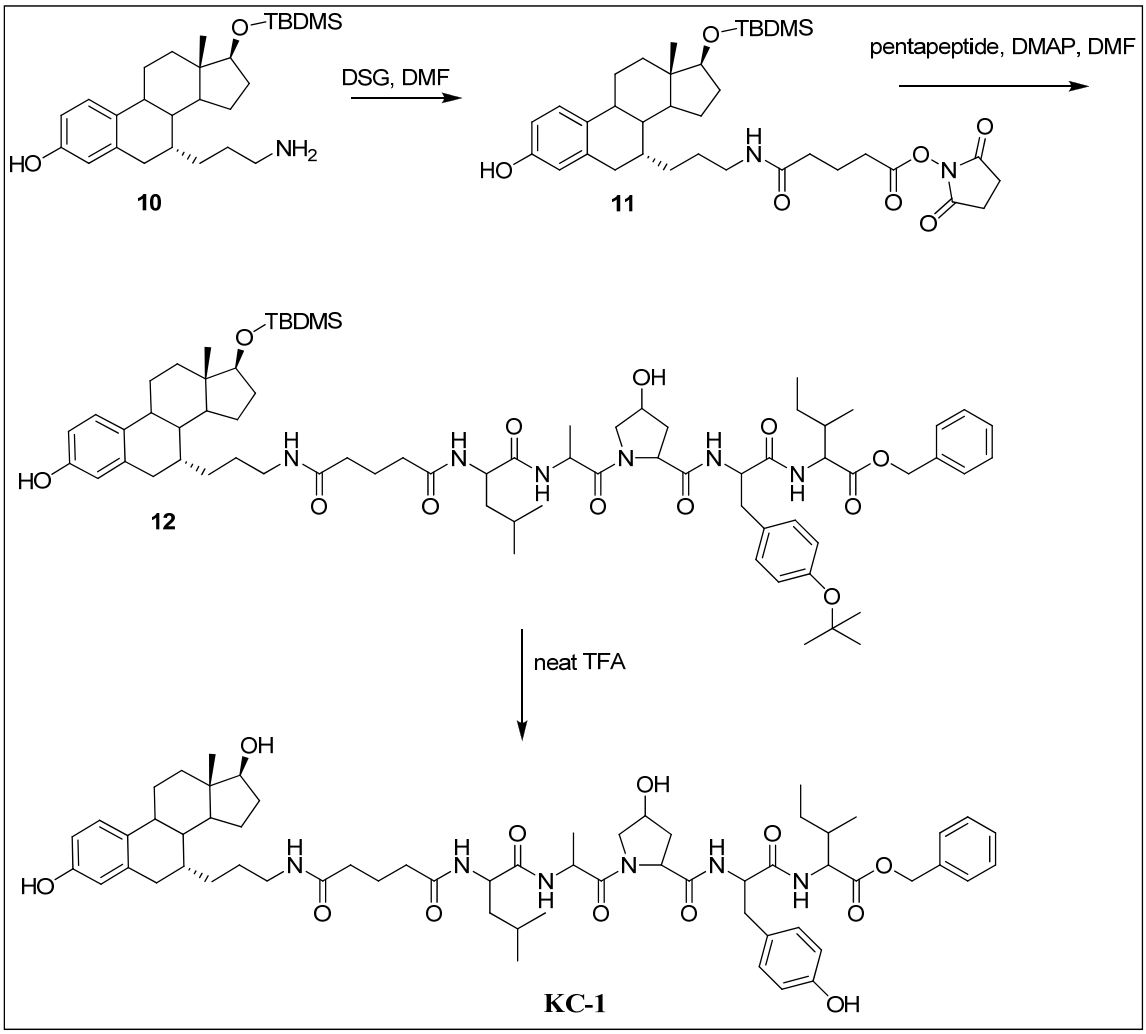

Synthesis of KC-1

Compound 11: Disuccinimidyl gluterate DSG (54 mg, 0.166 mmol) was added to the free amine "handle", **(10),** (37 mg, 0.083 mmol) and dissolved in DMF (2 ml). The mixture was stirred at room temp overnight. DMF was removed via high vacuum and column chromatography was performed (95:5, CH_2Cl_2: MeOH) to give the product as a white solid (25 mg, 46%). For this reaction two products were isolated having similar mobility on TLC. The upper product which was later identified by NMR to be the correct product was reactive while the other product was unreactive in subsequent reactions.
^{1}H NMR ($CDCl_3$, 300 MHz): δ 0.03 (s, 3H), 0.04 (s, 3H), 0.73 (s, 3H), 0.89 (s, 9H), 2.52 (t, *J* = 7 Hz, 2H), 2.63 (d, *J* = 16.5 Hz, 1H), 2.83 (s, 4H), 3.18 – 3.26 (m, 2H), 3.65 (t, *J* = 8.5 Hz, 1H), 5.92 (t, *J* = 5.5 Hz, 1H), 6.50 (d, *J* = 2.5 Hz, 1H), 6.62 (dd, *J* = 8.5, 2.5 Hz, 1H), 7.11 (d, *J* = 8.5 Hz, 1H).

Compound 12: Pentapeptide-1 (24 mg, 0.009 mmol) was added to **(11)**, (34 mg, 0.009 mmol) and then dissolved in DMF (1.5 ml). The reaction was stirred at room temp overnight. Solvent was removed *in vacuo* and column chromatography was performed (95:5 CH_2Cl_2: MeOH) to yield **(12)** as a white solid (34 mg, 70%).
^{1}H NMR ($CDCl_3$, 500 MHz): δ 0.03 (s, 3H), 0.04 (s, 3H), 0.74 (s, 3H), 0.77 – 0.85 (m, 6H), 0.87 – 0.94 (m, 6H), 0.89 (s, 9H), 1.30 (s, 9H), 2.63 (d, *J* = 16 Hz, 1H), 2.77 (s, 1H), 2.83 (dd, *J* = 17, 4.5 Hz, 1H), 2.93 – 3.10 (m, 3H), 3.57 (m, 1H), 3.64 (t, *J* = 8.5 Hz, 1H), 3.75 (d, *J* = 11 Hz, 1H), 4.36 – 4.67 (m, 6H), 5.11 (s, 2H), 6.53 (d, *J* = 2.5 Hz, 1H), 6.62 (dd, *J* = 8.5, 2.5 Hz, 1H), 6.74 (t, *J* = 5.5 Hz, 1H), 6.84 (d, *J* = 8 Hz, 2H), 7.04 (d, *J* = 8.5 Hz, 2H), 7.09 (d, *J* = 8.5 Hz, 1H), 7.16 (d, *J* = 7.5 Hz, 1H), 7.28 – 7.33 (m, 4H), 7.55 (d, *J* = 7.5 Hz, 1H), 7.59 (d, *J* = 7 Hz, 1H).

KC-1: t-Butyl from Tyr-OH and TBDMS protecting group at the O-17 position was simultaneously removed from **(12)**, (34 mg, 0.027 mmol) using neat TFA (2 ml) and stirring at room temperature until starting material disappeared ~30 min. After removal of TFA via high vacuum, column chromatography was performed using (95:5, CH_2Cl_2: MeOH) initially, then MeOH to isolate **KC-1** as a white solid (13.8 mg, 47%).

^{1}H NMR ($CDCl_3$, 500 MHz): δ 0.75 (s, 3H), 0.82 – 0.96 (m, 12H), 2.63 (d, *J* = 17 Hz, 1H), 3.19 (m, 1H), 3.49 (m, 1H), 3.57 (m, 1H), 3.68 (t, *J* = 8.5 Hz, 1H), 4.32 – 4.38 (m, 2H), 4.49 – 4.55 (m, 4H), 5.12 (s, 2H), 6.53 (d, *J* = 2.5 Hz, 1H), 6.62 (dd, *J* = 8.5, 2.5 Hz, 1H), 6.72 (d, *J* = 8.5 Hz, 2H), 7.00 (d, *J* = 8.5 Hz, 2H), 7.08 (d, *J* = 8.5 Hz, 1H), 7.28 (d, *J* = 8 Hz, 1H), 7.31 – 7.34 (m, 4H), 7.51 (d, *J* = 7 Hz, 1H), 7.71 (2d, *J* = 7 Hz, 2H). MS (MALDI, DHB) *m/z* 1130 ($M+Na^+$, calcd for $C_{62}H_{86}N_6O_{12}$ requires 1129.63)

Figure 3.6: Mass spectrum for KC-1

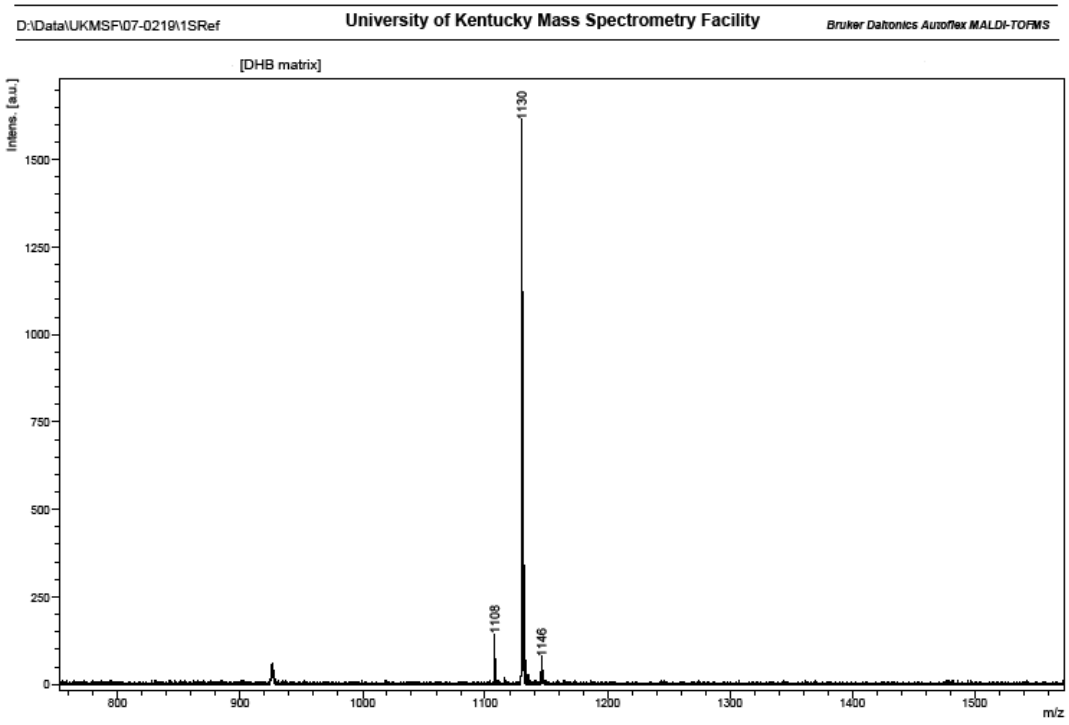

Scheme 3.5 Synthesis of KC-2 (12 atom linker)

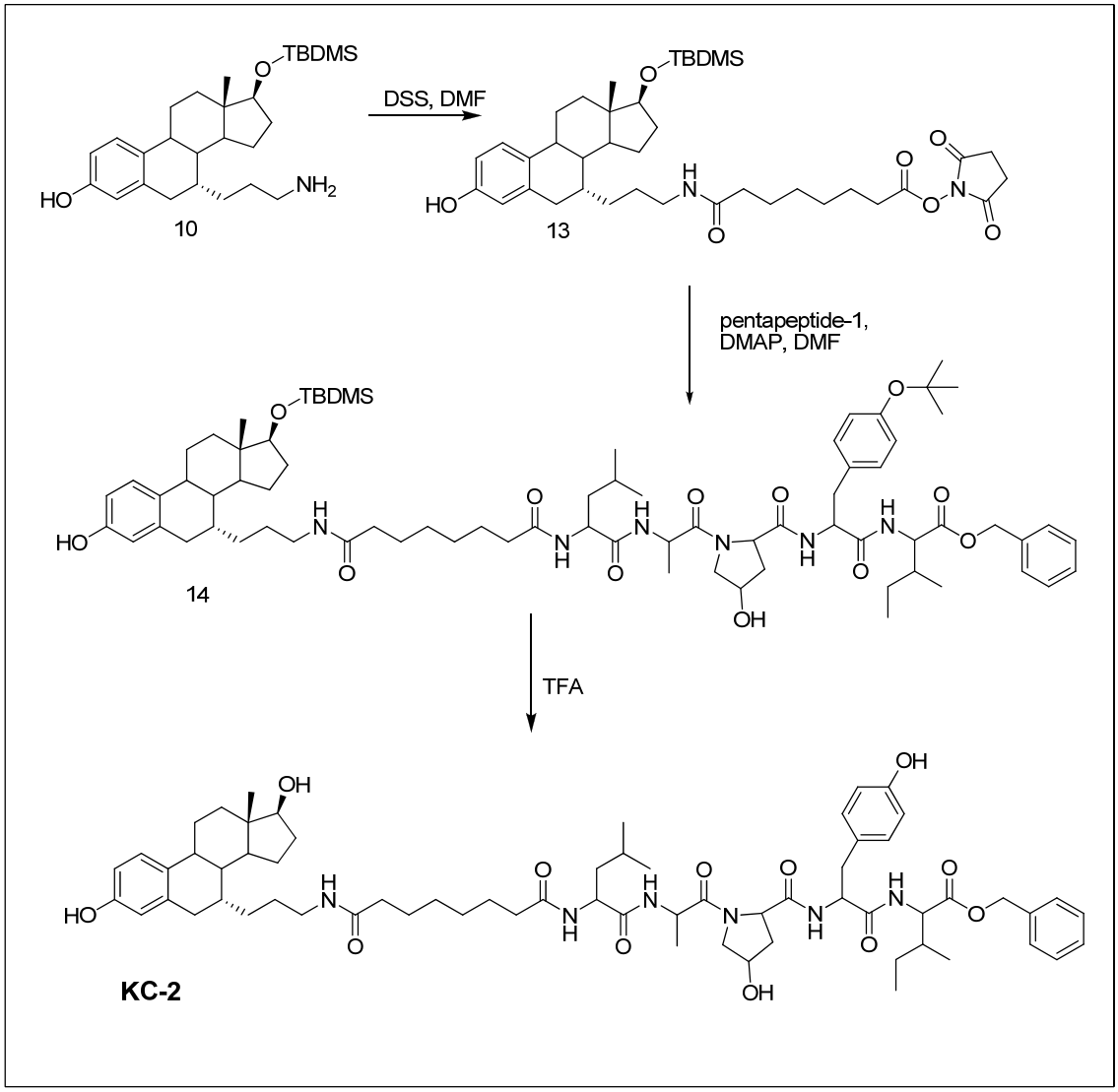

Synthesis of KC-2

Compound 13: Disuccinimidyl suberate (DSS), (12 mg, 0.033 mmol), was added to free amine "handle", **(10)**, (14.6 mg, 0.033 mmol) and dissolved then dissolved in DMF (1ml). The mixture was stirred at room temp overnight. DMF was removed via high vacuum and column was performed (95:5 CH_2Cl_2: MeOH) to give a white solid (5.7 mg, 25%). For this reaction two products were isolated having similar mobility on TLC. The

upper product which was later identified by NMR to be the correct product was reactive while the other isomer was unreactive in subsequent reactions.

^{1}H NMR ($CDCl_3$, 500 MHz): δ 0.03 (s, 3H), 0.04 (s, 3H), 0.73 (s, 3H), 0.89 (s, 9H), 2.12 (t, *J* = 7.5 Hz, 2H), 2.58 (t, *J* = 7.5 Hz, 2H), 2.65 (d, *J* = 16.5 Hz, 1H), 2.82 – 2.87 (m, 5H), 3.08 – 3.12 (m, 1H), 3.24 – 3.29 (m, 1H), 3.65 (t, *J* = 8.5 Hz, 1H), 5.76 (t, *J* = 5.5 Hz, 1H), 6.53 (d, *J* = 2.5 Hz, 1H), 6.61 (s, 1H), 6.64 (dd, *J* = 8.5, 2.5 Hz, 1H), 7.11 (d, *J* = 8.5 Hz, 1H).

Compound 14: Pentapeptide-1, (6 mg, 0.008 mmol) was added to **(13),** (5.7 mg, 0.008 mmol) and dissolved in DMF (1.5 ml). The reaction was stirred at room temp overnight. Solvent was removed *in vacuo* and column chromatography was performed using (95:5 CH_2Cl_2: MeOH) to yield **(14)** as a white solid (6.6 mg, 66%)

^{1}H NMR ($CDCl_3$, 500 MHz): δ 0.03 (s, 3H), 0.04 (s, 3H), 0.74 (s, 3H), 0.79 – 0.85 (m, 6H), 0.87 – 0.95 (m, 6H), 0.89 (s, 9H), 1.13 – 1.33 (m, 13H), 1.31 (s, 9H), 2.63 (d, *J* = 16.5 Hz, 1H), 2.83 (dd, *J* = 16.5, 4.5 Hz, 1H), 2.97 – 3.10 (m, 3H), 3.23 – 3.27 (m, 1H), 3.56 (dd, *J* = 11.1, 3.9 Hz, 1H), 3.64 (t, *J* = 8.5 Hz, 1H), 3.75 (d, *J* = 11 Hz, 1H), 4.47 – 4.62 (m, 6H), 5.11 (2s, 2H), 6.53 (d, *J* = 2.5 Hz, 1H), 6.62 (dd, *J* = 8.5, 2.5 Hz, 1H), 6.66 (d, *J* = 8 Hz, 1H), 6.84 (d, *J* = 8.5 Hz, 2H), 7.05 (d, *J* = 8.5 Hz, 2H), 7.08 (d, *J* = 8.5 Hz, 1H), 7.30 – 7.37 (m, 4H), 7.51 (d, *J* = 7 Hz, 1H).

KC-2: Trifluoroacetic acid (TFA) was used to remove both protecting groups (TBDMS and t-Bu). Neat TFA was added to **(14)**, (6.6 mg, 0.005 mmol), and the mixture was stirred at room temperature until starting material disappeared, (45 min) observed on TLC. Column chromatography was performed using (95:5, CH_2Cl_2: MeOH) initially, then column was flushed with MeOH to isolate **KC-2** as a white solid (2.5 mg, 42%).

^{1}H NMR ($CDCl_3$, 300 MHz): δ 0.74 (s, 3H), 0.79 – 0.85 (m, 6H), 0.87 – 0.95 (m, 6H), 2.63 (d, *J* = 16.5 Hz, 1H), 2.83 (dd, *J* = 16.5, 4.5 Hz, 1H), 2.97 – 3.10 (m, 3H), 3.23 – 3.27 (m, 1H), 3.53 (dd, *J* = 11.1, 3.9 Hz, 1H), 3.64 (t, *J* = 8.5 Hz, 1H), 3.75 (d, *J* = 11 Hz, 1H), 4.36 – 4.54 (m, 6H), 5.14 (s , 2H), 6.53 (d, *J* = 2.5 Hz, 1H), 6.62 (dd, *J* = 8.5, 2.5 Hz, 1H), 6.74 (d, *J* = 8 Hz, 1H), 7.02 (d, *J* = 8.5 Hz, 2H), 7.12 (d, *J* = 8.5 Hz, 1H), 7.25

(d, J = 8 Hz, 1H), 7.38 (s, 4H), 7.48 (d, J = 7.5 Hz, 1H), 7.54 (d, J = 7 Hz, 1H). MS (MALDI, DHB) *m/z* 1172 ($M+Na^+$, calcd for $C_{65}H_{92}N_6O_{12}$ requires 1171.68)

Figure 3.7: Mass spectrum for KC-2

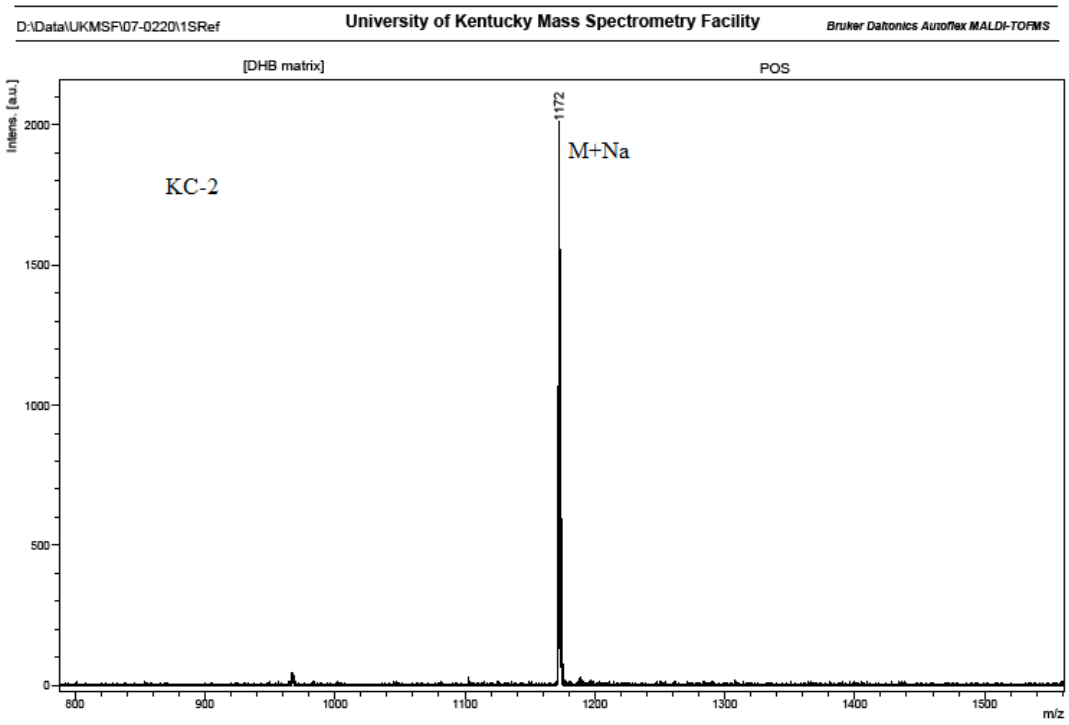

Scheme 3.6 Synthesis of KC-3 (16 atom linker)

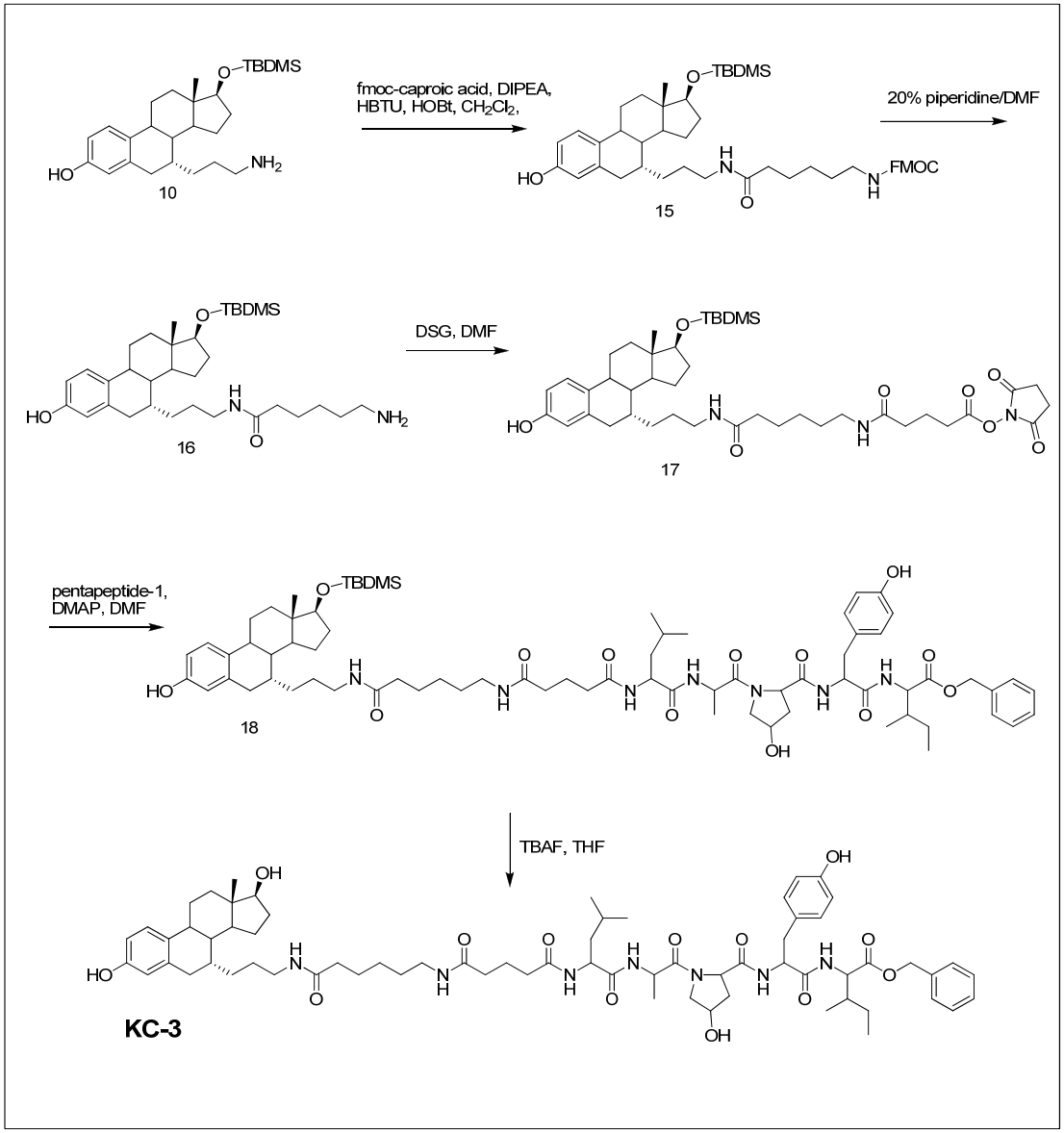

Synthesis of KC-3

Compound 15: Fmoc-6-aminohexanoic acid (6-Ahx-OH/caproic acid) (13.4 mg, 0.038 mmol) was added to free amine "handle" **(10),** (17 mg, 0.038 mmol) and dissolved in CH_2Cl_2. HBTU (21.6 mg, 0.057 mmol) and HoBt (8.73 mg, 0.057 mmol) was added to the mixture followed by DIPEA (2 drops) The mixture was stirred at room temp until all

free amine was coupled (15 min-1.5 hr). Column chromatography was performed (99:1 CH_2Cl_2: MeOH) yielding a white foamy solid (27 mg, 91%). A small amount of di-coupled product was isolated as well (5%). In some coupling reactions EDC was used as a coupling agent instead of HBTU providing cleaner reaction (only mono-coupled) product, but lower yields.

^{1}H NMR ($CDCl_3$, 500 MHz): δ 0.02 (s, 3H), 0.03 (s, 3H), 0.73 (s, 3H), 0.89 (s, 9H), 2.62 (d, *J* = 16.5 Hz, 1H), 2.85 (dd, *J* = 16.5, 4.7 Hz 1H), 3.04 – 3.10 (m, 1H), 3.14 (q, *J* = 6.5 Hz, 2H), 3.29 – 3.34 (m, 1H), 3.64 (t, *J* = 8.3 Hz, 1H), 4.21 (t, *J* = 7 Hz, 1H), 4.41 (d, *J* = 7 Hz, 2H), 4.97 (t, *J* = 6 Hz, 1H), 5.47 (t, *J* = 6 Hz, 1H), 6.53 (d, *J* = 2.5 Hz, 1H), 6.62 (dd, *J* = 8.5, 2.5 Hz, 1H), 7.10 (d, *J* = 8.5 Hz, 1H), 7.30 – 7.33 (td, *J* = 7.5, 1.2 Hz, 2H), 7.40 (t, *J* = 7.5 Hz, 2H), 7.59 (d, *J* = 7.5 Hz, 2H), 7.76 (d, *J* = 7.5 Hz, 2H).

Compound 16: Fmoc-group from **(15)** was removed using 20% piperidine in DMF (2 ml) for 10 minutes. Following removal of solvents *in vacuo*, flash column chromatography was performed using (CH_2Cl_2: MeOH 95:5) initially to remove by products and finally flushing with MeOH to isolate **(16)** as white solid (14 mg, 73%).

^{1}H NMR ($CDCl_3$, 300 MHz): δ 0.03 (s, 3H), 0.04 (s, 3H), 0.74 (s, 3H), 0.89 (s, 9H), 2.60 (d, *J* = 16.5 Hz, 1H), 2.87 (dd, *J* = 16.5, 4.7 Hz 1H), 3.36 – 3.48 (m, 4H), 3.65 (t, *J* = 8 Hz, 1H), 5.50 (t, *J* = 5.4 Hz, 1H), 6.49 (d, *J* = 2.5 Hz, 1H), 6.62 (dd, *J* = 8.5, 2.5 Hz, 1H), 7.11 (d, *J* = 8.5 Hz, 1H).

Compound 17: DSG (16.4 mg, 0.050 mmol) was added to **(16),** (14 mg, 0.025 mmol) and dissolved in DMF (1.5 ml). The mixture was stirred at room temp for 15 min. DMF was removed via high vacuum and column chromatography was performed using (99:1 CH_2Cl_2: MeOH) to remove excess DSG and then (95:5 CH_2Cl_2: MeOH) to give **(17)** as a white solid (7 mg, 37%).

^{1}H NMR ($CDCl_3$, 500 MHz): δ 0.03 (s, 3H), 0.04 (s, 3H), 0.74 (s, 3H), 0.89 (s, 9H), 2.60 (d, *J* = 16.5 Hz, 1H), 2.31 (t, *J* = 7 Hz, 2H), 2.67 (t, *J* = 7 Hz, 2H), 2.87 (s, 4H), 3.00 – 3.05 (m, 1H), 3.18 – 3.24 (m, 2H), 3.31 – 3.35 (m, 1H), 3.65 (t, *J* = 8 Hz, 1H), 5.69 (t, *J* = 5.5 Hz, 1H), 6.39 (t, *J* = 5.5 Hz, 1H), 6.56 (d, *J* = 2.5 Hz, 1H), 6.64 (dd, *J* = 8.5, 2.5 Hz, 1H), 7.11 (d, *J* = 8.5 Hz, 1H).

Compound 18: Pentapeptide-1 (10 mg, 0.013 mmol) was added to **(17)** (7 mg, 0.009 mmol) with catalytic amount of DMAP and then dissolved in DMF (1.5 ml). The reaction was stirred at room temp overnight. Solvent was removed *in vacuo* and column chromatography was performed (95:5 CH_2Cl_2: MeOH) to yield **(18)** as a white solid (9 mg, 74%)

^{1}H NMR (DMSO, 500 MHz): δ 0.03 (s, 3H), 0.04 (s, 3H), 0.69 (s, 3H), 0.79 - 0.86 (m, 12H), 0.87 (s, 9H), 1.25 (s, 9H), 2.58 (d, *J* = 16.5 Hz, 1H), 3.66 (t, *J* = 8 Hz, 1H), 4.22 – 4.33 (m, 4H), 4.42 (t, *J* = 6.7 Hz, 1H), 4.47 – 4.51 (m, 1H), 5.11 (s, 2H), 6.42 (d, *J* = 2.5 Hz, 1H), 6.51 (dd, *J* = 8.5, 2.5 Hz, 1H), 6.82 (d, J = 8.5 Hz, 2H), 7.05 (d, *J* = 8.5 Hz, 1H), 7.11 (d, *J* = 8.5 Hz, 2H), 7.36 – 7.37 (m, 4H), 7.71 (t, *J* = 5.5 Hz, 1H), 7.74 (t, *J* = 5.5 Hz, 1H), 7.82 (d, *J* = 8 Hz, 1H), 7.92 (d, J = 8 Hz, 1H), 8.03 (t, *J* = 7 Hz, 1H).

KC-3: (18), (9 mg, 0.005 mmol) was dissolved in THF (0.5 ml) and TBAF in THF (0.5 ml) was added to remove TBDMS protecting group from O-17 position. Mixture was stirred at room temperature until starting material disappeared (48 hrs). Column chromatography was performed using (CH_2Cl_2: MeOH 95:5) initially, then column was flushed with MeOH to isolate **KC-3** as a white solid (2.8 mg, 34%). In subsequent reactions the OH on tyrosine was protected and TFA was used to remove both protecting groups (TBDMS and t-Bu).

^{1}H NMR (DMSO, 500 MHz): δ 0.65 (s, 3H), 0.79 - 0.86 (m, 13H), 2.56 (d, *J* = 16.5 Hz, 1H), 2.75 (dd, *J* = 16.5, 4.5 Hz, 1H), 3.50 – 3.54 (m, 2H), 4.20 – 4.24 (m, 2H), 4.28 – 4.33 (m, 2H), 4.40 – 4.43 (m, 2H), 4.50 – 4.51 (m, 1H), 5.10 (s, 2H), 6.41 (d, *J* = 2.5 Hz, 1H), 6.49 (dd, *J* = 8.5, 2.5 Hz, 1H), 6.61 (d, *J* = 8.5 Hz, 2H), 6.98 (d, *J* = 8 Hz, 2H), 7.04 (d, *J* = 8.5 Hz, 1H), 7.36 (s, 4H), 7.71 (t, *J* = 5.5 Hz, 1H), 7.74 (t, J = 5.5 Hz, 1H), 7.77 (d, *J* = 8.5 Hz, 1H), 7.91 (d, J = 8 Hz, 1H), 8.00 (d, J = 8 Hz, 1H), 8.02 (d, *J* = 7 Hz, 1H).
MS (MALDI, CHCA) *m/z* 1243 ($M+Na^+$, calcd for $C_{68}H_{97}N_7O_{13}$ requires 1242.71)

Figure 3.8: Mass spectrum for KC-3

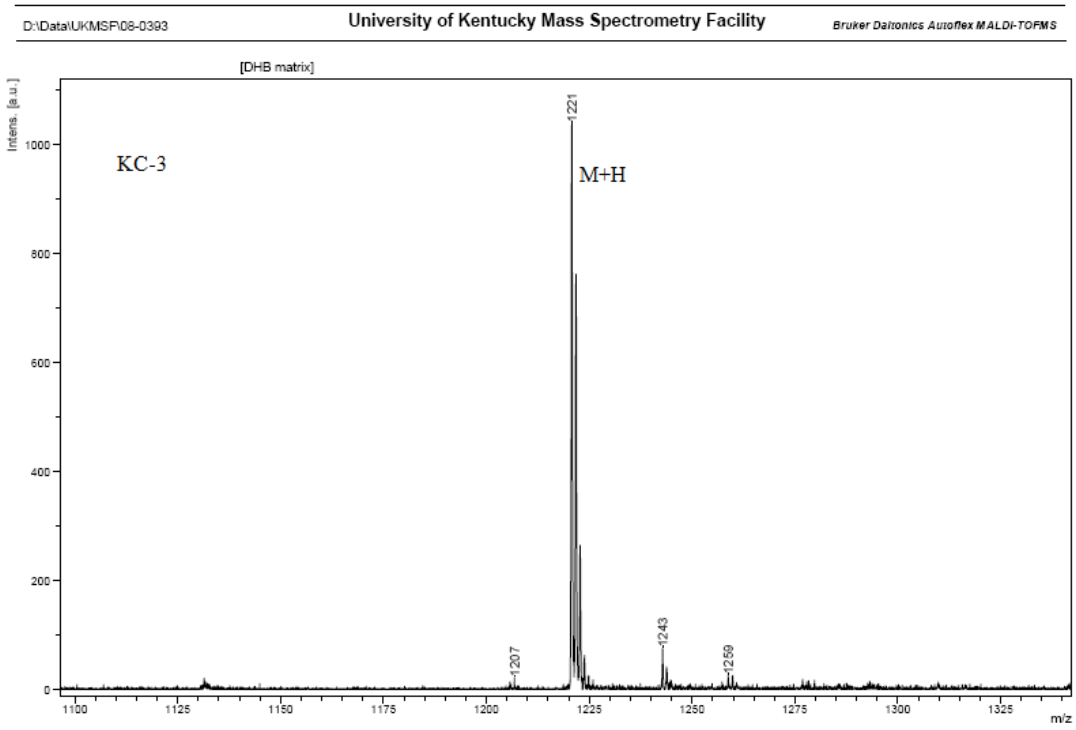

Scheme 3.7 Synthesis of KC-4 (19 atom linker)

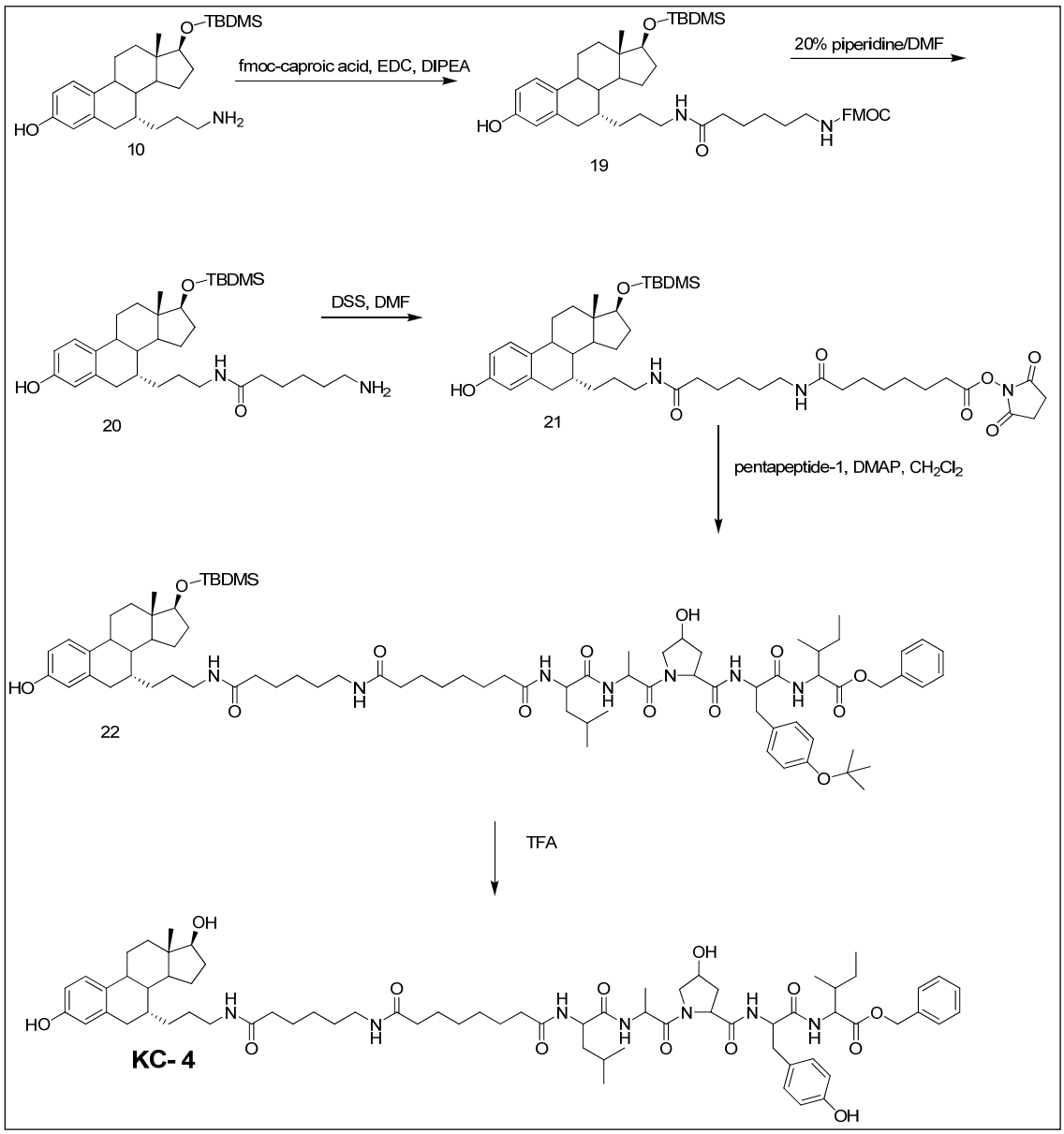

Synthesis of KC-4

Compound 19: Fmoc-6-aminohexanoic acid (6-Ahx-OH/caproic acid) (37 mg, 0.104 mmol) was added to the free amine "handle" **(10),** (46 mg, 0.104 mmol) and then dissolved in CH_2Cl_2. EDC, (28 mg, 0.156 mmol) was added to the mixture followed by DIPEA (2 drops). The mixture was stirred at room temp until all the free amine was

coupled (15 min-1.5 hr) monitored by TLC. Column chromatography was performed using (99:1, CH_2Cl_2: MeOH) to yield a white foamy solid (61 mg, 75%).
^{1}H NMR ($CDCl_3$, 500 MHz): δ 0.02 (s, 3H), 0.03 (s, 3H), 0.73 (s, 3H), 0.89 (s, 9H), 2.62 (d, *J* = 16.5 Hz, 1H), 2.85 (dd, J = 16.5, 4.7 Hz 1H), 3.04 – 3.10 (m, 1H), 3.14 (q, J = 6.5 Hz, 2H), 3.29 – 3.34 (m, 1H), 3.64 (t, J = 8.3 Hz, 1H), 4.21 (t, *J* = 7 Hz, 1H), 4.41 (d, *J* = 7 Hz, 2H), 4.97 (t, J = 6 Hz, 1H), 5.47 (t, J = 6 Hz, 1H), 6.53 (d, *J* = 2.5 Hz, 1H), 6.62 (dd, J = 8.5, 2.5 Hz, 1H), 7.10 (d, *J* = 8.5 Hz, 1H), 7.30 – 7.33 (td, *J* = 7.5, 1.2 Hz, 2H), 7.40 (t, J = 7.5 Hz, 2H), 7.59 (d, J = 7.5 Hz, 2H), 7.76 (d, J = 7.5 Hz, 2H).

Compound 20: Fmoc from (**19)** was deprotected using 20% piperidine in DMF (3.5 ml) for 15 minutes at room temp. Following removal of solvents *in vacuo* flash column chromatography was performed using (95:5, CH_2Cl_2: MeOH) initially to remove by-products and finally flushing with MeOH to isolate (**20)** as a white solid (39.5 mg, 91%).
^{1}H NMR ($CDCl_3$, 300 MHz): δ 0.03 (s, 3H), 0.04 (s, 3H), 0.74 (s, 3H), 0.89 (s, 9H), 2.60 (d, *J* = 16.5 Hz, 1H), 2.87 (dd, J = 16.5, 4.7 Hz 1H), 3.36 – 3.48 (m, 4H), 3.65 (t, J = 8 Hz, 1H), 5.50 (t, J = 5.4 Hz, 1H), 6.49 (d, J = 2.5 Hz, 1H), 6.62 (dd, J = 8.5, 2.5 Hz, 1H), 7.11 (d, *J* = 8.5 Hz, 1H).

Compound 21: DSS (52 mg, 0.142 mmol) was added to **(20)** (39.5 mg, 0.071 mmol) and dissolved in DMF (1.5 ml). The mixture was stirred at room temp overnight. DMF was removed via high vacuum and column was performed (99:1 CH_2Cl_2: MeOH) to give **(21)** as a white solid (17.6 mg, 31%). Coupling confirmed by negative Kaiser test.

Compound 22: Pentapeptide-1 (16 mg, 0.022 mmol) was added to **(21),** (17.6 mg, 0.022 mmol) with catalytic amount of DMAP and dissolved in CH_2Cl_2 (1.5 ml). The reaction was stirred at room temp overnight. Solvent was removed under reduced pressure and column chromatography was performed (95:5, CH_2Cl_2: MeOH) to yield **(22)** as a white solid (19 mg, 61%)
^{1}H NMR (500 MHz): δ 0.03 (s, 3H), 0.04 (s, 3H), 0.74 (s, 3H), 0.80 - 0.95 (m, 12H), 0.89 (s, 9H), 1.31 (s, 9H), 2.63 (d, J = 16.8 Hz, 1H), 2.85 (dd, J = 16.8, 4.2, 1H), 3.06 (d, J = 7.2 Hz, 3H), 3.13 – 3.27 (m, 4H), 3.55 (dd, J = 11.1, 3.6 Hz, 1H), 3.65 (t, J = 8 Hz,

1H), 4.40 – 4.43 (m, 2H), 4.48 – 4.56 (m, 4H), 4.47 – 4.51 (m, 1H), 5.12, (s, 2H), 6.35 (t, J = 5.7 Hz, 1H), 6.53 (d, *J* = 2.4 Hz, 1H), 6.63 (dd, J = 8.4, 2.4 Hz, 2H), 6.68 (t, J = 5.8 Hz, 1H), 6.86 (d, J = 8.4 Hz, 2H), 6.92 (d, J = 5 Hz, 1H), 6.95 (d, J = 5.7 Hz, 1H), 7.09 (d, J = 8.4 Hz, 1H), 7.10 (d, J = 8.4 Hz, 1H), 7.34 (s, 4H).

KC-4: TBDMS and t-Bu protecting groups were removed simultaneously by adding neat TFA (1ml) to **(22),** (19 mg, 0.013 mmol) and stirring at room temperature until all starting material disappeared (30 mim). TFA was removed *in vacuo* and column chromatography was performed using (95:5 CH_2Cl_2: MeOH) to isolate **KC-4** as a white solid (3.6 mg, 22%). MS (MALDI, SA) *m/z* 1262.8 (M+H, calcd for $C_{71}H_{103}N_7O_{13}$ requires 1261.76)

Figure 3.9: Mass spectrum for KC-4

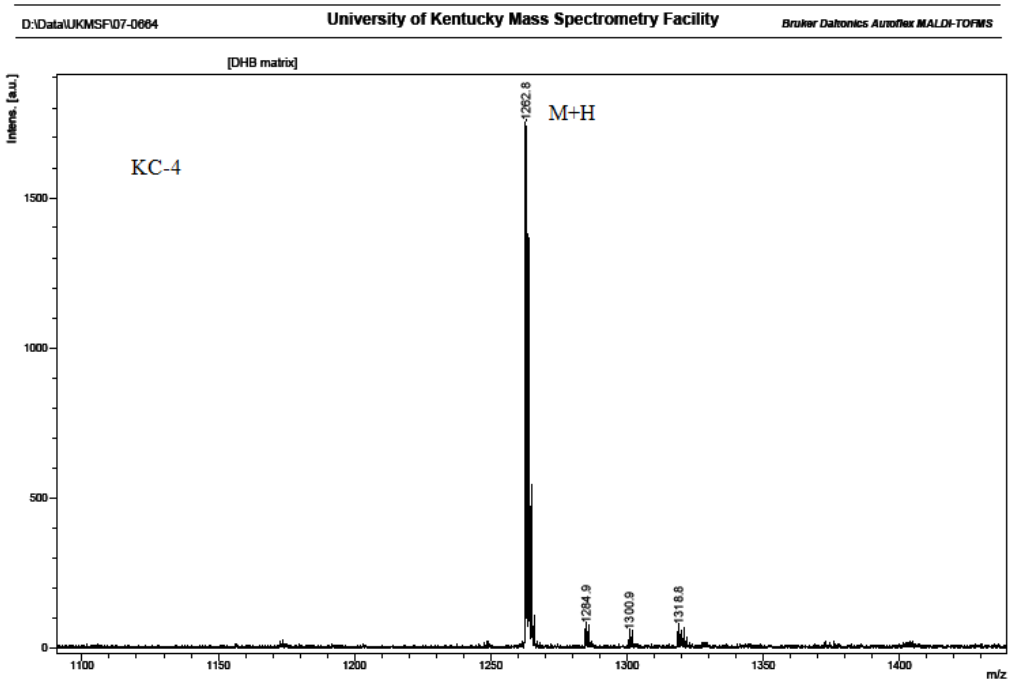

Scheme 3.8 Synthesis of KC-5 (21 atom linker)

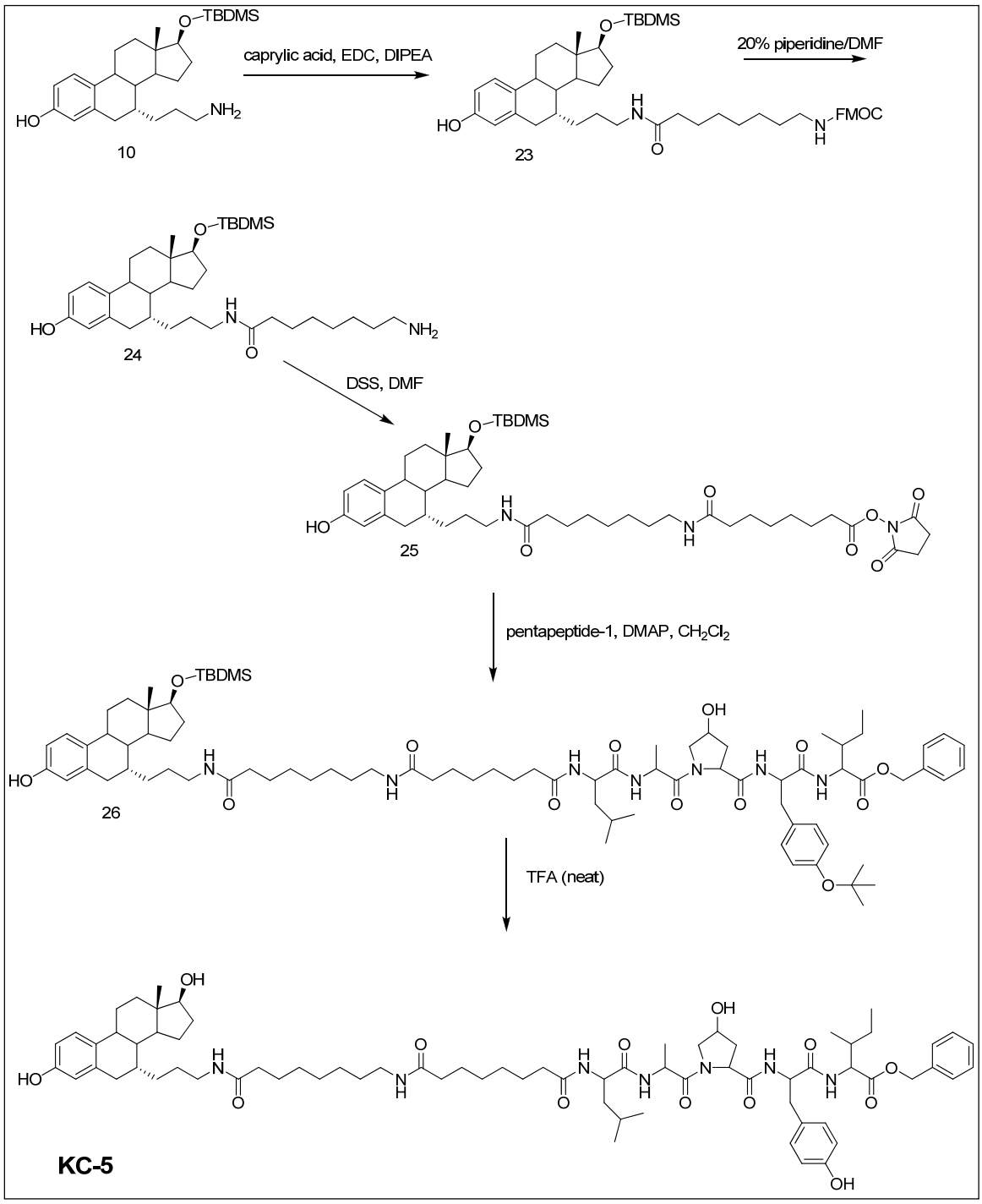

Synthesis of KC-5

Compound 23: Fmoc-caprylic acid (18 mg, 0.047 mmol) was added to the free amine "handle" **(10),** (21 mg, 0.047 mmol) already dissolved in CH_2Cl_2. EDC (13.5 mg, 0.070 mmol) was added to the mixture followed by DIPEA (2 drops) and mixture was stirred at room temp until all free amine was coupled (15 min-1.5 hr) monitored by TLC. Column chromatography was performed, (99:1, CH_2Cl_2: MeOH) yielding a white foamy solid (32 mg, 84%).

^{1}H NMR ($CDCl_3$, 500 MHz): δ 0.03 (s, 3H), 0.04 (s, 3H), 0.73 (s, 3H), 0.89 (s, 9H), 2.60 (d, *J* = 17 Hz, 1H), 2.85 (dd, J = 16.5, 4.7 Hz 1H), 3.04 – 3.10 (m, 1H), 3.12 (q, J = 7.4 Hz, 2H), 3.64 (t, J = 8.3 Hz, 1H), 4.17 (t, J = 7 Hz, 1H), 4.34 (d, J = 7 Hz, 2H), 5.00 (t, J = 6 Hz, 1H), 5.82 (t, J = 6 Hz, 1H), 6.51 (d, J = 2.5 Hz, 1H), 6.62 (dd, J = 8.5, 2.5 Hz, 1H), 7.06 (d, *J* = 8.5 Hz, 1H), 7.30 – 7.31 (td, J = 7.5, 1.0 Hz, 2H), 7.39 (t, J = 7.5 Hz, 2H), 7.56 (d, J = 7.5 Hz, 2H), 7.72 (d, J = 7.5 Hz, 2H).

Compound 24: Fmoc group from **(23),** (32 mg, 0.040 mmol) was removed using 20% piperidine in DMF (2ml) for 10 minutes at room temperature. Following removal of solvents *in vacuo* flash column chromatography was performed using (CH_2Cl_2: MeOH 95:5) initially to remove by-products and finally flushing with MeOH to isolate **(24)** as white solid (13 mg, 56%). Deprotection confirmed by Kaiser test.

Compound 25: DSS (42 mg, 0.111 mmol) was added to **(24)** (13 mg, 0.022 mmol) and the reagents were dissolved in DMF (2.5 ml) the mixture was stirred at room temp overnight. DMF was removed via high vacuum and column was performed (99:1 CH_2Cl_2: MeOH) to give **(25)** as a white solid (5.8 mg, 31%).

^{1}H NMR ($CDCl_3$, 300 MHz): δ 0.03 (s, 3H), 0.04 (s, 3H), 0.73 (s, 3H), 0.89 (s, 9H), 2.60 (t, *J* = 7.2 Hz, 1H), 2.84 (s, 2H), 3.21 – 3.28 (m, 2H), 3.64 (t, J = 8.3 Hz, 1H), 5.61(t, J = 5.7 Hz, 1H), 5.87 (t, J = 5.7 Hz, 1H), 6.55 (d, J = 2.5 Hz, 1H), 6.66 (dd, J = 8.5, 2.5 Hz, 1H), 7.11 (d, *J* = 8.5 Hz, 1H).

Compound 26: Pentapeptide-1 (5.2 mg, 0.007 mmol) was added to **(25)**, (5.8 mg, 0.007 mmol) with catalytic amount of DMAP and dissolved in CH_2Cl_2 (3 ml). The reaction was stirred at room temp overnight. Solvent was removed under reduced pressure and column chromatography was performed (95:5 CH_2Cl_2: MeOH) to yield **(26)** as a white solid (4.8 mg, 48%)

^{1}H NMR (500 MHz): δ 0.03 (s, 3H), 0.04 (s, 3H), 0.74 (s, 3H), 0.80 - 0.95 (m, 12H), 0.89 (s, 9H), 1.31 (s, 9H), 2.63 (d, J = 16.8 Hz, 1H), 2.85 (dd, J = 16.8, 4.2, 1H), 3.06 (d, J = 7.2 Hz, 3H), 3.13 – 3.27 (m, 4H), 3.55 (dd, J = 11.1, 3.6 Hz, 1H), 3.65 (t, J = 8 Hz, 1H), 4.40 – 4.43 (m, 2H), 4.48 – 4.56 (m, 4H), 4.47 – 4.51 (m, 1H), 5.13 (s, 2H), 6.35 (t, J = 5.7 Hz, 1H), 6.53 (d, *J* = 2.4 Hz, 1H), 6.63 (dd, J = 8.4, 2.4 Hz, 2H), 6.68 (t, J = 5.8 Hz, 1H), 6.86 (d, J = 8.4 Hz, 2H), 6.92 (d, J = 5 Hz, 1H), 6.95 (d, J = 5.7 Hz, 1H), 7.09 (d, J = 8.4 Hz, 1H), 7.10 (d, J = 8.4 Hz, 1H), 7.34 (s, 4H).

KC-5: TBDMS and t-Bu protecting groups were removed simultaneously by adding neat TFA (1ml) to 26 (4.8 mg, 0.003 mmol) and stirring at room temperature until all starting material disappeared (30 mim). TFA was removed *in vacuo* and column chromatography was performed (CH_2Cl_2: MeOH 95:5) to isolate **KC-5** as a white solid (0.8 mg, 19%). MS (MALDI, SA) *m/z* 1312 ($M+Na^+$, calcd for $C_{73}H_{107}N_7O_{13}$ requires 1312.79)

Figure 3.10: Mass spectrum for KC-5

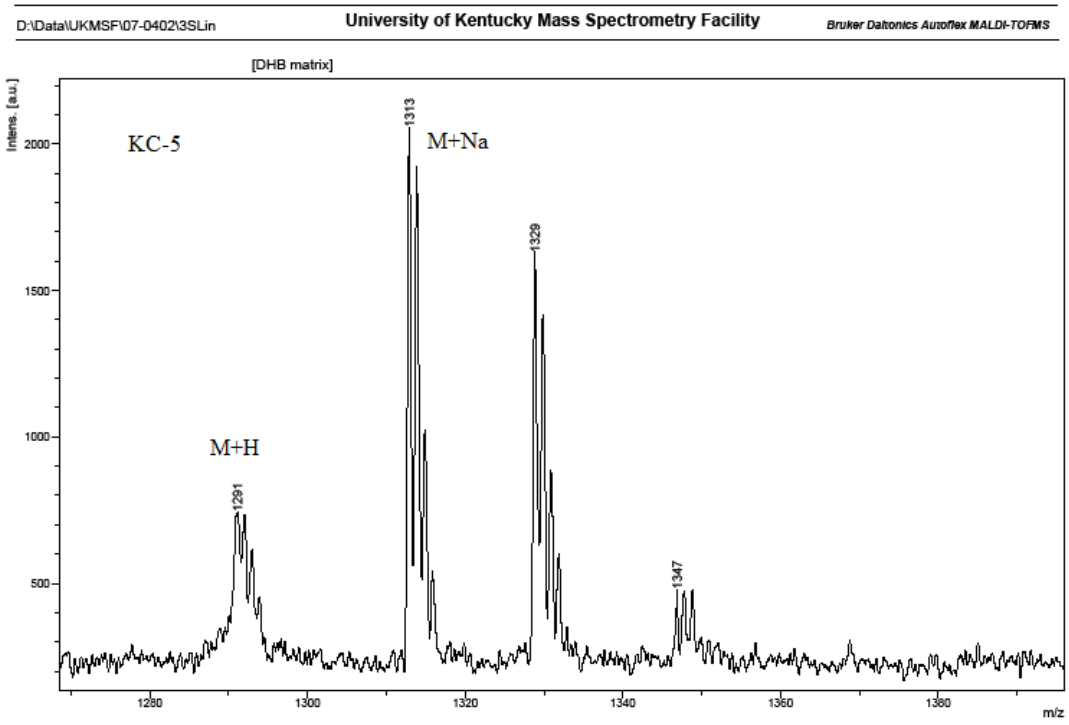

Scheme 3.9 Synthesis of KC-6 (12 atom linker attached at the C-terminus of HIF-pentapeptide)

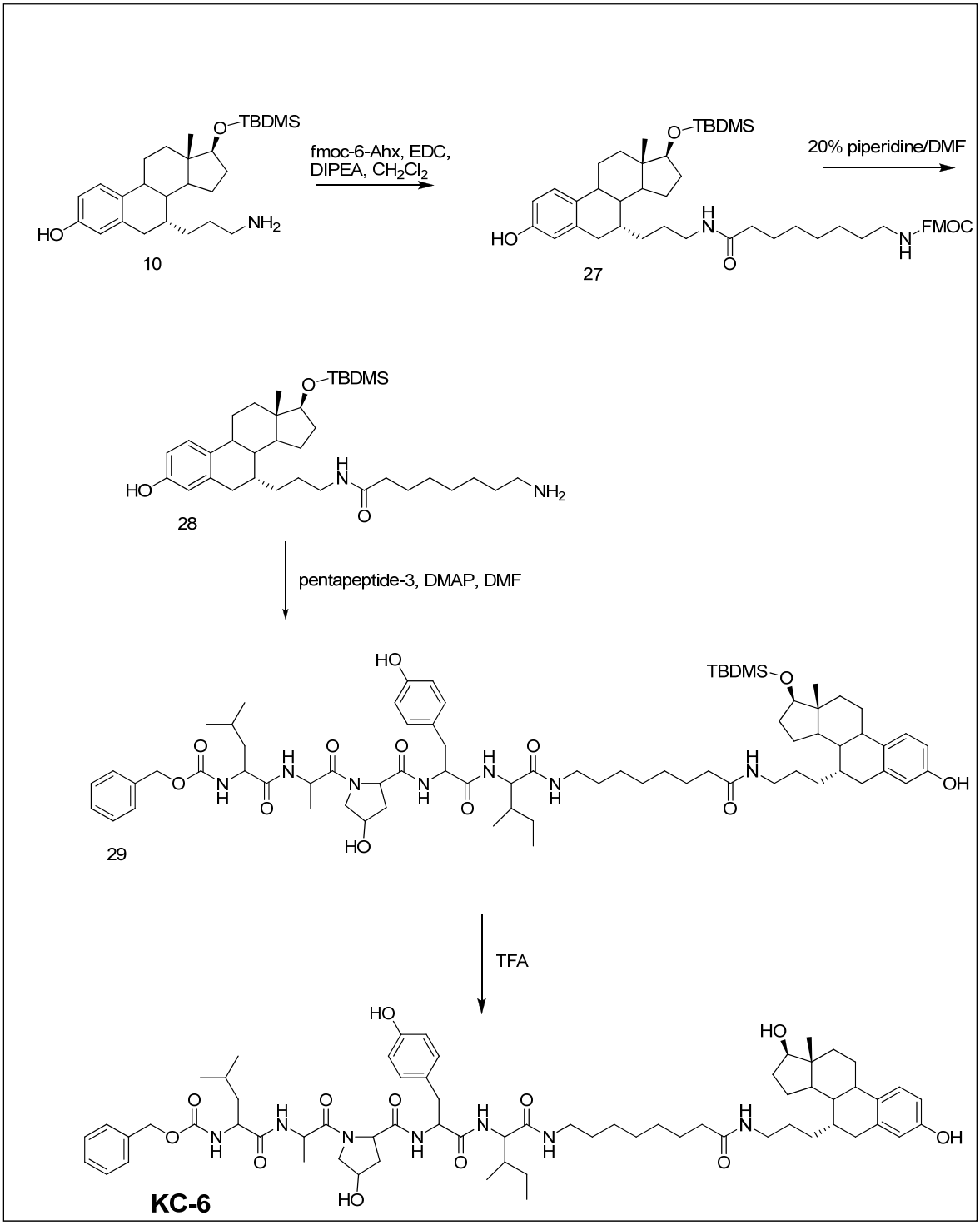

Synthesis of KC-6

Compound 27: Fmoc-caprylic acid (29.2 mg, 0.077 mmol) was added to the free amine "handle" **(10),** (34 mg, 0.077 mmol) and then dissolved in CH_2Cl_2. EDC (22 mg, 0.115 mmol) was added to the mixture followed by DIPEA (2 drops) and mixture was stirred at room temp until all free amine was coupled (15 min-1.5 hr), monitored by TLC. Column chromatography was performed (99:1, CH_2Cl_2: MeOH) yielding a white foamy solid (53 mg, 62%).

^{1}H NMR ($CDCl_3$, 300 MHz): δ 0.03 (s, 3H), 0.04 (s, 3H), 0.73 (s, 3H), 0.89 (s, 9H), 2.62 (d, *J* = 17 Hz, 1H), 2.85 (dd, J = 16.5, 4.7 Hz 1H), 3.06 – 3.30 (m, 4H), 3.64 (t, J = 8.3 Hz, 1H), 4.20 (t, J = 7 Hz, 1H), 4.40 (d, J = 7 Hz, 2H), 4.91 (t, J = 5.5 Hz, 1H), 5.54 (t, J = 5.5 Hz, 1H), 6.53 (d, J = 2.5 Hz, 1H), 6.64 (dd, J = 8.5, 2.5 Hz, 1H), 7.10 (d, *J* = 8.5 Hz, 1H), 7.32 (m, 2H), 7.39 (t, J = 7.5 Hz, 2H), 7.58 (d, J = 7.5 Hz, 2H), 7.75 (d, J = 7.5 Hz, 2H).

Compound 28: Fmoc from (**27),** (53 mg, 0.065 mmol) was deprotected using 20% piperidine in DMF (3 ml) for 10 minutes at room temperature. Following removal of the solvents *in vacuo*, flash column chromatography was performed using (95:5 CH_2Cl_2: MeOH) initially to remove by-products and finally flushing with MeOH to isolate **(28)** as white solid (30 mg, 79%).

Compound 29: Pentapeptide-3 (17 mg, 0.023 mmol) was added to **(28)** (13.6 mg, 0.023 mmol) and both were dissolved in DMF (1.5 ml). The reaction was stirred at room temp overnight. Solvent was removed *in vacuo* and column chromatography was performed (4:1 CH_2Cl_2: MeOH) to yield **(29)** as a white solid (17 mg, 56 %).

^{1}H NMR ($CDCl_3$, 300 MHz): δ 0.03 (s, 3H), 0.04 (s, 3H), 0.73 (s, 3H), 0.89 (s, 9H), 2.62 (d, *J* = 17 Hz, 1H), 2.85 (dd, J = 16.5, 4.7 Hz 1H), 3.00 – 3.26 (m, 5H), 3.64 (t, J = 8.3 Hz, 1H), 4.20 – 4.25 (m, 2H), 4.22 – 4.56 (m, 3H), 5.10 (s, 2H), 6.53 (d, J = 2.5 Hz, 1H), 6.63 (dd, J = 8.5, 2.5 Hz, 1H), 6.74 (t, *J* = 8 Hz, 2H), 6.94 (d, J = 8 Hz, 1H), 7.00 (d, J = 8 Hz, 2H), 7.11 (d, J = 8 Hz, 1H), 7.22 (d, J = 8 Hz, 1H), 7.31(m, 2H), 7.89 (d, J = 6 Hz, 1H).

KC-6: TBDMS protecting group was removed by adding neat TFA (1ml) to **(29)** (9.8 mg, 0.007 mmol) and stirring at room temperature for 30 mim. TFA was removed *in vacuo* and column chromatography was performed (CH_2Cl_2: MeOH 95:5) to isolate **KC-6** as a white solid (6 mg, 67%).

^{1}H NMR ($CDCl_3$, 300 MHz): 0.77 (s, 3H), 2.64 (d, *J* = 17 Hz, 1H), 2.85 (dd, J = 16.5, 4.7 Hz 1H), 3.04 – 3.20 (m, 4H), 3.67 (t, J = 8.3 Hz, 1H), 4.20 – 4.23 (m, 2H), 4.37 – 4.56 (m, 3H), 5.10 (s, 2H), 5.90 (d, J = 8 Hz, 1H), 5.96 (d, J = 8.5 Hz, 1H), 6.16 (d, J = 6 Hz, 1H), 6.53 (d, *J* = 2.5 Hz, 1H), 6.64 (dd, J = 8.5, 2.5 Hz, 1H), 6.73 (t, J = 8.5 Hz, 2H), 6.92 (d, J = 8.5 Hz, 1H), 6.98 (d, J = 8.5 Hz, 1H), 7.12 (d, J = 8.5 Hz, 2H), 7.27 – 7.32 (m, 2H), 7.56 (d, J = 6 Hz, 1H), 7.79 (d, J = 7 Hz, 1H). MS (MALDI, CHCA) *m/z* 1200.7 ($M+Na^+$, calcd for $C_{66}H_{95}N_7O_{12}$ requires 1200.7)

Figure 3.11: Mass spectrum for KC-6

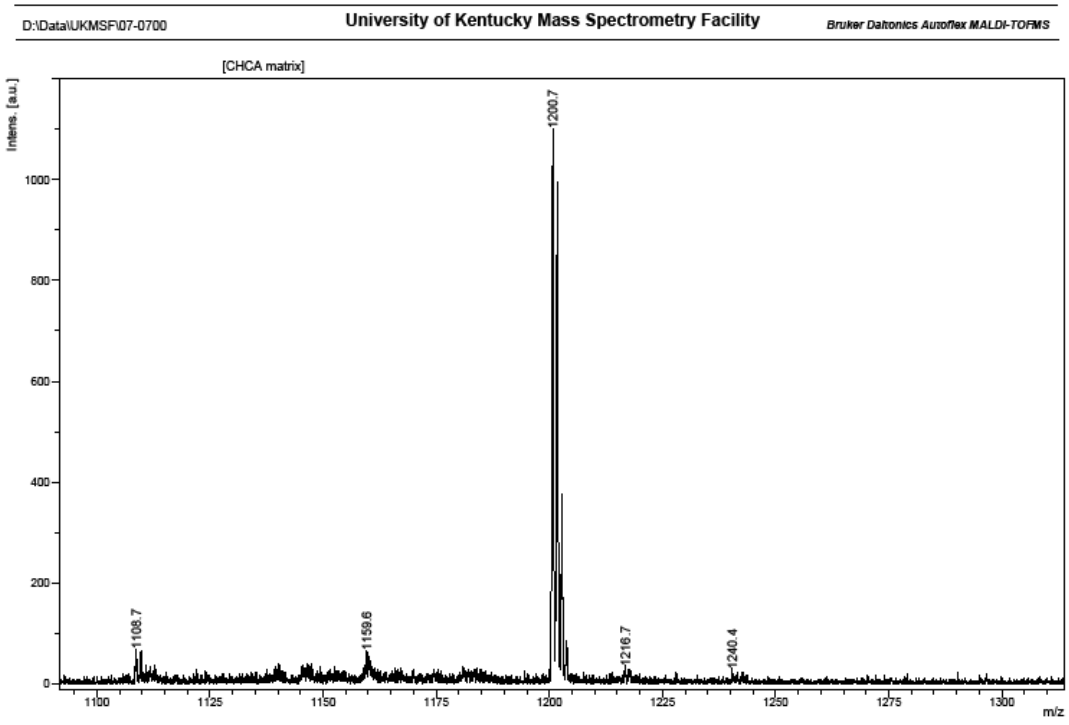

Scheme 3.10 Synthesis of NC – (negative control, HyP substituted with norleucine)

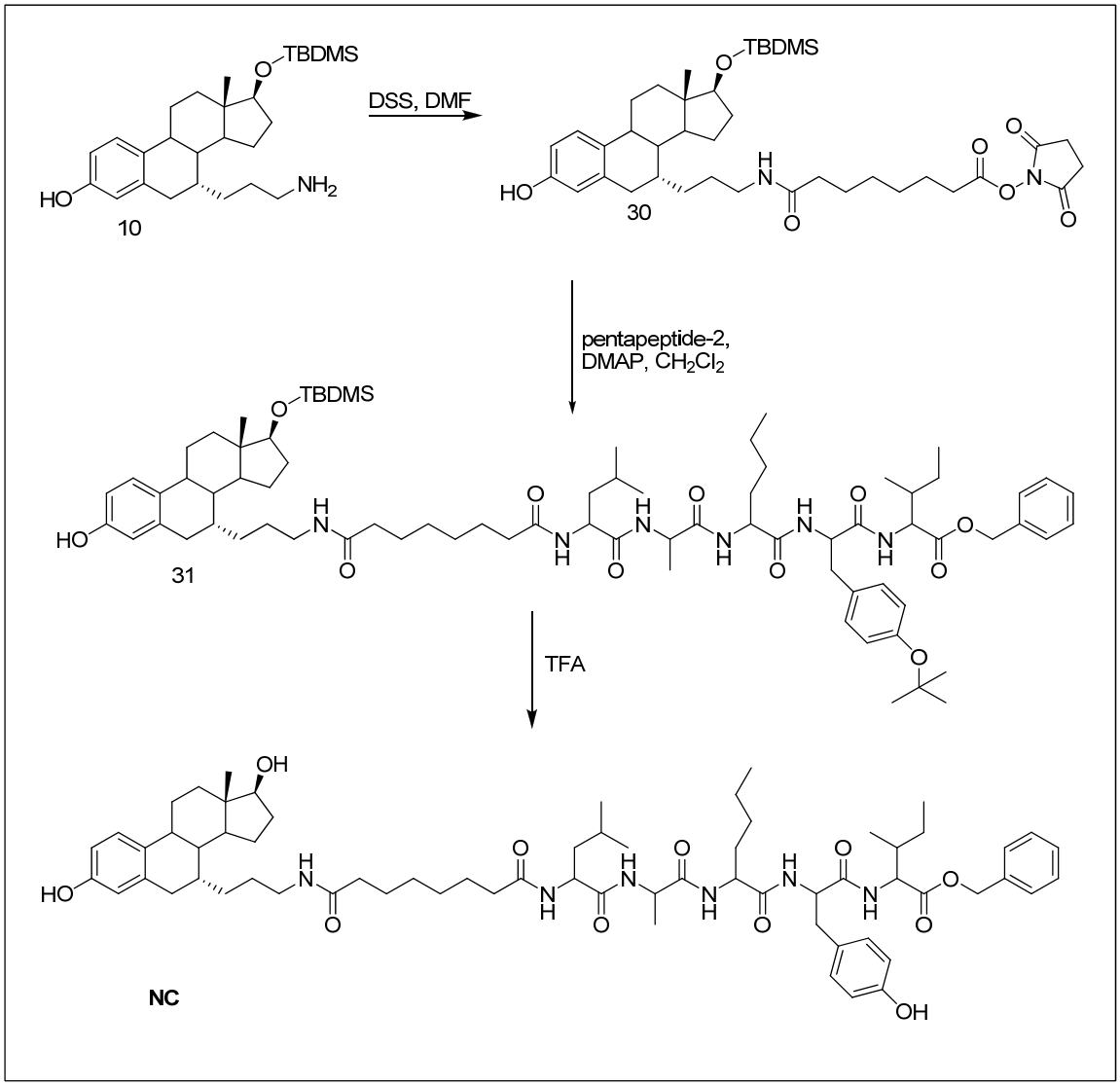

Synthesis of NC – negative control

Compound 30: DSS, (108 mg, 0.394 mmol) was added to the free amine "handle" **(10),** (35 mg, 0.079 mmol) and both were dissolved in DMF (5 ml). The mixture was stirred at room temp overnight. DMF was removed via high vacuum and column chromatography was performed (95:5, CH_2Cl_2: MeOH) to give a white solid (17 mg, 31%).

^{1}H NMR ($CDCl_3$, 500 MHz): δ 0.03 (s, 3H), 0.04 (s, 3H), 0.73 (s, 3H), 0.89 (s, 9H), 2.12 (t, *J* = 7.5 Hz, 2H), 2.58 (t, *J* = 7.5 Hz, 2H), 2.65 (d, *J* = 16.5 Hz, 1H), 2.82 – 2.87 (m, 5H), 3.08 – 3.12 (m, 1H), 3.24 – 3.29 (m, 1H), 3.65 (t, *J* = 8.5 Hz, 1H), 5.76 (t, *J* = 5.5 Hz, 1H), 6.53 (d, *J* = 2.5 Hz, 1H), 6.61 (s, 1H), 6.64 (dd, *J* = 8.5, 2.5 Hz, 1H), 7.11 (d, *J* = 8.5 Hz, 1H).

Compound 31: Pentapeptide-2, (8.5 mg, 0.011 mmol) was added to **(30),** (8 mg, 0.011 mmol) and both were dissolved in CH_2Cl_2 (1.5 ml). The reaction was stirred at room temp overnight. Solvent was removed under reduced pressure and column chromatography was performed (95:5 CH_2Cl_2: MeOH) to yield **(31)** as a white solid (9.3 mg, 62%)

^{1}H NMR ($CDCl_3$, 500 MHz): δ 0.03 (s, 3H), 0.04 (s, 3H), 0.74 (s, 3H), 0.81 – 0.95 (m, 12H), 0.89 (s, 9H), 1.30 (s, 9H), 2.65 (d, J = 16.5 Hz, 1H), 2.86 (dd, J = 16.5, 4.8 Hz, 1H), 2.92 (d, J = 6 Hz, 1H), 2.06 – 3.13 (m, 2H), 3.20 – 3.30 (m, 1H), 3.70 – 3.46 (m, 5H), 3.66 (t, J = 8.5 Hz, 1H), 4.21 – 4.36 (m, 3H), 4.47 -4.50 (m, 1H), 4.57 – 4.64 (m, 1H), 5.13 (s , 2H), 6.47 (d, J = 4.5 Hz, 1H), 6.22 (d, *J* = 8.5 Hz, 1H), 6.50 (dd, J = 8.5, 2.5 Hz, 1H), 6.85 (d, J = 8.5 Hz, 2H), 7.10 (d, J = 8.5 Hz, 2H), 7.12 (d, J = 8.5 Hz, 1H), 7.22 (d, J = 7.5 Hz, 1H), 7.26 (d, J = 8.5 Hz, 1H), 7.35 (s, 4H), 7.44 (d, J = 7.5 Hz, 1H), 7.57 (d, J = 8.5 Hz, 1H), 7.63 (d, J = 6 Hz, 1H).

NC: TBDMS and t-Bu protecting groups were removed simultaneously by adding neat TFA (1ml) to **(31)** (9.3 mg, 0.007 mmol) and stirring at room temperature for 30 min. TFA was removed *in vacuo* and column chromatography was performed (95:5, CH_2Cl_2: MeOH) to isolate NC as a white solid (2.9 mg, 36%).

MS (MALDI, SA) *m/z* 1149.8 (M+H, calcd for $C_{65}H_{92}N_6O_{12}$ requires 1149.68)

Figure 3.12: Mass spectrum for NC

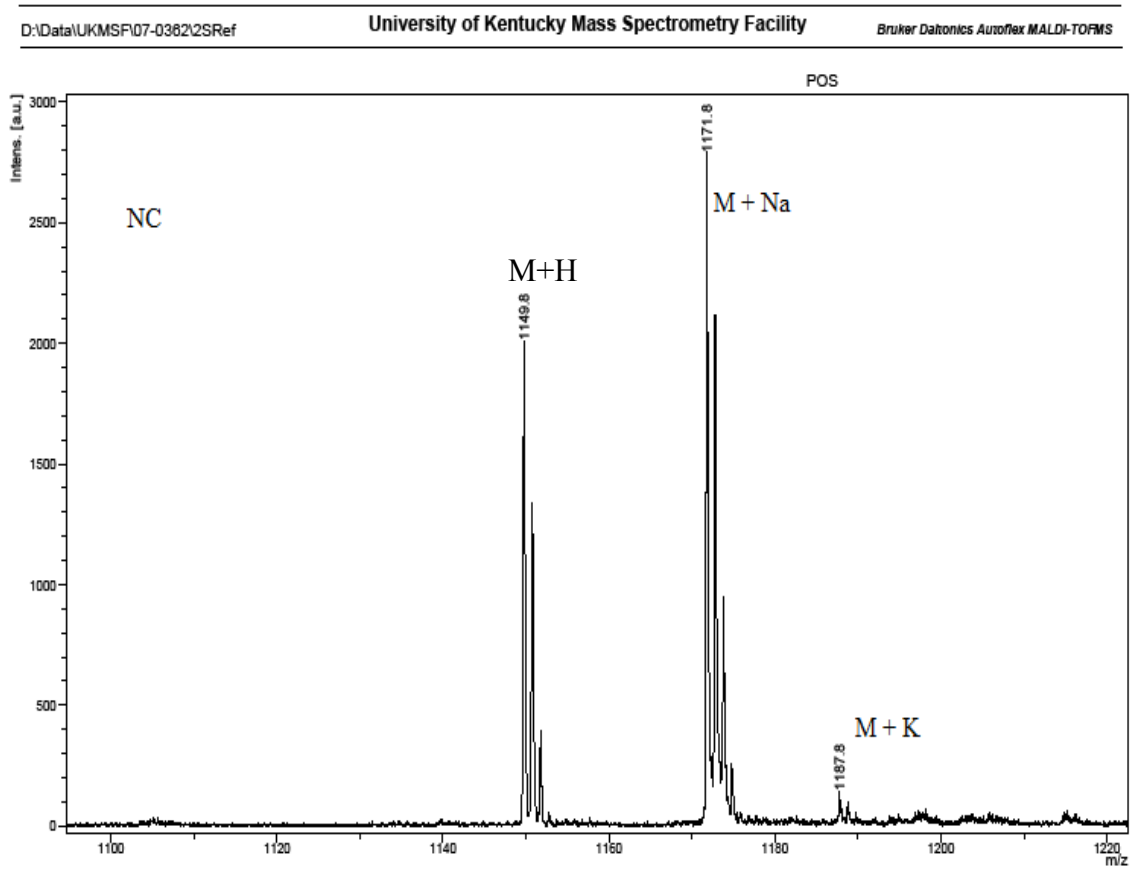

3.5 Synthesis of KC-7/Dimeric ligand PROTAC

Based on the fact that a number of proteins exist as dimers, (including the ER, which dimerizes upon E2 binding) attempts have been made to produce dimeric compounds that can interact with both members of such dimers [193, 194, 195]. It is thought that dimeric ligands that are suitably engineered, having a proper spacer between the two ligands, for example, should produce higher selectivity and potency when compared to their monomeric counterparts [194].

As such the synthesis of dimeric ligands as: anti-cancer agents, example, geldanamycin dimer targeting Hsp90 and HER2 [196] ; anti-HIV agents example disulfide benzamides (DIBAs) dimers, that were found to selectively target the HIV-1nucleocapsid protein zinc (NCp7 Zn) fingers [197]. Dimeric ER lignads have also been

synthesized from both steroidal and non steroidal ligands [195, 198, 199, 200]. Hexestrol dimers showed some antiestrogenic activities [198] and a triphenylethylene dimer containing six hydroxyls had similar activity to tamoxifen, but was not specific for ER positive breast cancer cells [201]. Estrone dimers were also synthesized but, had no antiestrogenic activity and in fact stimulated cell proliferation similar to E2 [200]. Other ER dimers were linked at the 17-β position on E2 and showed minimal cytotoxicity in MCF-7 cells when compared with tamoxifen, but were cytotoxic to murine skin cancer cells [195, 199].

Similar to the aforementioned studies, in an attempt to improve the efficiency of the PROTAC, a dimeric PROTAC was synthesized. The dimeric PROTAC was linked at the C-7α position on E2 (unlike the other ER targeting dimers previously mentioned aboved), which we hope would retain the binding affinity for the ER. The Scheme and reaction details for synthesis of the dimeric PROTAC are reported below.

.

Scheme 3.11 Synthesis of KC-7/dimeric ligand PROTAC

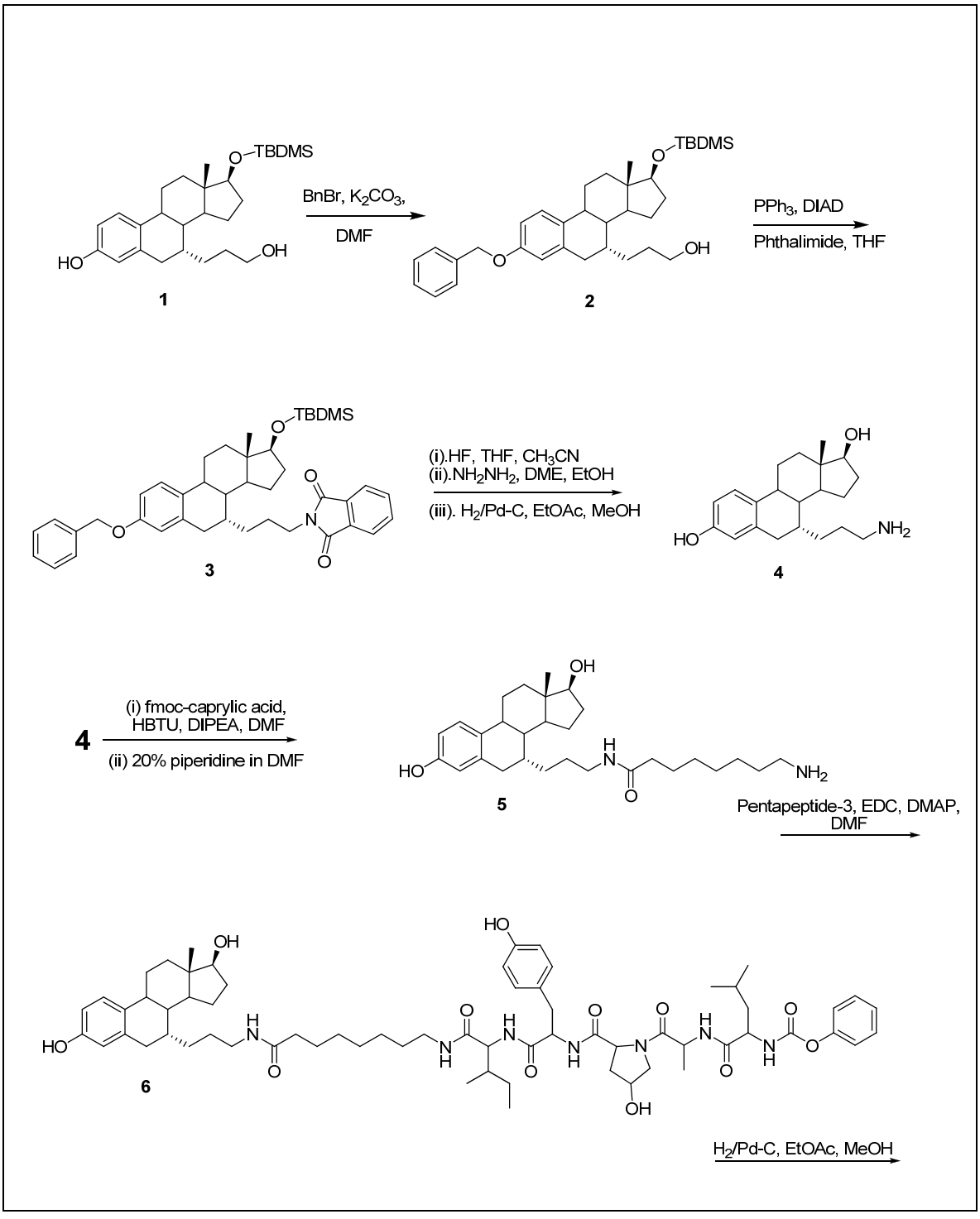

Scheme 3.11 Synthesis of KC-7/dimer continued

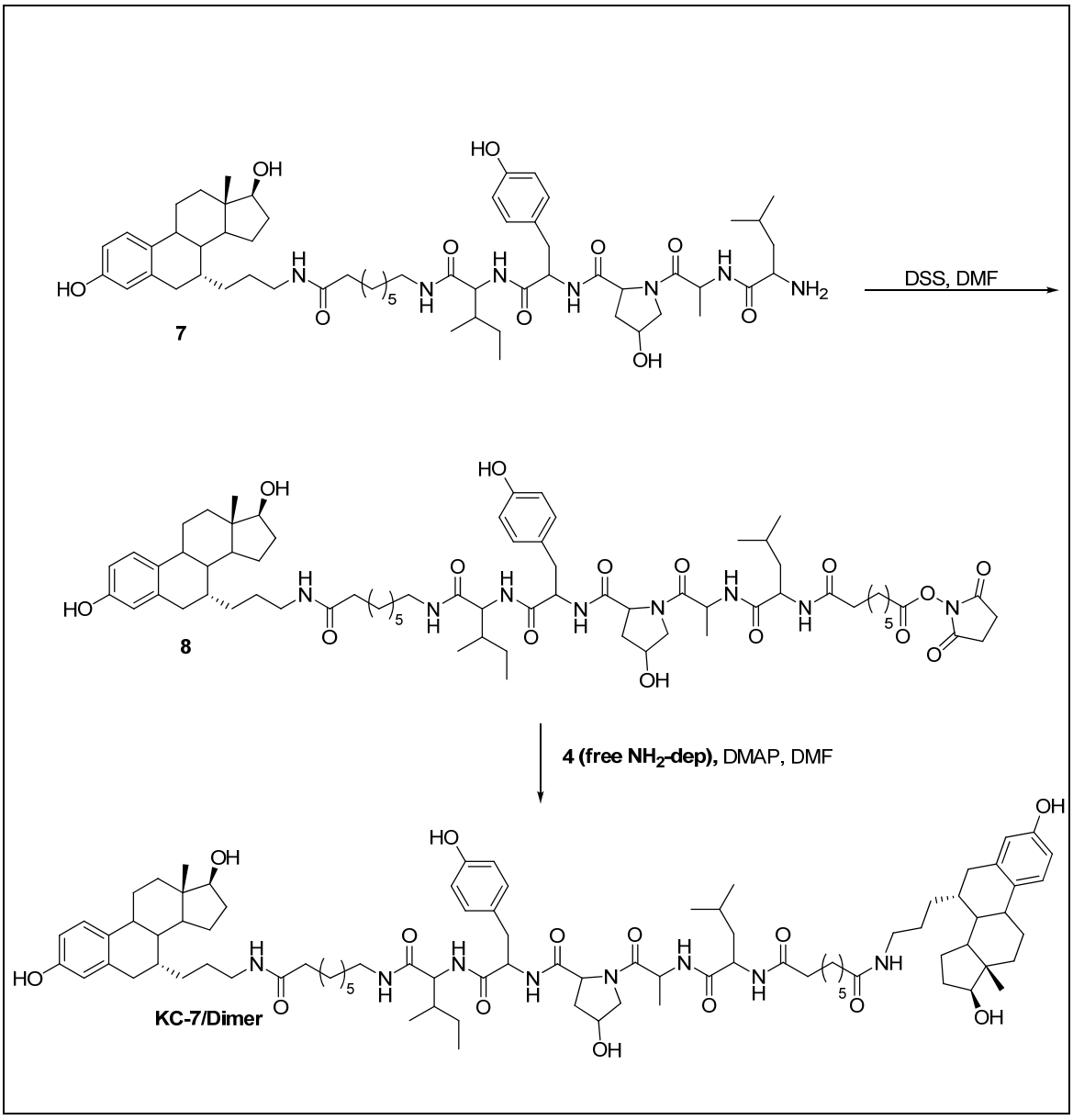

Reaction details for synthesis of KC-7/dimeric ligand PROTAC

Compound 2: The 3-OH deprotected compound isolated from the synthesis of **(8)** in scheme 3, was re-protected with a benzyl group. K_2CO_3 (1.2 g, 8.50 mmol) was added to **(8)** (470 mg, 1.06 mmol) and contents were dissolved in DMF, benzyl bromide (BnBr) (195 µl, 1.60 mmol) was then added and the reaction was stirred overnight at room

temperature. DMF was removed *in vacuo* and column chromatography was performed (5:1 Hex:EtOAc) to yield **(2)** (454 mg, 80%).

^{1}H NMR (CDCl3, 500 MHz): δ 0.02 (s, 3H), 0.03 (s, 3H), 0.74 (s, 3H), 0.89 (s, 9H), 2.73 (d, *J* = 16.5 Hz, 1H), 2.92 (dd, *J* = 17, 5 Hz, 1H), 3.60 (t, *J* = 6.2 Hz, 2H), 3.65 (t, *J* = 8 Hz, 1H), 5.02 (s, 2H), 6.70 (d, *J* = 2.5 Hz, 1H), 6.78 (dd, *J* = 8.7, 2.7 Hz, 1H), 7.20 (d, *J* = 8.5 Hz, 1H), 7.30- 7.44 (m, 5H)

Compound 3: To a cooled solution (0 °C) of PPh3 (443 mg, 1.70 mmol) in THF (10 mL) was added DIAD (dropwise) (332 µl, 1.70 mmol). A white precipitate of the ylide was observed, and the reaction was stirred for 40 min at 0 °C. A solution of **(2)**, (454 mg, 0.850 mmol) and phthalimide (249 mg, 1.70 mmol) dissolved in THF (5 mL) was then added to the ylide. The reaction was stirred for 1 h at 0 °C and then at room temperature overnight. The solvent was evaporated under reduced pressure and the residue was purified via flash chromatography (5:1 Hex:EtOAc) to give **(3)** as a white foam (369 mg, 65%).

^{1}H NMR (CDCl3, 500 MHz): δ 0.03 (s, 3H), 0.04 (s, 3H), 0.73 (s, 3H), 0.89 (s, 9H), 2.72 (d, *J* = 17 Hz, 1H), 2.92 (dd, *J* = 17, 5 Hz, 1H), 3.60 (t, *J* = 6.2 Hz, 2H), 3.65 (t, *J* = 8 Hz, 1H), 5.01 (s, 2H), 6.70 (d, *J* = 2.5 Hz, 1H), 6.76 (dd, *J* = 8.7, 2.7 Hz, 1H), 7.20 (d, *J* = 8.5 Hz, 1H), 7.30- 7.44 (m, 5H), 7.69- 7.71 (m, 2H), 7.82- 7.83 (m, 2H)

Compound 4: Three different deprotection reactions were performed to give **(4)**. (i) deprotection of TBDMS: hydrogen fluoride (HF) (540 µl) was added to a 25 ml round bottom flask containing **(3),** (172 mg, 0.260 mmol), already dissolved in THF and CH_3CN. The mixture was heated to approximately 60°C for 20 min. After cooling, the mixture was quenched with saturated $NaHCO_3$ and then solid $NaHCO_3$ until neutral, then extracted with CH_2Cl_2. After drying over Na_2SO_4 the solvent was evaporated under reduced pressure and the residue was purified via flash chromatography (5:1 Hex:EtOAc) (134 mg). (ii) release of free amine: Product (134 mg, 0.244 mmol) obtained from (i) above was dissolved in equal amounts of DME and EtOH (5 ml and 5 ml) and hydrazine (163 µl) was added and the mixture was refluxed for 2 h, during which time slightly brown precipitate formed on the sides and the solution turned slightly green. The reaction

was cooled, and 5% NaOH was added, dissolving the precipitate. After 30 min, water was added, and the solution was extracted with CH_2Cl_2, dried over Na_2SO_4 and the solvent was evaporated in vacuo. The residue was purified via flash chromatography (95:5, CH_2Cl_2: MeOH) to give the amine as a white foam solid (79 mg). (iii) hydrogenolysis: The amine from (ii) (79 mg) was dissolved in 1:1 EtOAc: MeOH and 10% palladium on charcoal (Pd-C) (12 mg) was added, hydrogen was bubbled through the mixture and the reaction was monitored by TLC until all starting material disappeared. Mixture was filtered through celite and solvent was evaporated to yield **(4)** as a white solid (58 mg, 96%).

^{1}H NMR (CDCl3, 500 MHz): δ 0.77 (s, 3H), 2.67 (d, *J* = 17 Hz, 1H), 2.88 (dd, *J* = 17, 5 Hz, 1H), 3.70 (t, *J* = 8 Hz, 1H), 6.54 (d, *J* = 2.3 Hz, 1H), 6.63 (dd, *J* = 8.5, 2.3 Hz, 1H), 7.11 (d, *J* = 8.5 Hz, 1H)

Compound 5: Fmoc-caprylic acid (28.6 mg, 0.075 mmol) was added to (**4),** (24.7 mg, 0.075 mmol) dissolved in CH_2Cl_2 and DMF. HBTU (43 mg, 0.112 mmol) and was added to the mixture followed by DIPEA (2 drops) and mixture was stirred at room temp for 30 min. solvents were removed *in vaccuo* and the residue was purified by column chromatography (CH_2Cl_2: MeOH 95:5) yielding a white foamy solid (17.5 mg, 34%). Fmoc from the product above (ii) (17.5 mg, 0.075 mmol) was deprotected using 20% piperidine in DMF. After solvent removal the residue was purified via flash column chromatography (CH_2Cl_2: MeOH 95:5) to yield **(5)**, (11 mg, 92%). Amine was confirmed using Kaiser test.

Compound 6: Pentapeptide-3 (18 mg, 0.023 mmol) and DMAP was added to **(5)** (11 mg, 0.023 mmol) and the contents were dissolved in DMF (2.5 ml). The reaction was stirred at room temp overnight. The solvents were removed *in vacuo* and column chromatography was performed (4:1 CH_2Cl_2: MeOH) to yield **(6)** as a white solid (17 mg, 63 %)

^{1}H NMR (CDCl3, 500 MHz): δ 0.66 (s, 3H), 0.67 – 0.87 (m, 16H), 2.57 (d, *J* = 16.5 Hz, 1H), 2.72 – 2.80 (m, 2H), 2.94 – 2.99 (m, 4H), 3.45 – 3.57 (m, 3H), 4.04 – 4.23 (m, 2H),

4.28 – 4.49 (m, 4H), 4.51 (d, J = 5 Hz, 1H), ( )5.02 (s, 2H), 6.41 (d, *J* = 2.5 Hz, 1H), 6.50 (dd, *J* = 8.5, 2.5 Hz, 1H), 6.60 – 6.63 (m, 2H), 6.97 – 7.01 (m, 2H), 7.05 (d, *J* = 8.5 Hz, 1H), 7.29 - 7.46 (m, 5H), 7.65 (d, *J* = 9.5 Hz, 1H), 7.82- 7.83 (m, 2H), 7.86 (d, *J* = 8 Hz, 1H), 8.00 (d, *J* = 7 Hz, 1H), 8.06 (d, *J* = 7 Hz, 1H), 8.19 (d, *J* = 6 Hz, 1H)

Compound 7: (**6),** (17 mg, 0.015 mmol) was dissolved in 1:1 EtOAc: MeOH, Pd-C was added and hydrogen was bubbled through the mixture for 1hr. The mixture was filtered through celite and solvent evaporated to give **(7)** as a pale yellow solid (15 mg, 98%). Free amine confirmed by Kaiser test.

Compound 8: DSS (15 mg, 0.042 mmol) was added to **(7)** (15 mg, 0.014 mmol) and dissolved in DMF (0.5 ml) the mixture was stirred at room temp overnight. DMF was removed via high vacuum and column chromatography was performed (95:5 CH_2Cl_2: MeOH) to give **(8)** as a yellow solid (5.5 mg, 31%).
^{1}H NMR (CDCl3, 500 MHz): δ 0.77 (s, 3H), 0.80 – 1.01 (m, 10 H), 1.02 (t, *J* = 6.5 Hz, 3H), 2.30 (t, *J* = 7.5 Hz, 2H), 2.60 (t, *J* = 7.5 Hz, 2H), 3.02 – 3.24 (m, 5H), 3.47 – 3.54 (m, 1H), 3.63 – 3.72 (m, 3H), 4.17 – 4.27 (m, 1H), 4.43 – 4.54 (m, 4H), 6.36 (t, *J* = 6 Hz, 1H), 6.40 (t, J = 6 Hz, 1H), 6.53 (d, *J* = 2.5 Hz, 1H), 6.63 (dd, *J* = 8.5, 2.5 Hz, 1H), 6.75 (t, *J* = 8.5 Hz, 2H), 6.95 (d, *J* = 8 Hz, 1H), 7.00 (d, *J* = 8.5 Hz, 1H), 7.10 (d, *J* = 8.5Hz, 1H), 7.14 (d, J = 4.5 Hz, 1H), 7.16(d, *J* = 4.5 Hz, 1H), 7.26 (d, J = 7Hz, 1H), 7.58 (t, *J* = 6 Hz, 1H), 7.73 (t, *J* = 6 Hz, 1H),

Compound 9: (8), (5.5 mg, 0.004 mmol), **(4)** (3 mg, 0.009 mmol) and DMAP was dissolved in DMF and mixture was stirred at room temperature overnight. Solvents were removed *in vaccuo* and flash column chromatography was performed (95:5 CH_2Cl_2: MeOH) to give the **(KC7/dimer)** as a yellow solid (4.1 mg, 68%). Mass spectrum indicated below. MS (MALDI, SA) *m/z* 1534 ($M+Na^+$, calcd for $C_{87}H_{130}N_8O_{14}$ requires 1533.97)

Figure 3.13: Mass spectrum for Dimer

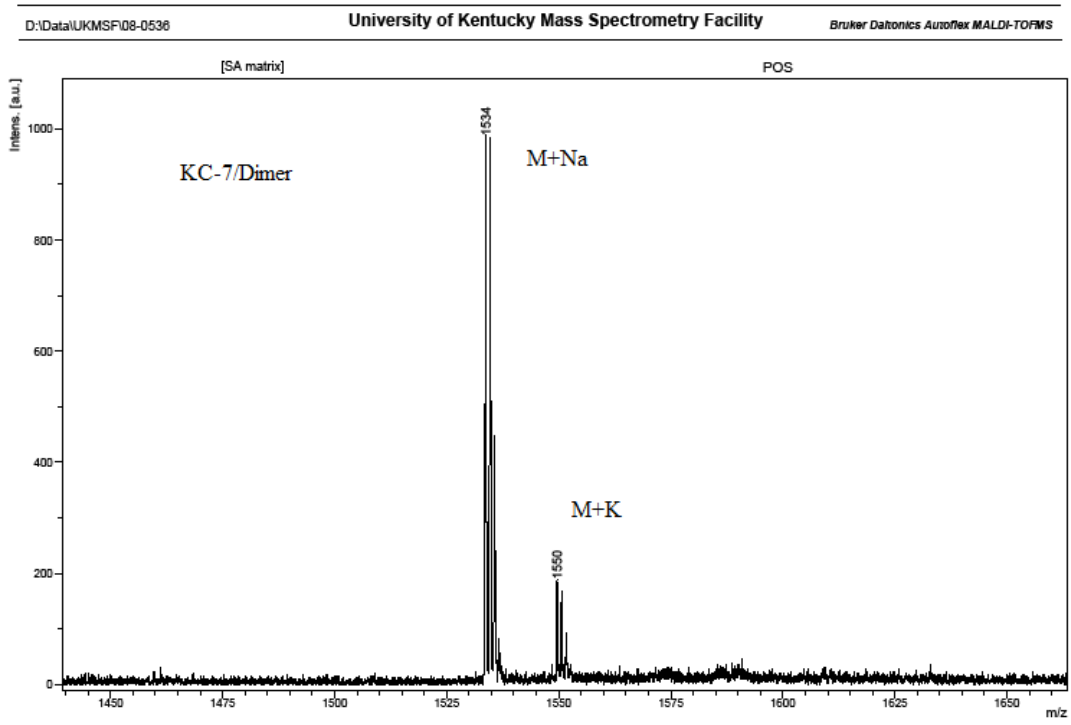

3.6 Summary

Syntheses resulted in the development of ten PROTACs. Two C-16α PROTACs, K1 and K2 were synthesized (Scheme 3.2) having a linker attached at the C-16α position via a carbon-carbon (C-C) bond. The C-C bond was used as an alternative to the ester bond used in the original ER-targeting PROTAC (Figure 3.1). The C-terminal benzyl protecting group on the HIF derived pentapeptide was not removed in K-1 in order to evaluate its potential in stabilizing the PROTAC while the benzyl group was removed from K-2 analogous to the O-17/E2-penta PROTAC.

All other PROTACs were synthesized as C-7α PROTACs. In this series eight PROTACs were developed. Five were developed in an attempt to optimize the linker length, KC-1, KC-2, KC-3, KC4, and KC-5, (Scheme 3.4 to 3.8). In an effort to decipher whether the location of attachment of the linker to the HIF pentapeptide was important, a

PROTAC KC6 (Scheme 3.9) was also synthesized having the linker attached at the C-terminal isoleucine residue. To help validate the mechanism of PROTAC action the critical Hyp was replaced with a nor-leucine reside. A dimeric PROTAC was also developed in the hope of improving the PROTAC efficiency.

CHAPTER 4: BIOLOGICAL CHARACTERIZATIONS

The data presented in this chapter were generated in collaboration with Marie Wehenkel (western blot, immunofluorescence, rt-PCR), Hyeong- Jun Han (MTS assay), Dr. Eun-Young Choi (binding assay) and, Dr. Wooin Lee's lab - Eun Young Jang & Kyungwha Kim (qrt-PCR). Thanks to the following laboratories for use of their equipment: Dr. Tai (microplate reader), Dr. Dr. Wooin Lee (fluorescence microscope) and Drs. Black, Graf, and Leggas (fluorescence microscope).

4.1 Introduction

PROTACs were tested in MCF-7 breast cancer cells for their ability to ER induce degradation. MCF-7 cells were treated with PROTACs and the effect of PROTACs on ERα protein levels was evaluated using western blot and immunofluorescence (IF). IC_{50} was also established for all compounds. Once an optimum compound was identified it was screened further for its potential effects on the ER downstream target gene, the progesterone receptor (PR). The belief is that if ER is degraded then genes that are normally dependent on ER for transcriptional activation will display only basal expression levels.

4.2 Materials and Methods

Reagents:

The following reagents were obtained from Bio-Rad: Tris-Cl Triton X-100, Protein Assay Dye Reagent Concentrate, Sodium Dodecyl Sulfate (SDS) 20% (w/v), 0.5M Tris-HCl Buffer pH 6.8, 1.5M Tris-HCl Buffer pH 8.8, 30% Acrylamide/Bis Solution 29:1, Immun-Blot PVDF Membrane, Blocking Grade Non-Fat Dry Milk, and Prestained SDS-PAGE Standards, Low Range.

The following reagents were obtained from Sigma-Aldrich: Protease Inhibitor Cocktail; Sample Buffer, Laemmli 2X Concentrate; Ammonium Persulfate (APS); N,N,N',N'-Tetramethylethylenediamine (TEMED); Bovine Serum, Albumin (BSA); Kodak GBX Developer/Replenisher; Kodak GBX Fixer/Replenisher; Kodak BioMax XAR Film;Sodium Bicarbonate; Glycero; HEPES; Magnesium Chloride ($MgCl_2$) hexahydrate, 99%, ACS reagent; TWEEN® 20; Ethylenediaminetetraacetic acid (EDTA); Phosphatase Inhibitor Cocktail 1; Dithiothreitol (DTT); and Sodium Orthovanadate (Na_3VO_4).

The following reagents were obtained from Gibco: Goat Serum; Fetal Bovine Serum (FBS) heat inactivated; 10X Hanks' Balanced Salt Solution (HBSS); Penicillin-Streptomycin (P/S); RPMI Medium 1640; 10X Trypsin-EDTA (TE); and RPMI 1640 Medium phenol-red free.

Additional reagents were supplied by other companies. The Amersham ECL Western Blotting Detection Reagents were purchased from GE Healthcare, Sodium Chloride and Methylsulfoxide (DMSO) were purchased from EMD, Nonidet-P40 was purchased from Fluka, PVDF membranes were purchased from Biorad, Prolong Gold antifade w/ DAPI was purchased from Invitrogen, CellTiter 96® Aqueous One Solution Cell Proliferation Assay was purchased from Promega, Charcoal/Dextran Treated Fetal Bovine Serum was purchased from Hyclone, Antibody Dilutant w/ Background Reducing Components was purchased from DAKO, Potassium Chloride (KCl) ACS Grade was purchased from EM Science, Formaldehyde, Para (PFA), Laboratory Grade was purchased from Fisher Scientific, Potassium Phosphate Monobasic (KH_2PO_4) and Sodium Phosphate Dibasic Heptahydrate (Na_2HPO_4) were both purchased from Mallinckrodt Baker. β-glycerolphosphate was a kind gift from Dr. Penni Black.

Antibodies:

The following primary antibodies were used for western blotting: Estrogen Receptor-α (ERα), Histone deacetylase 1 (HDAC1), (Santa Cruz). Cyclin D1, (NeoMarkers) and β-actin (Novus Biologicals).

Secondary antibodies: Anti-Mouse IgG horseradish peroxidase (Host: Goat) (Zymed); Anti-Rabbit IgG horseradish peroxidase (Host: Donkey), (Amersham).

Antibodies for immunofluorescence: Primary antibody, ERα (Abcam). Conjugated secondary antibody Alexa Fluor 488 (FITC) goat anti-rabbit IgG (Invitrogen). Also from Invitrogen was the f-actin stain Rhodamin Phallodin, which was first dissolved in methanol according to the manufacturer's instructions and then used at a concentration of 1:1000 in PBS [R415].

Cell Culture & Treatment:

MCF7 cells were purchased from the American Type Culture Collection (Manassas, VA) and maintained in RPMI 1640 Medium supplemented with 10% (v/v) fetal bovine serum and a mixture of 100U/mL penicillin and 100µg/mL streptomycin (P/S). Cells were grown in an incubator at 37°C with a 5% carbon dioxide atmosphere. Media was changed to RMPI plus P/S with 5% Charcoal/Dextran-treated FBS after washing with HBSS and at least 24 hours prior to treatment of the cells with compounds. Cells were added to 12 or 24 well plates and treated once they reached 70% confluence. Compounds were treated in a DMSO vehicle at the appropriate dilutions for 48 hours, unless noted otherwise.

Western Blotting:

Whole cell lysates were prepared by incubating cells in nondenaturing lysis buffer (50nM Tris-Cl, 150mM NaCl, 1% NP40, 1% Triton X-100, and 1% protease inhibitor cocktail) on ice for 1 hour. Cells were then centrifuged at 14,000 rpm for 10 min at 4◦C (Sorvall Biofuge Primo R, Kendro Laboratory Products, Newtown, CT). Supernatants were collected and subjected to protein assay via method of Bradford using Protein Assay Dye Reagent Concentrate. Protein concentrations were determined by a GENESYS 10 spectrophotometer, Thermo Spectronic (VWR, Arlington Heights, IL). The supernatants were then added 2x Laemmli Sample Buffer and heated in boiling water for 10 min. Subsequently, the denatured whole cell lysates were resolved by 8%-12% SDS-PAGE and transferred to PVDF membranes. Membranes were blocked with 5% skim milk or BSA for 1 hour at room temperature on the rotator. Appropriate primary and secondary antibodies were used to incubate the membranes for 1 hour at room temperature on the

rotator or overnight at 4◦C. Finally, Amersham ECL Western Blotting Detection Reagents were used to visualize protein of interests on Kodak BioMax XAR Films. Antibodies were used at the following dilutions: ERα (1:200), β-actin (1:5000), anti-rabbit (1:10000 or 1:5000), and anti-mouse (1:5000). Exposure: ERα (1-5 minutes), and β-actin (5-60 seconds).

Quantification:

The intensities of the bands on western blot films were quantified using volumetric densitometry (Quantity One, Bio-Rad). The estrogen receptor-alpha values were normalized to β-actin and DMSO was arbitrarily assigned a value of 100% for comparison purposes.

Cell Proliferation Assay:

Cells were seeded in a 96 well plate at a concentration of 5,000 cells per well and allowed to attach for 24 hours. The media was changed to 5% Charcoal RPMI for 24 hours prior to the addition of compounds. During the 48 hour treatment, ten concentrations were tested plus one vehicle and one media control. At the end of the treatment time, 20µL of the CellTiter 96® assay dye was added to the media in each well and allowed to react at 37°C for one hour. Absorbance was then measured at 490nm on a microplate reader using the KC4 data analysis program from BioTek®. In GraphPad Prism® (San Diego, USA), IC_{50} values were obtained from a sigmoid dose-response curve using a nonlinear regression to a logarithmic function. The data represent at least three replicates.

Immunofluorescence:

Coverslips were sterilized with ethanol and UV light exposure in 35mm dishes. Cells were added directly to the dish and allowed to attach for 24 hours. The media was then changed to phenol-red free RPMI with 5% Charcoal/Dextran-treated FBS until treatment with compounds. Compounds were diluted in the phenol-red free media, and treated as detailed previously.

After treatment, cells were fixed with 4% PFA at 37°C for 7 minutes, washed with PBS, and then permeablized with 0.2% Triton-X in PBS at 37°C for 30 minutes. Between all subsequent steps coverslips were washed in PBST (PBS with 0.05% Tween-20). Blocking in 10% goat serum with 0.1% BSA in PBST was performed at 37°C for 1 hour or 4°C overnight. Primary antibody (ERα) was added directly to the coverslip at a concentration of 1:1000 in DAKO antibody dilutant at 37°C for one hour, then secondary antibody (FITC) was added in the same way for 30 minutes. The f-actin stain was diluted to 1:1000 in PBS, added directly to the coverslip, and incubated at 37°C for 30 minutes. After extra washing, the coverslips were removed from the dishes and dried briefly. 20μL of Prolong Gold with DAPI per coverslip was added to clean slides and the mounted slides were allowed to dry overnight. After drying, the coverslips were rimmed with clear nail polish and visualized on a fluorescent microscope.

Competitive Ligand Binding Assay:

Competitive ligand binding assays were performed according to the manufacturer's protocol (Invitrogen). Purified human recombinant estrogen receptor (approximately 10 nM) was added to a saturating amount of [^{3}H]-labeled estradiol (20 nM) and the indicated concentrations of E2 or PROTACs. After incubating for 2 hr at room temperature or overnight at 4^{o}C, a 50% hydroxy apatite slurry was added to bind the receptor/ligand complex and the sample was centrifuged. The resuspended pellet was then analyzed for tritium activity using scintillation counting and the percent specific binding affinity was calculated. IC_{50} values were obtained using one site competition equation ($Y = Bottom + (Top-Bottom) / 1 + 10^{X-LogEC50}$) provided by the Graph Pad Prism® software. Relative binding affinity (RBA) was calculated using the following equation, $RBA = [IC_{50}\ (E2)/IC_{50}\ (sample)] \times 100$.

qRT-PCR:

MCF-7 cells were seeded in 6 well plates at a density of 250,000 cells per well and given 24 hours to attach. The media was changed to 5% Charcoal RPMI for 24 hours prior to the addition of compounds. Wells (four per condition) were treated with the

indicated concentrations of compounds for 48 hours. Cells were collected by trypsinization and stored at -80°C until lysis.

RNA was extracted from the cell pellets using the TRIzol reagent (Invitrogen) according to the manufacturer's instructions. RNA concentration was determined using NanoDrop (Thermo Scientific). One microgram of total RNA was employed to create cDNA utilizing the iScript™ cDNA synthesis kit (Bio-Rad) according to the manufacturer's instructions. Reaction conditions: 25µL total volume, 5 minutes at 25°C, 30 minutes at 42°C, 5 minutes at 85°C, followed by a hold at 4°C. The cDNA was stored at -20°C until qrt-PCR was performed.

The real time reactions (run in triplicate) were performed using an iCycler (Bio-Rad) with the iQ SYBR Green Supermix (Bio-Rad), 200nM of the forward/reverse primers, and 2µL of cDNA. The following gene-specific primers reported previously [202] were used: PR (fwd): 5'-ATCAGGCTGTCATTATGGTGT-3'; PR (rev): 5'-AAATTTTCGACCTCCAAGGAC-3'; β-actin (fwd): 5'-GCATCCTCACCCTGAAGTAC-3'; β-actin (rev): 5'-GATAGCACAGCCTGGATAGC-3'. The reactions for PR were carried out with annealing at 60℃ for 40 cycles while the reactions for β-actin were carried out with annealing at 65℃ for 40 cycles. A melting curve analysis was included in each real time reaction to ensure the specificity of the amplified products. Average cycle threshold (Ct) values for PR was calculated and normalized to Ct values for β-actin, using the ΔΔCt method as an internal control, with the fold-change plotted in GraphPad Prism® and the product of four independent replicates.

4.3 Results

Initial western blot screening assessed the effects of C-16α PROTACs vs. O-17/E2-penta PROTAC (the first generation PROTAC). The result showed (**Figure 3.4**) that the C-16α PROTAC was not better at degrading the ER than the original PROTAC; however, K-1, which has a C-terminal benzyl protecting group, showed better activity against the ER when compared to K-2, which is not protected (Scheme 3.2 for structures). Further evaluation using the C- terminus protected O-17/E2-penta PROTAC **(Figure 3.5),** indicated a possible role for benzyl protection at the C-terminus of the pentapeptide in enhancing PROTAC activity. Based on the data from these western blot studies it was decided that the C-16α position was not ideal for linker attachment and further length optimization of the PROTAC. As such, addditional PROTACs with the linker attached at the C-7α position on E2 and a benzyl protecting group at the C-terminus of the pentapeptide was synthesized.

Analysis of C-7 PROTACs

C-7 vs C-16 PROTACs:

The C-7α position was chosen for further optimization based on the reported success of compounds derivatized at that position [178, 203, 204, 205]. Length optimization was performed at the C-7α position (chapter 3). The different PROTACs were analyzed for their ability to degrade the ER in a dose dependent manner. ER levels were evaluated by western blot **(Figure 4.1).** The C-7α PROTAC containing the DSS extender, (KC-2), was compared to the C-16α PROTACs, which also has the DSS extender. As observed in **Figure 4.1,** K-1 and KC-2 showed similar ability to degrade the ER in a dose dependent manner, while K-2 did not show a dose dependent increase in ER degradation, again highlighting a possible role for benzyl protection, as both K-1 and KC-2 contain the benzyl protecting group.

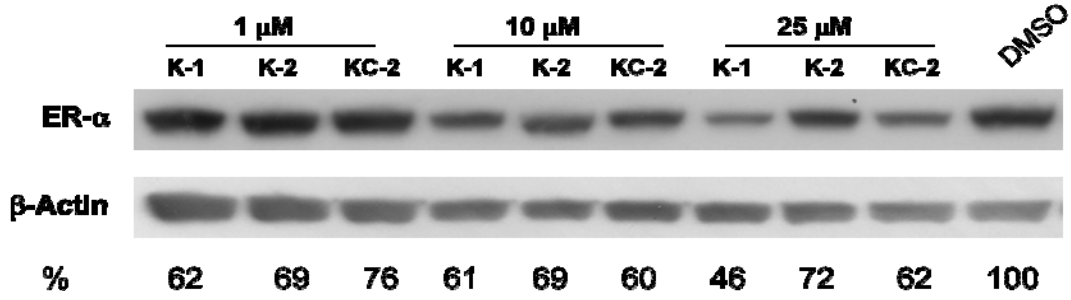

Figure 4.1 Dose dependent degradation of ERα by C-16α and C-7α PROTACs: K-1, K-2 and KC-2 respectively. MCF-7 cells were treated with PROTACs at the indicated concentrations or with DMSO for 48hrs. Cells were lysed and analyzed via western blot using anti ERα antibody. The intensities of the bands were quantified (%) using volumetric densitometry (Quantity One, Bio-Rad). The ERα values were normalized to β-actin and DMSO was arbitrarily assigned a value of 100% for comparison purposes. K-1 (C-16 PROTAC- protected C-terminus), K-2 (C-16 PROTAC - unprotected C-terminus), KC-2 (C-7 PROTAC –benzyl protected C-terminus).

C-7α PROTACs bind to ERα with higher affinity than C-16α PROTACs:

An efficient PROTAC should be able to maintain relatively good binding for the ER; therefore, competitive binding assays were employed to establish the affinities of the PROTACs for the ER. Comparison of the binding affinities of selected C-7α PROTACs with C-16α PROTACs demonstrates that the C-7α PROTACs bind the ER with a significantly higher affinity than the C-16α PROTACs (**Figure 4.2**). The dimeric PROTAC and its monomeric counterparts KC-2 and KC-6 bind to ER with the best affinity followed by the KC-3 PROTAC. The lower ER-binding affinity of C-16 PROTACs may explain the low ER degradation induced by the C-16 PROTACs. Based on this data and the data from **Figure 3.4**, it was concluded that a C-16α based PROTAC will not be a useful PROTAC strategy.

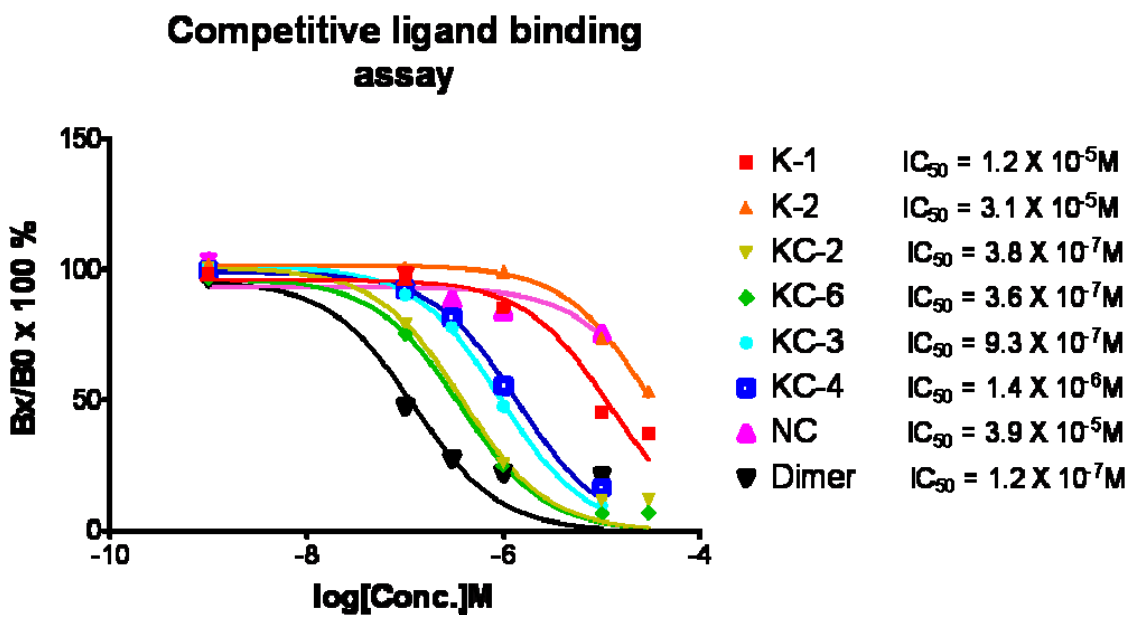

Figure 4.2 Relative binding affinities of C-7α PROTACs and C-16α PROTACs. Competitive ligand binding assays were performed as described in "Materials and Methods" using purified ERα . The ordinate is Bx/Bo, specifically bound radioligand in the presence of a given amount of competitor (Bx) divided by specifically bound radioligand in the absence of competitor. The values represent the mean ± SE and are represented as percent of that obtained using [^{3}H]-17β estradiol alone.

Comparison of linker lengths 9, 12 and 16 atoms (KC-1, KC-2 and KC-3 respectively):

The linker between the two moieties of the PROTAC has not been optimized; therefore, to establish the optimal linker length required for PROTAC activity, five PROTACs with varying linker lengths were developed (chapter 3). The short linker PROTACs within the series, KC-1 and KC-2 was compared to KC-3, the mid-length PROTAC for their ability to degrade the ER in MCF-7 cells. As evidenced in **Figure 4.3** western blot data indicated that all PROTACs were capable of degrading the ER at the concentrations tested.

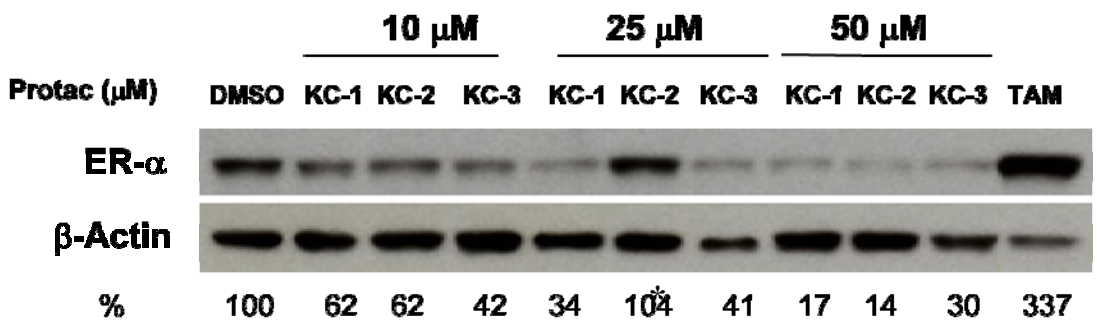

Figure 4.3 Analyses of C-7α PROTACs KC-1, KC-2 and KC-3 on ER degradation. MCF-7 cells were treated with PROTACs at the indicated concentrations or with DMSO or TAM (5 μM) for 48hrs. Cells were lysed and analyzed via western blot using anti ERα antibody. The intensities of the bands were quantified (%) using volumetric densitometry (Quantity One, Bio-Rad). The ERα values were normalized to β-actin and DMSO was arbitrarily assigned a value of 100% for comparison purposes. *data are not typical of KC-2 at that concentration.

Comparison of linker lengths 16, 19 and 21 atoms (KC-3, KC-4 and KC-5 respectively)

We next wanted to determine the maximum linker length required for PROTAC activity. Accordingly, the activity of the two longest linker PROTACs, KC-4 and KC-5, were evaluated along with KC-3 for their ability to degrade the ER. Western blot analysis indicates a higher level of ER degradation, in a dose dependent manner, in the presence of KC-3 while KC-4 and KC-5 had very little effect on inducing ER degradation, (**Figure 4.4**). This suggests that the linkers between the two moieties in KC-4 and KC-5 may be too long to allow for effective ubiquitin transfer to the ER and as such is unable to recruit the ER to the proteasome for degradation.

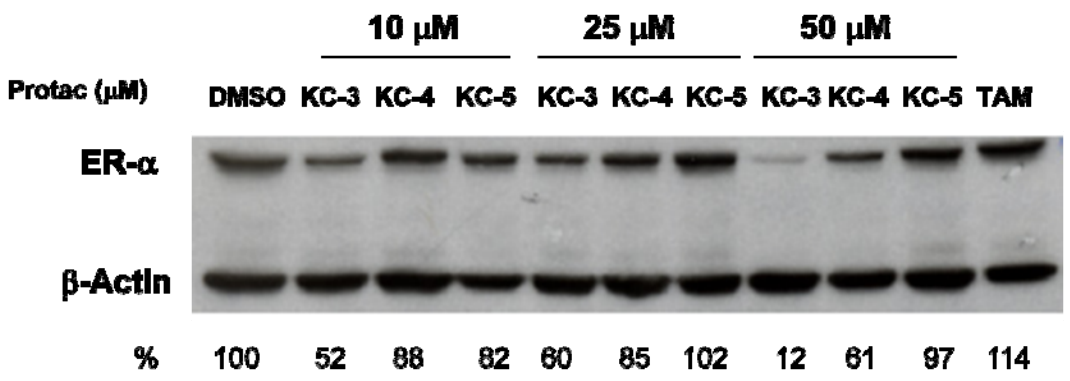

Figure 4.4 ER degradation by KC-3, KC-4 and KC-5. MCF-7 cells were treated with PROTACs at the indicated concentrations or with DMSO or TAM (5 μM) for 48hrs. Cells were lysed and analyzed via western blot using anti ERα antibody. The intensities of the bands were quantified (%) using volumetric densitometry (Quantity One, Bio-Rad). The ERα values were normalized to β-actin and DMSO was arbitrarily assigned a value of 1 for comparison purposes.

Effects of low PROTAC dose on the degradation of ER:

Based on the fact that KC-1, KC-2 and KC-3 showed an ability to induce ER degradation (**Figure 4.3**); we wanted to investigate the ability of all the PROTACs to degrade ER at a low dose to determine which was more potent. All PROTACs, with the exception of KC-3, caused a significant accumulation of the ER that was comparable to the levels induced by tamoxifen. KC-3 had no significant effect on ER accumulation at low concentrations (**Figure 4.5**), suggesting again a possible role for linker length in PROTAC activity, where KC-3 could represent an optimal spacer between the two moieties.

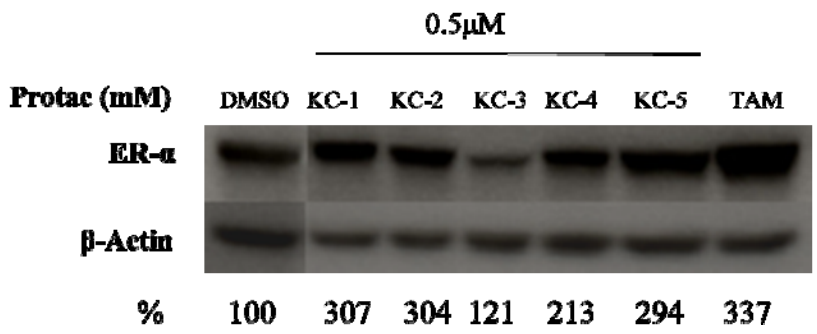

Figure 4.5: Effect on ER degradation at low doses of PROTACs. MCF-7 cells were treated with PROTACs at the indicated concentrations or with DMSO or TAM (5 μM) for 48hrs. Cells were lysed and analyzed via western blot using anti ERα antibody. The intensities of the bands were quantified (%) using volumetric densitometry (Quantity One, Bio-Rad). The ERα values were normalized to β-actin and DMSO was arbitrarily assigned a value of 100% for comparison purposes.

Proteasome dependent ER degradation induced by PROTAC:

An appropriately designed PROTAC will require the ubiquitin proteasome pathway for its action. The proposed mechanism of action of PROTACs, as discussed in Chapter 2, is that upon binding of the PROTAC to the ER the HIF-1α derived pentapeptide will be recognized by the pVHL, and the ER-PROTAC complex will be ubiquitinated and ultimately degraded by the proteasome. In order to examine the proteasome dependence of the PROTAC, a specific proteasome inhibitor, epoxomicin (epx), was used (**Figures 4.6 and 4.7**). The results showed that epoxomicin significantly inhibited ER degradation at a concentration of 100 nM, indicating that ER degradation by the PROTACs is proteasome-dependent.

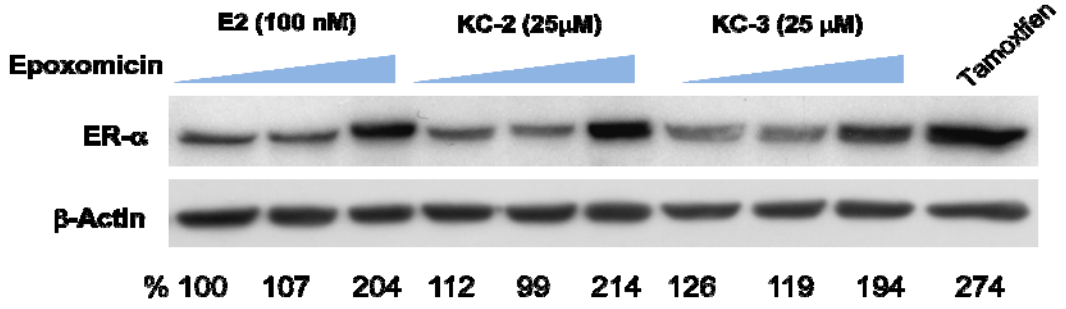

Figure 4.6 Proteasome dependent degradation of ER by PROTACs. MCF-7 cells were co-treated with increasing concentrations (10, 50, 100 nM) of the proteasome inhibitor epoxomicin and PROTACs (25 μM) or E2 (100 nM) or TAM (5 μM, positive control) for 48hrs. Cells were lysed and analyzed via western blot using anti ERα antibody. The intensities of the bands were quantified (%) using volumetric densitometry (Quantity One, Bio-Rad). The ERα values were normalized to β-actin and DMSO was arbitrarily assigned a value of 100% for comparison purposes.

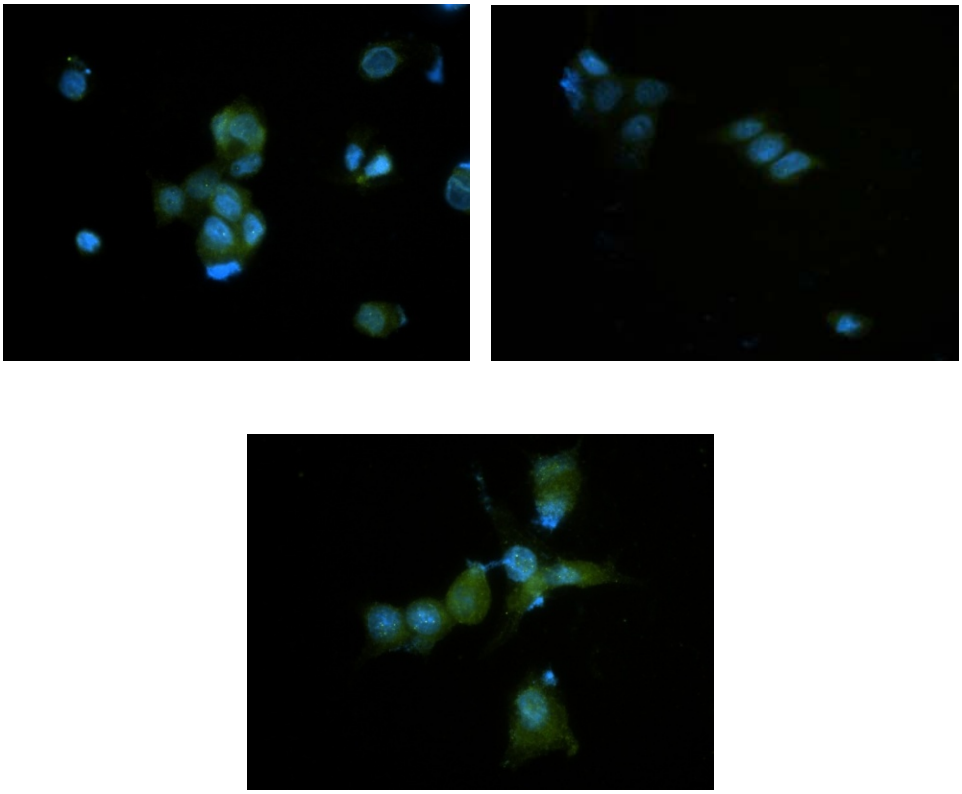

Figure 4.7 Determination of ER degradation via immunofluorescence following treatment with DMSO, KC-3 PROTAC and proteasome inhibitor epoxomicin (Epx). MCF-7 cells were treated with DMSO or KC-3 or KC-3 and Epx for 48 hrs. Cells were then fixed on glass slides and treated with ERα monoclonal antibody, DAPI and secondary antibody FITC. Green (estrogen receptor-FITC), blue (DAPI nuclear stain)

Protac is dependent on E3 ubiquitin ligase:

It is not sufficient to show proteasome dependence as the ER itself is targeted for degradation by the UPS. In that case, degradation of ER is tied to E2-ER induced transcriptional activation of target genes [206, 207]. The ability of the PROTACs to be specifically recognized by the pVHL E3 ligase complex is key for the action of PROTACs. In that respect a negative control PROTAC, NC, was synthesized lacking the critical hydroxyl proline required for pVHL E3 ubiquitin ligase recognition. Evaluation

of NC and KC-2, that both contain the same linker length suggests that the pVHL is required for the PROTAC-induced ER degradation (**Figure 4.8**), as KC-2, which has the proline residue, was better at inducing ER degradation, than NC.

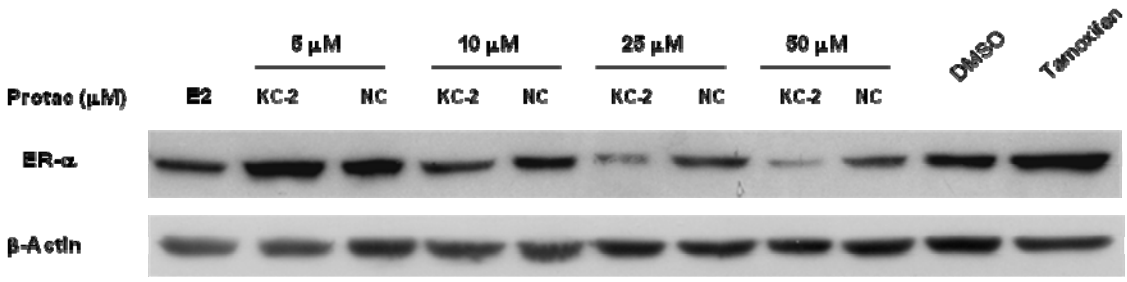

Figure 4.8 Evaluation of the pVHL dependence for PROTAC activity. MCF-7 cells were treated with PROTACs at the indicated concentrations or with DMSO, E2 (10 nM), or TAM (5 μM) for 48hrs. Cells were lysed and analyzed via western blot using anti ERα antibody. NC (negative control PROTAC)

C- vs. N-terminus pentapeptide coupling

Coupling of the pentapeptide to the linker is through the N-terminal Leu residue while the C-terminal Ile is protected with a benzyl group. To investigate whether the site for coupling of the linker to the pentapeptide is important for PROTAC activity, an alternative PROTAC, KC-6, which has an N-terminal Z group and is coupled to the linker via the C-terminal Ile was developed. KC-2, which has the same linker as KC-6, but is connected to the linker via the N terminal Leu residue, was compared with KC-6. Western blot analysis showed that KC-2 was more effective at causing degradation of the ER, indicating a possible role for peptide orientation in PROTAC activity (**Figure 4.9**).

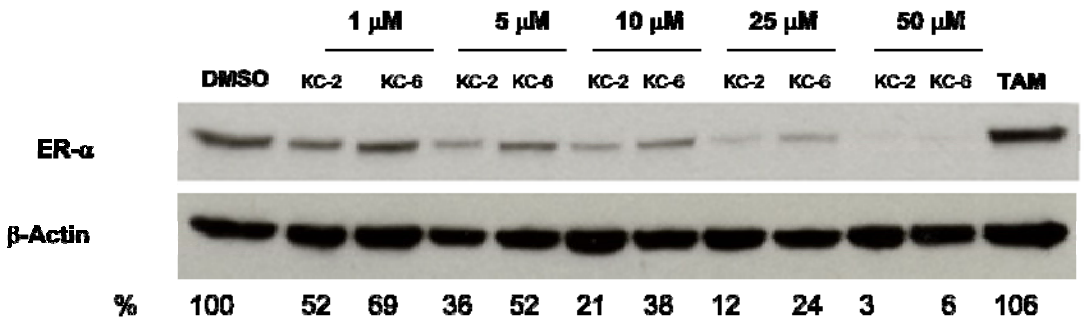

Figure 4.9 N- terminus (KC-2) coupling vs C- terminus (KC-6). MCF-7 cells were treated with increasing concentrations of PROTACs DMSO or TAM (5 μM) for 48hrs. Cells were lysed and analyzed via western blot using anti ERα antibody. The intensities of the bands were quantified (%) using volumetric densitometry (Quantity One, Bio-Rad). The ERα values were normalized to β-actin and DMSO was arbitrarily assigned a value of 100%.

KC-3 inhibits MCF-7 cell proliferation with an IC_{50} similar to that of tamoxifen

An optimum PROTAC will have the ability to block the proliferation of MCF-7 cells which express high levels of ER. A cell viability assay (MTS) as described in materials and methods was used to test the effects of PROTACs on MCF-7 cell proliferation. The dose response curves **(Figure 4.10)** and the IC_{50} for the various PROTACs are summarized in Table 4.1. Although a number of PROTACs were capable of degrading the ER, an investigation of the IC_{50} values indicated that the KC-3 PROTAC was most effective in blocking proliferation of MCF-7 cells, displaying values comparable to tamoxifen (Table 4.1). This data combined with the degradation data, suggested that the KC-3 PROTAC may the optimal length PROTAC among the monomeric PROTACs.

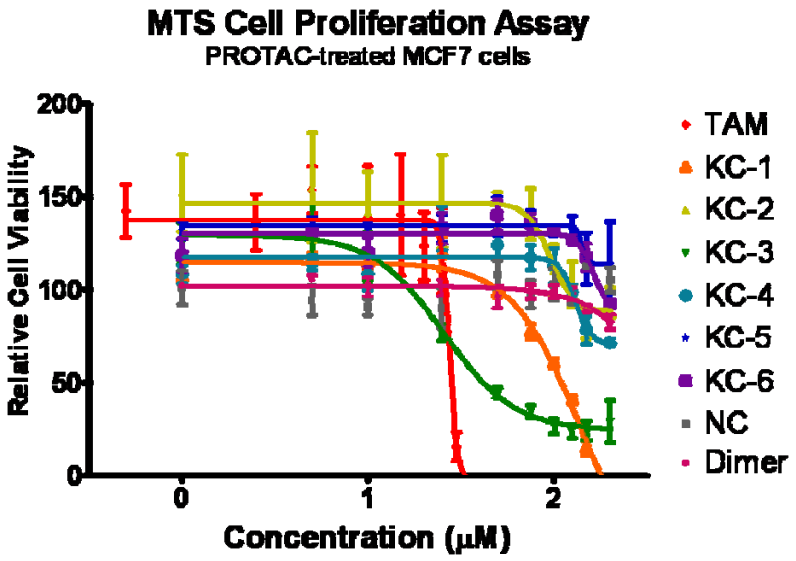

Figure 4.10 Dose response curves from MTS cell proliferation assay. Following the treatment of MCF-7 cells with PROTACs or Tamoxifen for 48 hrs, MTS assay was performed as stated in "Materials and Methods". The IC_{50} values (Table 4.1) were obtained In GraphPad Prism® (San Diego, USA), from a sigmoid dose-response curve using a nonlinear regression to a logarithmic function. Data represent at least three replicates.

Table 4.1 IC_{50} values of PROTACs

Compound	Dosage	IC_{50} (μM)	Error 95% CI
Tamoxifen	0.50μM to 50μM	27.43	± 2.59
KC-1	1μM to 200μM	139.3	± 49.85
KC-2	1μM to 200μM	94.82	± 18.66
KC-3	1μM to 200μM	25.68	± 5.83
KC-4	1μM to 200μM	> 200	---
KC-5	1μM to 200μM	> 200	---
KC-6	1μM to 200μM	162.9	± 90.23
NC	1μM to 200μM	> 200	---
Dimer	1μM to 200μM	> 200	---

KC-3 does not induce ER-regulated progesterone receptor (PR) to the same extent as E2.

To assess the capability of the optimal length PROTAC to influence ER regulated transcriptional activity, the PR, a known downstream target of the ER, was analyzed using qRT-PCR. As indicated in **Figure 4.11**, while E2 resulted in an approximately 10-fold increase in PR mRNA relative to control neither tamoxifen nor KC-3 displayed such a high increase in PR transcription, indicating that the binding of KC-3 to the ER, results in some agonistic activity, but not to the same extent as E2. A higher concentration of KC-3 may be required to cause significant PR downregulation.

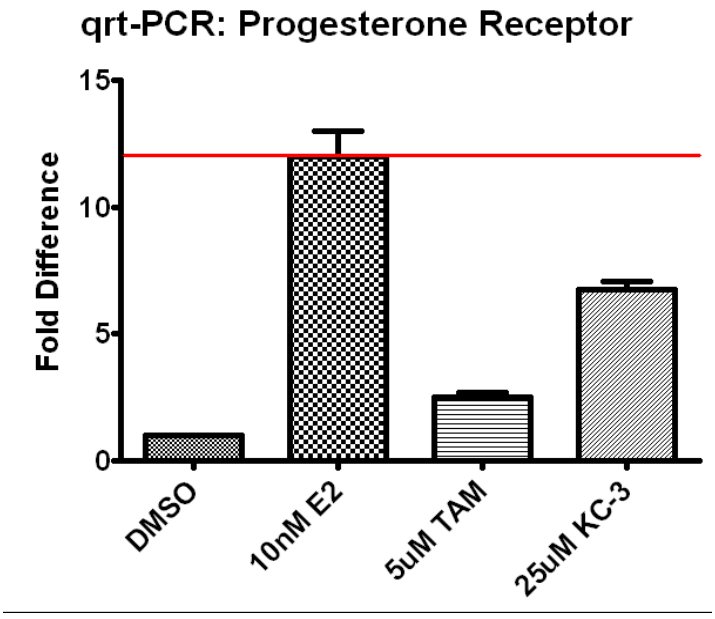

Figure 4.11 qrt-PCR for progesterone receptor (PR). Graph represents the fold difference in PR mRNA levels following 48 hr treatment of MCF-7 cells with DMSO, E2, KC-3 or TAM. The mRNA levels are quantified by normalization to β-actin. Data represent at least three replicates.

Activity of KC-7/dimeric PROTAC vs monomeric PROTACs KC-2, KC-6 and NC

A dimeric PROTAC was developed in order to determine whether a PROTAC strategy that uses two ligands is more efficient at targeting the ER than a monomeric one. The dimeric PROTAC was evaluated for its action on ER. Western blot analysis and immunofluorescence was used to analyze the abundance of ER following treatment with dimeric PROTAC. Data revealed that the dimeric PROTAC had a significant effect on ER degradation in comparison to its monomeric counterparts; at 10 μM the dimer was capable of degrading relatively all the ER as indicated in **Figure 4.12**. The activity of the dimer also appear to be proteasome dependent, as addition of the proteasome inhibitor epoxomicin (Epx) blocked the degradation of ER, as indicated by the immunofluorescence data (**Figure 4.13**). The effect of dimer on proliferation was also evaluated in Table 4.1 and the results indicated, surprisingly, that the dimer had no effect on proliferation at concentrations up to 200μM. This may indicate that the dimer functions as an ER agonist as ER agonists are known to induce ER degradation in concert with transcriptional activation [208].

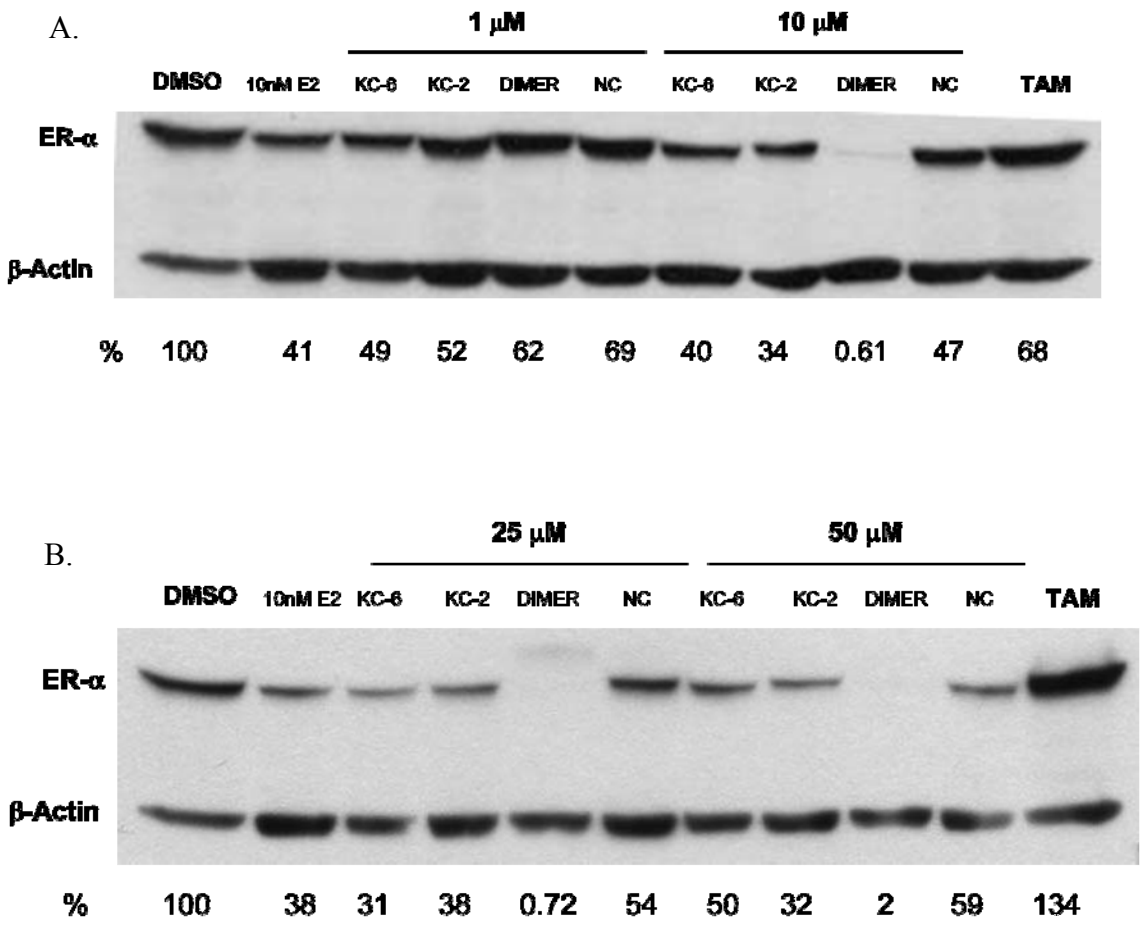

Figure 4.12 Comparison of KC-7/dimeric PROTAC with monomeric KC-2, KC-6 and NC. MCF-7 cells were with increasing concentrations of PROTACs DMSO or TAM (5 μM) for 48hrs. Cells were lysed and analyzed via western blot using anti ERα antibody. The intensities of the bands on western blot films were quantified (%) using volumetric densitometry (Quantity One, Bio-Rad). The ERα values were normalized to β-actin and DMSO was arbitrarily assigned a value of 100% for comparison purposes.

Media only

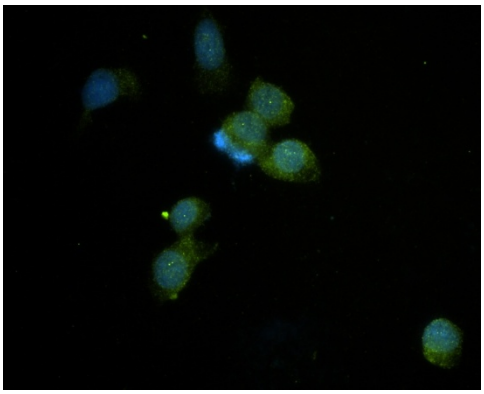

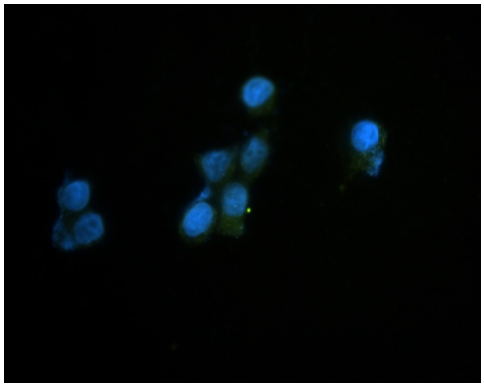

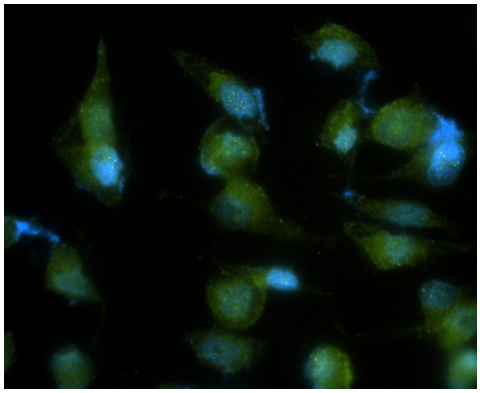

10μM dimer

10μM dimer + Epx

Figure 4.13: Analysis of ER status via immunofluorescence following treatment with dimer PROTAC and proteasome inhibitor epoxomicin (Epx). MCF-7 cells were treated with DMSO or dimer or dimer and Epx for 48 hrs. Cells were then fixed on glass slides and treated with ERα monoclonal antibody, DAPI and secondary antibody FITC. Green (estrogen receptor-FITC), blue (DAPI nuclear stain).

CHAPTER 5: CONCLUSIONS AND DISCUSSION

5.1 Conclusions and discussion

The data contained herein provides a rational blueprint for the optimization of the design of an ER-targeting PROTAC. First, data obtained from the original E2-penta (O-17 derivative) and C-16α PROTACs demonstrate that derivatizations at the C-16α position does not improve the ability of the PROTAC to degrade the ER when compared to the original PROTAC. While the presence of C-C bond instead of an ester bond may offer increased resistance to *in vivo* esterases, additional factors, such as binding affinity, are likewise essential for the judicious design of PROTACs. Interestingly, conjugation at the C-16α position showed efficient ER degradation for an E2-Geldanamycin hybrid [182], probably by disrupting the ER:HSP90 complex. However, the hybrid's mode of action is not entirely clear. Consistent with our results, earlier works by Fevig et al. suggested that the tolerance for long, bulky substituents at the C-16α position is generally not high [209]. Nonetheless, the lesson from these C-16α PROTACs is that a benzyl protecting group at the C-terminal of the E3 ubiquitin ligase recognition motif enhances PROTAC activity compared to unprotected counterparts (Figure 3.4 and 3.5). It is believed that the benzyl group mimics the ODD region of HIF-1α, which is flanked by polypeptides and as such, the benzyl group may provide structural stability as well as protect the pentapeptide from peptidase attack.

Based on the conclusions drawn from the C-16α data, all remaining PROTACs were synthesized using the benzyl protected E3 ligase recognition motif. Several studies suggest that the C-7α position can be modified using long linkers without significant loss of ER binding affinity [178, 203, 204, 205]. Thus, we derivatized the C-7α position of estradiol to attach linkers of varying lengths for the optimization of the ER-targeting PROTAC.

As Corson et al. point out, a linker has to be long enough to allow flexibility with the proper interactions between each moiety and its respective protein target, but short enough to allow for the proper interface between the two units [210]. This is in accordance with this data using C-7 derivatized PROTACs. Specifically, it has been shown here that linker length selection is crucial for promoting the desired PROTAC activity. A linker that is too short may generate steric hindrance between the two partner proteins,

preventing efficient ubiquitin transfer to the target. On the other hand, a linker that is too long may hinder the proper interaction between the E3 ubiquitin ligase and target protein.

While PROTACs with nine and twelve atom linker length, KC-1 and KC-2, respectively, showed an ability to degrade the ER in a concentration dependent manner, they are considered less effective than KC-3. Both KC-1 and KC-2 induced ER accumulation at low concentrations (500 nM), whereas KC-3, (16-atom length linker), did not induce significant accumulation of the ER at the concentrations tested. Overall, KC-3 was the most effective PROTAC as it induced potent ER degradation and successfully inhibited MCF-7 cell proliferation. Given that most ER regulated genes are associated with cell proliferation [158], increased degradation of the ER by the PROTAC should elicit a lower expression of these genes, inhibiting cell proliferation. The effectiveness of the KC-3 PROTAC may be due its linker length, wherein the 16-atom spacer allows for the most effective interaction between ER and the E3 ligase complex.

Another important lesson from these studies concerns the coupling of the ligand to the pentapeptide. Attachment of the small molecule ligand at the N-terminus of the HIF-1α pentapeptide is favored for PROTAC activity, as the activity of the PROTAC decreased when estradiol was attached at the C-terminus of the HIF-1α pentapeptide. Prior studies revealed a possible role for Tyr in enhancing the interaction of pVHL to the ODD, while other residues in the ODD were not essential [99]. However, if the residue following Ile in the ODD sequence is considered, the Pro structure may be emulated by the benzyl ring at the C-ternimus of the pentapeptide. Such homology might well account for the superiority of the N-terminal coupling.

The negative control PROTAC (NC), in which, the critical hydroxy-proline is replaced with norleucine, did not induce ER degradation. This is significant because its active counterpart, KC-2, effectively induces ER degradation. Replacement of the hydroxy-proline abrogrates the interaction between the HIF derived pentapeptide and the pVHL E3-ligase complex, which is essential for the action of the PROTAC.

The synthesis of a dimeric PROTAC was undertaken in an attempt to improve the efficiency of the PROTAC strategy. The hypothesis for the design of the dimeric PROTAC was twofold; first, since dimerization of the ER is a consequence of ligand binding, association of a dimeric PROTAC with the ER could theoretically mirror this

process. Additionally, it was thought that the presence of two ligands on either end of the HIF pentapeptide should increase the likelihood of an interaction between the PROTAC and ER. As shown in Figure 4.11, administration of the dimer resulted in very effective ER degradation at concentrations lower than either of its corresponding monomeric halves, KC-2 and KC-6.

However, the enhanced ER degradation by dimer did not translate to an effect on MCF-7 cell proliferation, as demonstrated by the high IC_{50} value (Table 4.1). This result is similar to a previous study conducted using estrone dimers. The estrone dimers were incapable of inhibiting breast cancer cell proliferation and displayed IC_{50} values similar to E2 (>200 μM), leading the authors to postulate that the dimers may function as an E2-like compound [200]. This is a reasonable justification of the data seen with the dimeric PROTAC, as it too displayed no effect on MCF-7 cell proliferation.

There are a few likely rationales for this discrepancy between the monomeric and dimeric PROTACs. The first point to consider is that the dimeric PROTAC may bind either to one ER or to a pair of ERs, resulting in their dimerization. Dimer binding to a pair of ERs may thus result in agonistic activity similar to the binding of the cognate ligand. Binding of the cognate ligand results in transcriptional activation of target genes a process that requires degradation of the ER [208]. Likewise, since the linker between each E2 and the HIF-1α pentapeptide is 12 atoms, its inherent flexibility might promote conformational changes that impede the interaction between the pentapeptide and the E3 ligase. This hindrance of E3-PROTAC interaction would effectively prevent the pVHL-mediated ubiquitination and degradation of the ER, while likely leading to transcriptional activation of target genes and subsequent degradation of the ER. .

While the current dimer PROTAC did not have many advantageous properties, the binding affinity experiment clearly indicates that the dimer has high affinity for the ER. This demonstrates the potential for a dimeric PROTAC approach to effectively bind a target protein, which may result in the efficient recruitment of the target protein to the E3 ubiquitin ligase. To further validate the dimeric PROTAC approach, a dimeric PROTAC that uses tamoxifen (antagonist) instead of the agonist (estradiol) should be explored. This will eliminate the agonistic activity of the dimeric PROTAC that was observed in this study. To conclusively determine the mode of action of the dimeric

PROTAC, a negative control dimer should be prepared as well. Additionally, analogous to what was done for the monomeric PROTACs, it will be interesting to develop dimers with varying spacers to assess the optimal linker for a dimeric PROTAC.

Therefore, the general conclusions that can be made from these studies are as follows:

1. An optimum ER-targeting monomeric PROTAC (KC-3) has a spacer of about 16 atoms between the E2, attached at the C-7α position, and the HIF-1α pentapeptide attached at the N-terminus.

2. The monomeric PROTAC is capable of targeting the ER for degradation in a proteasome- and pVHL-dependent manner.

3. The optimal PROTAC (KC-3) inhibits proliferation of MCF-7 cells with an IC_{50} similar to that of tamoxifen.

4. KC-3 alone does not induce the transcription of PR, a downstream target of the ER, to the same extent as E2.

5. A dimeric PROTAC binds the ER, induces ER degradation and functions in a proteasome dependent manner, but more studies are needed to validate the dimeric PROTAC approach.

5.2 Future directions:

While this project has provided a great deal of information about the overall design of an ER-targeting PROTAC, there are still some avenues that are currently unexplored. For example, what is the potential of an ER-targeting PROTAC as a therapeutic agent? The effect of ER-targeting PROTACs has only been analyzed in MCF-7 cell lines. An analysis of the actions of PROTAC in other ER expressing cells or tissues such as the uterus and bone should be undertaken in the future to decide whether PROTAC activity varies from one tissue to the other. This is essential information to obtain prior to the consideration of an ER-targeting PROTAC as a therapeutic agent. Also, in terms of therapeutic value, an ER-targeting PROTAC could be of tremendous

benefit in cases where resistance to tamoxifen and other antiestrogens have developed, as the ER is still present and functional in cases of resistance; therefore the activity of KC-3 in tamoxifen/antiestrogen resistant cells should be evaluated.

Additionally, the effect of other ER ligands, such as tamoxifen and genistein (phytoestrogen) among others, should be explored. Tamoxifen is a known SERM that binds the ER and displays both antagonistic and agonistic activities depending on its tissue binding, whereas genistein is a flavone that binds the ER and induce estrogen-like activities. The mechanism of PROTAC activity currently presumes that any ligand capable of binding the ER should engender a stable complex facilitating the ubiquitination and degradation of the ER. Showing that any ligand capable of binding the ER can target the protein for degradation in a PROTAC-dependent manner will further strengthen the idea of the approach.

A major drawback to the PROTAC approach as it is utilized currently is the inclusion of a peptide moeity. The pentapetide as the E3-ligase recognition motif may be subjected to peptidase activity *in vivo*, thus replacement of the pentapeptide with a non-peptide moiety such as a peptidomimetic or a small molecule may be useful in future design of a PROTAC. This change in the structure of the PROTAC may require a reoptimization of the linker length.

One of the goals in undertaking this study was to provide a potential blueprint for the design of PROTACs targeting other proteins. From the studies conducted up to this point, a few generalizations can be made. First, the PROTAC has been shown to be a tool that can be used to target any protein with a known ligand specifically to the UPS for degradation. Secondly, these studies demonstrate that a pentapeptide derived from HIF-1α is sufficient for the activity of these PROTACs. Additionally, both the location of the attachment to the linker and length of the linker moiety are critical for the optimization of the PROTAC design. A sixteen atom linker proved to be optimal for a monomeric ER-targeting PROTAC; however, more experiments should be conducted to ascertain whether this linker length will be generally applicable in the design of PROTACs targeting other proteins.

More specifically, the design of the ER-targeting PROTAC may provide some insights for the design of other PROTACs targeting nuclear receptors, as they are

structurally similar to the ER. Still, adjustments will likely be required to accommodate the specific ligands for these other protein targets. However, because of the high homology within the nuclear receptor family, the ER-PROTAC may provide a good starting point for the design of other nuclear receptor-targeting PROTACs.

Overall, the PROTAC approach could be a useful strategy for probing proteins with known ligands. More studies need to be done using the current model to develop PROTACs that target other proteins to validate the general application of this strategy.

REFERENCES

1. Sakamoto, K.M., et al., Protacs: chimeric molecules that target proteins to the Skp1-Cullin-F box complex for ubiquitination and degradation. Proc Natl Acad Sci U S A, 2001. **98**(15): p. 8554-9.

2. Bargagna-Mohan, P., et al., Use of PROTACS as molecular probes of angiogenesis. Bioorganic & Medicinal Chemistry Letters, 2005. **15**(11): p. 2724-2727.

3. Puppala, D., et al., Development of an aryl hydrocarbon receptor antagonist using the proteolysis-targeting chimeric molecules approach: a potential tool for chemoprevention. Mol Pharmacol, 2008. **73**(4): p. 1064-71.

4. Rodriguez-Gonzalez, A., Cyrus, K., et al., Targeting steroid hormone receptors for ubiquitination and degradation in breast and prostate cancer. Oncogene, 2008. **27**(57): p. 7201-11.

5. Sakamoto, K.M. and J.D. Raymond, Chimeric Molecules to Target Proteins for Ubiquitination and Degradation, in *Methods in Enzymology*. 2005, Academic Press. p. 833-847.

6. Schneekloth, J.S., et al., Chemical Genetic Control of Protein Levels: Selective in Vivo Targeted Degradation. Journal of the American Chemical Society, 2004. **126**(12): p. 3748-3754.

7. Zhang, D., et al., Targeted Degradation of Proteins by Small Molecules: A Novel Tool for Functional Proteomics. Combinatorial Chemistry & High Throughput Screening, 2004. **7**(7): p. 689-697.

8. Zhang, D., et al., Degradation of target protein in living cells by small-molecule proteolysis inducer. Bioorganic & Medicinal Chemistry Letters, 2004. **14**(3): p. 645-648.

9. Lee, H., et al., Targeted degradation of the aryl hydrocarbon receptor by the PROTAC approach: a useful chemical genetic tool. Chembiochem, 2007. **8**(17): p. 2058-62.

10. Enmark, E. and J.A. Gustafsson, Oestrogen receptors - an overview. J Intern Med, 1999. **246**(2): p. 133-8.

11. Macgregor, J.I. and V.C. Jordan, Basic Guide to the Mechanisms of Antiestrogen Action. Pharmacol Rev, 1998. **50**(2): p. 151-196.

12. Ring, A. and M. Dowsett, Mechanisms of tamoxifen resistance. Endocr Relat Cancer, 2004. **11**(4): p. 643-58.

13. Sarwar, N., et al., Phosphorylation of ER{alpha} at serine 118 in primary breast cancer and in tamoxifen-resistant tumours is indicative of a complex role for ER{alpha} phosphorylation in breast cancer progression. Endocr Relat Cancer, 2006. **13**(3): p. 851-861.

14. Holm, C., et al., Phosphorylation of the oestrogen receptor alpha at serine 305 and prediction of tamoxifen resistance in breast cancer. J Pathol, 2009. **217**(3): p. 372-9.

15. Schneekloth, J.S., Jr. and C.M. Crews, Chemical approaches to controlling intracellular protein degradation. Chembiochem, 2005. **6**(1): p. 40-6.

16. Schreiber, S.L., Chemical genetics resulting from a passion for synthetic organic chemistry. Bioorg Med Chem, 1998. **6**(8): p. 1127-52.

17. Kawasumi, M. and P. Nghiem, Chemical genetics: elucidating biological systems with small-molecule compounds. J Invest Dermatol, 2007. **127**(7): p. 1577-84.

18. Walsh, D.P. and Y.T. Chang, Chemical genetics. Chem Rev, 2006. **106**(6): p. 2476-530.

19. Stockwell, B.R., Frontiers in chemical genetics. Trends Biotechnol, 2000. **18**(11): p. 449-55.

20. Darvas, F., et al., Recent advances in chemical genomics. Curr Med Chem, 2004. **11**(23): p. 3119-45.

21. Blackwell, H.E. and Y. Zhao, Chemical genetic approaches to plant biology. Plant Physiol, 2003. **133**(2): p. 448-55.

22. Asami, T., et al., The Influence of Chemical Genetics on Plant Science: Shedding Light on Functions and Mechanism of Action of Brassinosteroids Using Biosynthesis Inhibitors. J Plant Growth Regul, 2003. **22**(4): p. 336-349.

23. Zheng, X.F. and T.F. Chan, Chemical genomics in the global study of protein functions. Drug Discov Today, 2002. **7**(3): p. 197-205.

24. Lewandoski, M., Conditional control of gene expression in the mouse. Nat Rev Genet, 2001. **2**(10): p. 743-55.

25. Yarranton, G.T., Inducible vectors for expression in mammalian cells. Curr Opin Biotechnol, 1992. **3**(5): p. 506-11.

26. Hannon, G.J., RNA interference. Nature, 2002. **418**(6894): p. 244-51.

27. Bernstein, E., et al., Role for a bidentate ribonuclease in the initiation step of RNA interference. Nature, 2001. **409**(6818): p. 363-6.

28. Zamore, P.D., et al., RNAi: double-stranded RNA directs the ATP-dependent cleavage of mRNA at 21 to 23 nucleotide intervals. Cell, 2000. **101**(1): p. 25-33.

29. Spring, D.R., Chemical genetics to chemical genomics: small molecules offer big insights. Chem Soc Rev, 2005. **34**(6): p. 472-82.

30. Mayer, T.U., Chemical genetics: tailoring tools for cell biology. Trends Cell Biol, 2003. **13**(5): p. 270-7.

31. Shuker, D.E.G., Chemical Genetics. Annu. Rep. Prog. Chem., Sect. B: Org. Chem., 2004. **100**: p. 191-205.

32. Ward, G.E., K.L. Carey, and N.J. Westwood, Using small molecules to study big questions in cellular microbiology. Cell Microbiol, 2002. **4**(8): p. 471-82.

33. MacBeath, G., Chemical genomics: what will it take and who gets to play? Genome Biol, 2001. **2**(6): p. COMMENT2005.

34. Lehar, J., et al., Combination chemical genetics. Nat Chem Biol, 2008. **4**(11): p. 674-81.

35. Shokat, K. and M. Velleca, Novel chemical genetic approaches to the discovery of signal transduction inhibitors. Drug Discov Today, 2002. **7**(16): p. 872-9.

36. Zheng, X.S., T.F. Chan, and H.H. Zhou, Genetic and genomic approaches to identify and study the targets of bioactive small molecules. Chem Biol, 2004. **11**(5): p. 609-18.

37. Alaimo, P.J., M.A. Shogren-Knaak, and K.M. Shokat, Chemical genetic approaches for the elucidation of signaling pathways. Curr Opin Chem Biol, 2001. **5**(4): p. 360-7.

38. Knight, Z.A. and K.M. Shokat, Chemical genetics: where genetics and pharmacology meet. Cell, 2007. **128**(3): p. 425-30.

39. Haggarty, S.J., et al., Domain-selective small-molecule inhibitor of histone deacetylase 6 (HDAC6)-mediated tubulin deacetylation. Proc Natl Acad Sci U S A, 2003. **100**(8): p. 4389-94.

40. Hideshima, T., et al., Small-molecule inhibition of proteasome and aggresome function induces synergistic antitumor activity in multiple myeloma. Proc Natl Acad Sci U S A, 2005. **102**(24): p. 8567-72.

41. Knight, Z.A., et al., A pharmacological map of the PI3-K family defines a role for p110alpha in insulin signaling. Cell, 2006. **125**(4): p. 733-47.

42. He, M.M., et al., Small-molecule inhibition of TNF-alpha. Science, 2005. **310**(5750): p. 1022-5.

43. Halazy, S., Chemical genetics: toward the next generation of molecular medicines. Pharmacogenomics, 2004. **5**(7): p. 757-61.

44. Abel, U., et al., Modern methods to produce natural-product libraries. Current Opinion in Chemical Biology, 2002. **6**(4): p. 453-458.

45. Lokey, R.S., Forward chemical genetics: progress and obstacles on the path to a new pharmacopoeia. Current Opinion in Chemical Biology, 2003. **7**(1): p. 91-96.

46. Khersonsky, S.M. and Y.T. Chang, Strategies for facilitated forward chemical genetics. Chembiochem, 2004. **5**(7): p. 903-8.

47. Arya, P., R. Joseph, and D.T. Chou, Toward high-throughput synthesis of complex natural product-like compounds in the genomics and proteomics age. Chem Biol, 2002. **9**(2): p. 145-56.

48. Knepper, K., C. Gil, and S. Brase, Natural product-like and other biologically active heterocyclic libraries using solid-phase techniques in the post-genomic era. Comb Chem High Throughput Screen, 2003. **6**(7): p. 673-91.

49. Breinbauer, R., I.R. Vetter, and H. Waldmann, From protein domains to drug candidates-natural products as guiding principles in the design and synthesis of compound libraries. Angew Chem Int Ed Engl, 2002. **41**(16): p. 2879-90.

50. Brohm, D., et al., Natural products are biologically validated starting points in structural space for compound library development: solid-phase synthesis of dysidiolide-derived phosphatase inhibitors. Angew Chem Int Ed Engl, 2002. **41**(2): p. 307-11.

51. Brohm, D., et al., Solid-phase synthesis of dysidiolide-derived protein phosphatase inhibitors. J Am Chem Soc, 2002. **124**(44): p. 13171-8.

52. Nicolaou, K.C., et al., Natural Product-like Combinatorial Libraries Based on Privileged Structures. 3. The “Libraries from Libraries” Principle for Diversity Enhancement of Benzopyran Libraries. Journal of the American Chemical Society, 2000. **122**(41): p. 9968-9976.

53. Nicolaou, K.C., et al., Natural Product-like Combinatorial Libraries Based on Privileged Structures. 2. Construction of a 10 000-Membered Benzopyran Library by Directed Split-and-Pool Chemistry Using NanoKans and Optical Encoding. Journal of the American Chemical Society, 2000. **122**(41): p. 9954-9967.

54. Nicolaou, K.C., et al., Natural Product-like Combinatorial Libraries Based on Privileged Structures. 1. General Principles and Solid-Phase Synthesis of Benzopyrans. Journal of the American Chemical Society, 2000. **122**(41): p. 9939-9953.

55. Tan, D.S., et al., Synthesis and Preliminary Evaluation of a Library of Polycyclic Small Molecules for Use in Chemical Genetic Assays. Journal of the American Chemical Society, 1999. **121**(39): p. 9073-9087.

56. Pelish, H.E., et al., Use of biomimetic diversity-oriented synthesis to discover galanthamine-like molecules with biological properties beyond those of the natural product. J Am Chem Soc, 2001. **123**(27): p. 6740-1.

57. Mitsopoulos, G., D.P. Walsh, and Y.-T. Chang, Tagged library approach to chemical genomics and proteomics. Current Opinion in Chemical Biology, 2004. **8**(1): p. 26-32.

58. Nicolas Winssinger, J.L.H.B.J.B.P.G.S., From Split-Pool Libraries to Spatially Addressable Microarrays and Its Application to Functional Proteomic Profiling13. Angewandte Chemie International Edition, 2001. **40**(17): p. 3152-3155.

59. Schreiber, S.L., Target-Oriented and Diversity-Oriented Organic Synthesis in Drug Discovery. Science, 2000. **287**(5460): p. 1964-1969.

60. Lam, K.S., et al., A new type of synthetic peptide library for identifying ligand-binding activity. Nature, 1991. **354**(6348): p. 82-4.

61. Houghten, R.A., et al., Generation and use of synthetic peptide combinatorial libraries for basic research and drug discovery. Nature, 1991. **354**(6348): p. 84-6.

62. Stockwell, B.R., Chemical genetics: ligand-based discovery of gene function. Nat Rev Genet, 2000. **1**(2): p. 116-25.

63. Kino, T., et al., FK-506, a novel immunosuppressant isolated from a Streptomyces. I. Fermentation, isolation, and physico-chemical and biological characteristics. J Antibiot (Tokyo), 1987. **40**(9): p. 1249-55.

64. Kino, T., et al., FK-506, a novel immunosuppressant isolated from a Streptomyces. II. Immunosuppressive effect of FK-506 in vitro. J Antibiot (Tokyo), 1987. **40**(9): p. 1256-65.

65. Harding, M.W., et al., A receptor for the immunosuppressant FK506 is a cis-trans peptidyl-prolyl isomerase. Nature, 1989. **341**(6244): p. 758-60.

66. Liu, J., et al., Calcineurin is a common target of cyclophilin-cyclosporin A and FKBP-FK506 complexes. Cell, 1991. **66**(4): p. 807-15.

67. Stockwell, B.R., S.J. Haggarty, and S.L. Schreiber, High-throughput screening of small molecules in miniaturized mammalian cell-based assays involving post-translational modifications. Chem Biol, 1999. **6**(2): p. 71-83.

68. Mayer, T.U., et al., Small Molecule Inhibitor of Mitotic Spindle Bipolarity Identified in a Phenotype-Based Screen. Science, 1999. **286**(5441): p. 971-974.

69. Thorpe, D.S., Forward & reverse chemical genetics using SPOS-based combinatorial chemistry. Comb Chem High Throughput Screen, 2003. **6**(7): p. 623-47.

70. Sakamoto, K.M., et al., Development of Protacs to target cancer-promoting proteins for ubiquitination and degradation. Mol Cell Proteomics, 2003. **2**(12): p. 1350-8.

71. Hicke, L., Gettin' down with ubiquitin: turning off cell-surface receptors, transporters and channels. Trends in Cell Biology, 1999. **9**(3): p. 107-112.

72. Pickart, C.M., Ubiquitin in chains. Trends Biochem Sci, 2000. **25**(11): p. 544-8.

73. Pelzer, C., et al., UBE1L2, a Novel E1 Enzyme Specific for Ubiquitin. J. Biol. Chem., 2007. **282**(32): p. 23010-23014.

74. Jin, J., et al., Dual E1 activation systems for ubiquitin differentially regulate E2 enzyme charging. Nature, 2007. **447**(7148): p. 1135-1138.

75. Hershko, A., Ubiquitin-mediated protein degradation. J Biol Chem, 1988. **263**(30): p. 15237-40.

76. Hershko, A. and A. Ciechanover, The ubiquitin system. Annu Rev Biochem, 1998. **67**: p. 425-79.

77. Hershko, A. and A. Ciechanover, The Ubiquitin System for Protein Degradation. Annual Review of Biochemistry, 1992. **61**(1): p. 761-807.

78. Pickart, C.M., MECHANISMS UNDERLYING UBIQUITINATION. Annual Review of Biochemistry, 2001. **70**(1): p. 503-533.

79. Ciechanover, A., Glickman, M H., The Ubiquitin-mediated Proteolytic System, in *Life sciences for the 21st Century*, S.I. Keinan E., Sela M., Editor. 2004, Wiley-VCH verlag GmbH & Co. p. 93-150.

80. Huibregtse, J.M., et al., A family of proteins structurally and functionally related to the E6-AP ubiquitin-protein ligase. Proc Natl Acad Sci U S A, 1995. **92**(11): p. 5249.

81. Scheffner, M., U. Nuber, and J.M. Huibregtse, Protein ubiquitination involving an E1-E2-E3 enzyme ubiquitin thioester cascade. Nature, 1995. **373**(6509): p. 81-3.

82. Abriel, H., et al., Defective regulation of the epithelial Na+ channel by Nedd4 in Liddle's syndrome. J Clin Invest, 1999. **103**(5): p. 667-73.

83. Zheng, N., et al., Structure of a c-Cbl-UbcH7 Complex: RING Domain Function in Ubiquitin-Protein Ligases. Cell, 2000. **102**(4): p. 533-539.

84. Fang, S., et al., Mdm2 Is a RING Finger-dependent Ubiquitin Protein Ligase for Itself and p53. J. Biol. Chem., 2000. **275**(12): p. 8945-8951.

85. Honda, R. and H. Yasuda, Activity of MDM2, a ubiquitin ligase, toward p53 or itself is dependent on the RING finger domain of the ligase. Oncogene, 2000. **19**(11): p. 1473-6.

86. Zhang, Y., et al., Parkin functions as an E2-dependent ubiquitinâ€“ protein ligase and promotes the degradation of the synaptic vesicle-associated protein, CDCrel-1. Proceedings of the National Academy of Sciences of the United States of America, 2000. **97**(24): p. 13354-13359.

87. Shimura, H., et al., Familial Parkinson disease gene product, parkin, is a ubiquitin-protein ligase. Nat Genet, 2000. **25**(3): p. 302-5.

88. Deshaies, R.J., SCF AND CULLIN/RING H2-BASED UBIQUITIN LIGASES. Annual Review of Cell and Developmental Biology, 1999. **15**(1): p. 435-467.

89. Page, A.M. and P. Hieter, THE ANAPHASE-PROMOTING COMPLEX: New Subunits and Regulators. Annual Review of Biochemistry, 1999. **68**(1): p. 583.

90. Lisztwan, J., et al., The von Hippel-Lindau tumor suppressor protein is a component of an E3 ubiquitin-protein ligase activity. Genes Dev, 1999. **13**(14): p. 1822-33.

91. Iwai, K., et al., Identification of the von Hippelâ€“Lindau tumor-suppressor protein as part of an active E3 ubiquitin ligase complex. Proceedings of the National Academy of Sciences of the United States of America, 1999. **96**(22): p. 12436-12441.

92. Kamura, T., et al., Activation of HIF1Î± ubiquitination by a reconstituted von Hippel-Lindau (VHL) tumor suppressor complex. Proceedings of the National Academy of Sciences of the United States of America, 2000. **97**(19): p. 10430-10435.

93. Semenza, G.L., HIF-1 and human disease: one highly involved factor. Genes Dev, 2000. **14**(16): p. 1983-91.

94. Ivan, M. and W.G. Kaelin, Jr., The von Hippel-Lindau tumor suppressor protein. Curr Opin Genet Dev, 2001. **11**(1): p. 27-34.

95. Ivan, M., et al., HIFalpha Targeted for VHL-Mediated Destruction by Proline Hydroxylation: Implications for O2 Sensing. Science, 2001. **292**(5516): p. 464-468.

96. Ohh, M., et al., Ubiquitination of hypoxia-inducible factor requires direct binding to the beta-domain of the von Hippel-Lindau protein. Nat Cell Biol, 2000. **2**(7): p. 423-7.

97. Huang, L.E., et al., Regulation of hypoxia-inducible factor 1[alpha] is mediated by an oxygen-dependent domain via the ubiquitin-proteasome pathway. Proc. Natl Acad. Sci. USA, 1998. **95**: p. 7987-7992.

98. Masson, N. and P.J. Ratcliffe, HIF prolyl and asparaginyl hydroxylases in the biological response to intracellular O2 levels. J Cell Sci, 2003. **116**(15): p. 3041-3049.

99. Jaakkola, P., et al., Targeting of HIF-alpha to the von Hippel-Lindau Ubiquitylation Complex by O2-Regulated Prolyl Hydroxylation. Science, 2001. **292**(5516): p. 468-472.

100. Min, J.-H., et al., Structure of an HIF-1alpha -pVHL Complex: Hydroxyproline Recognition in Signaling. Science, 2002. **296**(5574): p. 1886-1889.

101. Pickart, C.M. and R.E. Cohen, Proteasomes and their kin: proteases in the machine age. Nat Rev Mol Cell Biol, 2004. **5**(3): p. 177-187.

102. Pamer, E. and P. Cresswell, MECHANISMS OF MHC CLASS Iâ€“RESTRICTED ANTIGEN PROCESSING. Annual Review of Immunology, 1998. **16**(1): p. 323-358.

103. DeMartino, G.N. and T.G. Gillette, Proteasomes: Machines for All Reasons. Cell, 2007. **129**(4): p. 659-662.

104. Dick, T.P., et al., Contribution of Proteasomal beta -Subunits to the Cleavage of Peptide Substrates Analyzed with Yeast Mutants. J. Biol. Chem., 1998. **273**(40): p. 25637-25646.

105. Bochtler, M., et al., THE PROTEASOME. Annual Review of Biophysics and Biomolecular Structure, 1999. **28**(1): p. 295-317.

106. Groll, M., et al., Structure of 20S proteasome from yeast at 2.4 A resolution. Nature, 1997. **386**(6624): p. 463-71.

107. Groll, M., et al., A gated channel into the proteasome core particle. Nat Struct Biol, 2000. **7**(11): p. 1062-7.

108. Lam, Y.A., et al., A proteasomal ATPase subunit recognizes the polyubiquitin degradation signal. Nature, 2002. **416**(6882): p. 763-7.

109. Deveraux, Q., et al., A 26 S protease subunit that binds ubiquitin conjugates. J. Biol. Chem., 1994. **269**(10): p. 7059-7061.

110. Yao, T. and R.E. Cohen, A cryptic protease couples deubiquitination and degradation by the proteasome. Nature, 2002. **419**(6905): p. 403-7.

111. Koulich, E., X. Li, and G.N. DeMartino, Relative Structural and Functional Roles of Multiple Deubiquitylating Proteins Associated with Mammalian 26S Proteasome. Mol. Biol. Cell, 2008. **19**(3): p. 1072-1082.

112. Köhler, A., et al., The Axial Channel of the Proteasome Core Particle Is Gated by the Rpt2 ATPase and Controls Both Substrate Entry and Product Release. Molecular Cell, 2001. **7**(6): p. 1143-1152.

113. Green, S., et al., Cloning of the human oestrogen receptor cDNA. J Steroid Biochem, 1986. **24**(1): p. 77-83.

114. Jensen, E.V. and V.C. Jordan, The estrogen receptor: a model for molecular medicine. Clin Cancer Res, 2003. **9**(6): p. 1980-9.

115. Kuiper, G.G., et al., Cloning of a novel receptor expressed in rat prostate and ovary. Proc. Natl. Acad. Sci. USA, 1996. **93**: p. 5925.

116. Beato, M., P. Herrlich, and G. Schütz, Steroid hormone receptors: Many Actors in search of a plot. Cell, 1995. **83**(6): p. 851-857.

117. Fuller, P.J., The steroid receptor superfamily: mechanisms of diversity. FASEB J., 1991. **5**(15): p. 3092-3099.

118. Edwards, D.P., REGULATION OF SIGNAL TRANSDUCTION PATHWAYS BY ESTROGEN AND PROGESTERONE. Annual Review of Physiology, 2005. **67**(1): p. 335-376.

119. Green, S. and P. Chambon, Nuclear receptors enhance our understanding of transcription regulation. Trends in Genetics, 1988. **4**(11): p. 309-314.

120. Schwabe, J.W.R., et al., The crystal structure of the estrogen receptor DNA-binding domain bound to DNA: How receptors discriminate between their response elements. Cell, 1993. **75**(3): p. 567-578.

121. Kumar, V. and P. Chambon, The estrogen receptor binds tightly to its responsive element as a ligand-induced homodimer. Cell, 1988. **55**(1): p. 145-156.

122. Kumar, V., et al., Functional domains of the human estrogen receptor. Cell, 1987. **51**(6): p. 941-951.

123. Umesono, K. and R.M. Evans, Determinants of target gene specificity for steroid/thyroid hormone receptors. Cell, 1989. **57**(7): p. 1139-1146.

124. O'Malley, B., MINIREVIEW: The Steroid Receptor Superfamily: More Excitement Predicted for the Future. Mol Endocrinol, 1990. **4**(3): p. 363-369.

125. Picard, D., et al., Signal transduction by steroid hormones: nuclear localization is differentially regulated in estrogen and glucocorticoid receptors. Cell Regul, 1990. **1**(3): p. 291-9.

126. Ylikomi, T., et al., Cooperation of proto-signals for nuclear accumulation of estrogen and progesterone receptors. EMBO J, 1992. **11**(10): p. 3681-94.

127. Kumar, V., et al., Localisation of the oestradiol-binding and putative DNA-binding domains of the human oestrogen receptor. EMBO J, 1986. **5**(9): p. 2231-6.

128. MacGregor, J.I. and V.C. Jordan, Basic guide to the mechanisms of antiestrogen action. Pharmacol Rev, 1998. **50**(2): p. 151-96.

129. Brzozowski, A.M., et al., Molecular basis of agonism and antagonism in the oestrogen receptor. Nature, 1997. **389**(6652): p. 753-758.

130. Leclercq, G., et al., Estrogen receptor alpha: impact of ligands on intracellular shuttling and turnover rate in breast cancer cells. Curr Cancer Drug Targets, 2006. **6**(1): p. 39-64.

131. Schwartz, J.A., et al., Mutations Targeted to a Predicted Helix in the Extreme Carboxyl-terminal Region of the Human Estrogen Receptor-alpha Alter Its Response to Estradiol and 4-Hydroxytamoxifen. J. Biol. Chem., 2002. **277**(15): p. 13202-13209.

132. Wang, Y. and C.H.K. Cheng, ER[alpha] and STAT5a cross-talk: interaction through C-terminal portions of the proteins decreases STAT5a phosphorylation, nuclear translocation and DNA-binding. FEBS Letters, 2004. **572**(1-3): p. 238-244.

133. Peters, G.A. and S.A. Khan, Estrogen Receptor Domains E and F: Role in Dimerization and Interaction with Coactivator RIP-140. Mol Endocrinol, 1999. **13**(2): p. 286-296.

134. Lonard, D.M., et al., The 26S Proteasome Is Required for Estrogen Receptor-[alpha] and Coactivator Turnover and for Efficient Estrogen Receptor-[alpha] Transactivation. Molecular Cell, 2000. **5**(6): p. 939-948.

135. Kuiper, G.G., et al., Comparison of the ligand binding specificity and transcript tissue distribution of estrogen receptors alpha and beta. Endocrinology, 1997. **138**(3): p. 863-70.

136. Katzenellenbogen, B.S. and J.A. Katzenellenbogen, Estrogen receptor transcription and transactivation: Estrogen receptor alpha and estrogen receptor beta: regulation by selective estrogen receptor modulators and importance in breast cancer. Breast Cancer Res, 2000. **2**(5): p. 335-44.

137. Hall, J.M. and D.P. McDonnell, The estrogen receptor beta-isoform (ERbeta) of the human estrogen receptor modulates ERalpha transcriptional activity and is a key regulator of the cellular response to estrogens and antiestrogens. Endocrinology, 1999. **140**(12): p. 5566-78.

138. Mosselman, S., J. Polman, and R. Dijkema, ER beta: identification and characterization of a novel human estrogen receptor. FEBS Lett, 1996. **392**(1): p. 49-53.

139. Deroo, B.J., Estrogen receptors and human disease. The Journal of Clinical Investigation, 2006. **116**(3): p. 561-570.

140. Hewitt, S.C., J.C. Harrell, and K.S. Korach, LESSONS IN ESTROGEN BIOLOGY FROM KNOCKOUT AND TRANSGENIC ANIMALS. Annual Review of Physiology, 2005. **67**(1): p. 285-308.

141. Parker, M.G., Structure and function of estrogen receptors. Vitam. Horm., 1995. **51**: p. 267.

142. Levin, E.R., Integration of the extranuclear and nuclear actions of estrogen. Mol Endocrinol, 2005. **19**(8): p. 1951-9.

143. Levin, E.R., Cell localization, physiology, and nongenomic actions of estrogen receptors. J Appl Physiol, 2001. **91**(4): p. 1860-7.

144. McKenna, N.J., et al., Nuclear receptor coactivators: multiple enzymes, multiple complexes, multiple functionsProceedings of Xth International Congress on Hormonal Steroids, Quebec, Canada, 17-21 June 1998. The Journal of Steroid Biochemistry and Molecular Biology, 1999. **69**(1-6): p. 3-12.

145. O'Lone, R., et al., Genomic Targets of Nuclear Estrogen Receptors. Mol Endocrinol, 2004. **18**(8): p. 1859-1875.

146. Fujimoto, N., H. Honda, and S. Kitamura, Effects of environmental estrogenic chemicals on AP1 mediated transcription with estrogen receptors alpha and beta. J Steroid Biochem Mol Biol, 2004. **88**(1): p. 53-9.

147. Marino, M., et al., Distinct Nongenomic Signal Transduction Pathways Controlled by 17beta -Estradiol Regulate DNA Synthesis and Cyclin D1 Gene Transcription in HepG2 Cells. Mol. Biol. Cell, 2002. **13**(10): p. 3720-3729.

148. Aranda, A. and A. Pascual, Nuclear Hormone Receptors and Gene Expression. Physiol. Rev., 2001. **81**(3): p. 1269-1304.

149. Paech, K., et al., Differential ligand activation of estrogen receptors ERalpha and ERbeta at AP1 sites. Science, 1997. **277**: p. 1508.

150. Marino, M., P. Galluzzo, and P. Ascenzi, Estrogen signaling multiple pathways to impact gene transcription. Curr Genomics, 2006. **7**(8): p. 497-508.

151. Saville, B., et al., Ligand-, cell-, and estrogen receptor subtype (alpha/beta)-dependent activation at GC-rich (Sp1) promoter elements. J Biol Chem, 2000. **275**(8): p. 5379-87.

152. Li, C., et al., Requirement of Sp1 and Estrogen Receptor {{alpha}} Interaction in 17{beta}-Estradiol-Mediated Transcriptional Activation of the Low Density Lipoprotein Receptor Gene Expression. Endocrinology, 2001. **142**(4): p. 1546-1553.

153. Sun, G., W. Porter, and S. Safe, Estrogen-induced retinoic acid receptor alpha 1 gene expression: role of estrogen receptor-Sp1 complex. Mol Endocrinol, 1998. **12**(6): p. 882-90.

154. Migliaccio, A., et al., Tyrosine kinase/p21ras/MAP-kinase pathway activation by estradiol-receptor complex in MCF-7 cells. EMBO J., 1996. **15**: p. 1292.

155. Klinge, C.M., et al., Resveratrol and Estradiol Rapidly Activate MAPK Signaling through Estrogen Receptors {alpha} and {beta} in Endothelial Cells. J. Biol. Chem., 2005. **280**(9): p. 7460-7468.

156. Kahlert, S., et al., Estrogen Receptor alpha Rapidly Activates the IGF-1 Receptor Pathway. J. Biol. Chem., 2000. **275**(24): p. 18447-18453.

157. Jemal, A., et al., Cancer Statistics, 2009. CA Cancer J Clin, 2009. **59**(4): p. 225-249.

158. Frasor, J., et al., Profiling of estrogen up- and down-regulated gene expression in human breast cancer cells: insights into gene networks and pathways underlying estrogenic control of proliferation and cell phenotype. Endocrinology, 2003. **144**(10): p. 4562-74.

159. Brodie, A.M., et al., Aromatase inhibitors and hormone-dependent cancers. J Steroid Biochem Mol Biol, 1990. **37**(3): p. 327-33.

160. Macedo, L.F., G. Sabnis, and A. Brodie, Aromatase inhibitors and breast cancer. Ann N Y Acad Sci, 2009. **1155**: p. 162-73.

161. Alba, E., et al., [Antiestrogen therapy in the treatment of breast neoplasms]. Minerva Ginecol, 2002. **54**(3): p. 245-51.

162. Anderson, E., R.B. Clarke, and A. Howell, Estrogen responsiveness and control of normal human breast proliferation. J Mammary Gland Biol Neoplasia, 1998. **3**(1): p. 23-35.

163. Ariazi, E.A., et al., Estrogen receptors as therapeutic targets in breast cancer. Curr Top Med Chem, 2006. **6**(3): p. 181-202.

164. Barron-Gonzalez, A., J. Arias-Martinez, and I. Castro-Romero, [Antiestrogens: mechanism of action and clinical applications]. Salud Publica Mex, 2001. **43**(6): p. 577-84.

165. Benshushan, A. and A. Brzezinski, Hormonal manipulations and breast cancer. Obstet Gynecol Surv, 2002. **57**(5): p. 314-23.

166. Bentrem, D.J. and V.C. Jordan, Antiestrogens: the past and the future. Zentralbl Gynakol, 2002. **124**(12): p. 551-8.

167. Bergeron, C., [Effect of estrogens and antiestrogens on the endometrium]. Gynecol Obstet Fertil, 2002. **30**(12): p. 933-7.

168. Barker, S., Non-steroidal anti-estrogens in the treatment of breast cancer. Curr Opin Investig Drugs, 2006. **7**(12): p. 1085-91.

169. Shiau, A.K., et al., The structural basis of estrogen receptor/coactivator recognition and the antagonism of this interaction by tamoxifen. Cell, 1998. **95**(7): p. 927-37.

170. Tzukerman, M.T., et al., Human estrogen receptor transactivational capacity is determined by both cellular and promoter context and mediated by two functionally distinct intramolecular regions. Mol Endocrinol, 1994. **8**(1): p. 21-30.

171. McDonnell, D.P., et al., Analysis of estrogen receptor function in vitro reveals three distinct classes of antiestrogens. Mol Endocrinol, 1995. **9**(6): p. 659-69.

172. Tamoxifen for early breast cancer: an overview of the randomised trials. Early Breast Cancer Trialists' Collaborative Group. Lancet, 1998. **351**(9114): p. 1451-67.

173. Dowsett, M., et al., Mechanisms of resistance to aromatase inhibitors. J Steroid Biochem Mol Biol, 2005. **95**(1-5): p. 167-72.

174. Nicholson, R.I., et al., The biology of antihormone failure in breast cancer. Breast Cancer Res Treat, 2003. **80 Suppl 1**: p. S29-34; discussion S35.

175. Gutierrez, M.C., et al., Molecular changes in tamoxifen-resistant breast cancer: relationship between estrogen receptor, HER-2, and p38 mitogen-activated protein kinase. J Clin Oncol, 2005. **23**(11): p. 2469-76.

176. Knowlden, J.M., et al., Elevated Levels of Epidermal Growth Factor Receptor/c-erbB2 Heterodimers Mediate an Autocrine Growth Regulatory Pathway in Tamoxifen-Resistant MCF-7 Cells. Endocrinology, 2003. **144**(3): p. 1032-1044.

177. Robertson, J.F., Oestrogen receptor: a stable phenotype in breast cancer. Br J Cancer, 1996. **73**(1): p. 5-12.

178. Robertson, J.F., Faslodex (ICI 182, 780), a novel estrogen receptor downregulator--future possibilities in breast cancer. J Steroid Biochem Mol Biol, 2001. **79**(1-5): p. 209-12.

179. Robertson, J.F., ICI 182,780 (Fulvestrant)--the first oestrogen receptor down-regulator--current clinical data. Br J Cancer, 2001. **85 Suppl 2**: p. 11-4.

180. Zhao, L., K. O'Neill, and R.D. Brinton, Estrogenic agonist activity of ICI 182,780 (Faslodex) in hippocampal neurons: implications for basic science understanding of estrogen signaling and development of estrogen modulators with a dual therapeutic profile. J Pharmacol Exp Ther, 2006. **319**(3): p. 1124-32.

181. Anstead, G.M., K.E. Carlson, and J.A. Katzenellenbogen, The estradiol pharmacophore: ligand structure-estrogen receptor binding affinity relationships and a model for the receptor binding site. Steroids, 1997. **62**(3): p. 268-303.

182. Kuduk, S.D., et al., Synthesis and evaluation of geldanamycin-estradiol hybrids. Bioorg Med Chem Lett, 1999. **9**(9): p. 1233-8.

183. Fevig, T.L. and J.A. Katzenellenbogen, A short, stereoselective route to 16.alpha.-(substituted-alkyl)estradiol derivatives. The Journal of Organic Chemistry, 2002. **52**(2): p. 247-251.

184. Kiesewetter, D.O., et al., Synthesis of 16-fluoroestrogens by unusually facile fluoride ion displacement reactions: prospects for the preparation of fluorine-18 labeled estrogens. The Journal of Organic Chemistry, 2002. **49**(25): p. 4900-4905.

185. Osborne, C.K., A. Wakeling, and R.I. Nicholson, Fulvestrant: an oestrogen receptor antagonist with a novel mechanism of action. Br J Cancer, 2004. **90 Suppl 1**: p. S2-6.

186. Wakeling, A.E. and J. Bowler, ICI 182,780, a new antioestrogen with clinical potential. J Steroid Biochem Mol Biol, 1992. **43**(1-3): p. 173-7.

187. Wakeling, A.E. and J. Bowler, Development of novel oestrogen-receptor antagonists. Biochem Soc Trans, 1991. **19**(4): p. 899-901.

188. Wakeling, A.E., M. Dukes, and J. Bowler, A Potent Specific Pure Antiestrogen with Clinical Potential. Cancer Res, 1991. **51**(15): p. 3867-3873.

189. Tedesco, R., R. Fiaschi, and E. Napolitano, 6-Oxoestradiols from Estradiols: Exploiting Site Selective Metalation of Aralkyl Systems with Superbases. Synthesis, 1995. **1995**(12): p. 1493-5.

190. Tedesco, R., J.A. Katzenellenbogen, and E. Napolitano, An Expeditious Route to 7α- Substituted Estradiol Derivatives. Tetrahedron Lett., 1997. **38**(46): p. 7997-8000.

191. Skaddan, M.B., F.R. Wust, and J.A. Katzenellenbogen, Synthesis and Binding Affinities of Novel Re-Containing 7α-Substituted Estradiol Complexes: Models for Breast Cancer Imaging Agents. The Journal of Organic Chemistry, 1999. **64**(22): p. 8108-8121.

192. Hussey, S.L., E. He, and B.R. Peterson, Synthesis of Chimeric 7α-Substituted Estradiol Derivatives Linked to Cholesterol and Cholesterylamine. Organic Letters, 2002. **4**(3): p. 415-418.

193. Hadden, M.K. and B.S. Blagg, Dimeric approaches to anti-cancer chemotherapeutics. Anticancer Agents Med Chem, 2008. **8**(7): p. 807-16.

194. Berube, G., Natural and synthetic biologically active dimeric molecules: anticancer agents, anti-HIV agents, steroid derivatives and opioid antagonists. Curr Med Chem, 2006. **13**(2): p. 131-54.

195. Bérubé, G., et al., Synthesis of unique 17[beta]-estradiol homo-dimers, estrogen receptors binding affinity evaluation and cytocidal activity on breast, intestinal and skin cancer cell lines. Steroids, 2006. **71**(10): p. 911-921.

196. Zheng, F.F., et al., Identification of a geldanamycin dimer that induces the selective degradation of HER-family tyrosine kinases. Cancer Res, 2000. **60**(8): p. 2090-4.

197. Rice, W.G., et al., Inhibitors of HIV nucleocapsid protein zinc fingers as candidates for the treatment of AIDS. Science, 1995. **270**(5239): p. 1194-7.

198. Bergmann, K.E., et al., Bivalent ligands as probes of estrogen receptor action. The Journal of Steroid Biochemistry and Molecular Biology, 1994. **49**(2-3): p. 139-152.

199. Rabouin, D., et al., A facile synthesis of C2-symmetric 17[beta]-estradiol dimers. Bioorganic & Medicinal Chemistry Letters, 2003. **13**(3): p. 557-560.

200. Rabouina, D., et al., Synthesis and Preliminary Biological Evaluation of Estrone Dimers. Letters in Drug Design & Discovery, 2007. **4**(3): p. 171-174.

201. Groleau, S., et al., Synthesis and Preliminary in Vitro Cytotoxic Activity of New Triphenylethylene Dimers. Bioorganic Chemistry, 1999. **27**(5): p. 383-394.

202. Fuchsjager-Mayrl, G., et al., Identification of Estrogen and Progesterone Receptor mRNA Expression in the Conjunctiva of Premenopausal Women. Invest. Ophthalmol. Vis. Sci., 2002. **43**(9): p. 2841-2844.

203. Robertson, J.F. and M. Harrison, Fulvestrant: pharmacokinetics and pharmacology. Br J Cancer, 2004. **90 Suppl 1**: p. S7-10.

204. Sharma, U., et al., Design, synthesis, and evaluation of estradiol-linked genotoxicants as anti-cancer agents. Bioorg Med Chem Lett, 2004. **14**(14): p. 3829-33.

205. Zhao, L., et al., Design, synthesis, and estrogenic activity of a novel estrogen receptor modulator--a hybrid structure of 17beta-estradiol and vitamin E in hippocampal neurons. J Med Chem, 2007. **50**(18): p. 4471-81.

206. Reid, G., et al., Human estrogen receptor-alpha: regulation by synthesis, modification and degradation. Cell Mol Life Sci, 2002. **59**(5): p. 821-31.

207. Reid, G., et al., Cyclic, Proteasome-Mediated Turnover of Unliganded and Liganded ER[alpha] on Responsive Promoters Is an Integral Feature of Estrogen Signaling. Molecular Cell, 2003. **11**(3): p. 695-707.

208. Preisler-Mashek, M.T., et al., Ligand-specific regulation of proteasome-mediated proteolysis of estrogen receptor-alpha. Am J Physiol Endocrinol Metab, 2002. **282**(4): p. E891-898.

209. Fevig, T.L., M.K. Mao, and J.A. Katzenellenbogen, Estrogen receptor binding tolerance of 16 alpha-substituted estradiol derivatives. Steroids, 1988. **51**(5-6): p. 471-97.

210. Corson, T.W., N. Aberle, and C.M. Crews, Design and Applications of Bifunctional Small Molecules: Why Two Heads Are Better Than One. ACS Chem Biol, 2008. **3**(11): p. 677-692.

VITA

Kedra C. Cyrus

Birth

August 28, 1978

St. George's, Grenada

Education

1998 ~ 2002	Bachelor of Science, Biology, Medgar Evers College-CUNY, Brooklyn, New York

PROFESSIONAL POSITIONS

2003 ~ present	Graduate student research assistant, University of Kentucky, Lexington KY
2001 ~ 2002	Undergraduate research assistant, Medgar Evers College, New York State Louis- Stokes Alliance for Minority Participation (NYS-LSAMP) in Science Engineering and Mathematics.
2001	Summer research fellow, National University of Singapore, NIH Minority International Research Training (MIRT) Program.

SCHOLASTIC AND PROFESSIONAL HONORS

2008	Student Role Model award, Minority Access, Inc. National Role Models conference
2003 ~ 2006	Lyman T. Johnson Fellowship, University of Kentucky
2002	Certificate of academic excellence award, Medgar Evers College – CUNY
2002	Certificate for outstanding performance in research, Medgar Evers College – CUNY
2001~ 2002	New York State Louis- Stokes Alliance for Minority Participation (NYS-LSAMP) scholarship
2001	NIH- MIRT, Fogarty International Research Fellowship
2005 ~ present	Rho Chi Society
2002	*Summa cum Laude*, Medgar Evers College-CUNY
1999 ~ 2002	Dean's list, Medgar Evers College-CUNY

PROFESSIONAL PUBLICATIONS

- Cyrus, K, Wehenkel, M, Han, H.J, Ban, J.O and Kim, K.B. "Chemical Genetic Control of Protein Levels: Effective PROTAC Design Strategy" *in preparation* (2009)
- Cyrus, K, Wehenkel, M, Han, H.J and Kim, K.B. "Dimeric Ligand Based Protac: An Effective New Tool for Targeted Degradation of Protein" *in preparation* (2009)
- Rodriguez-Gonzalez, A., Cyrus, K. et al. "Targeting steroid hormone receptors for ubiquitination and degradation in breast and prostate cancer." *Oncogene*. 2008 27(57): 7201-11.
- Ho, A.; Kim, Y.E.; Lee, H; Cyrus, K; Baek, S.H and Kim, K.B. "SAR studies of 2-methoxyestradiol and development of its analogs as probes of anti-tumor mechanism." *Bioorg. Med. Chem. Lett.* 2006 16(13):3383-7
- Ho, A.; Cyrus, K. and Kim, K.B. "Towards immunoproteasome specific inhibitors: An improved synthesis of dihydroeponemycin." *Eur. J. Org. Chem.* 2005 22:4829-483

SCIENTIFIC MEETINGS/PRESENTATIONS

- Kedra Cyrus, Yang-eon Kim, Kyung Bo Kim. "Chemical Genetics approach to breast cancer therapy." American Chemical Society Fall National Meeting, San Francisco, poster presentation, abstract #65 (September 9 -14, 2006)
- Kedra Cyrus, Yang-eon Kim, Kyung Bo Kim. "Chemical Genetics approach to breast cancer therapy." 30th National Medicinal Chemistry Symposium, University of Washington, poster presentation, abstract #140. (June 24-29, 2006)
- Kedra Cyrus, Mohammed Bangura, Farah Jean, Umesh Nagarkatte. "Analysis of urban air samples using mathematical methods." Florida-Georgia Louis Stokes Alliance for Minority Participation in Science, Technology, Engineering and Mathematics, Florida State University, poster presentation, (2002).
- Kedra Cyrus, Leong May Ling, Nga Been Hen. "Genes encoding proteins responsible for the biosynthesis of daunorubicin in the actinomycete NS3- 166." National Minority Research Symposium, Cancun, Mexico, poster presentation (October 17- 20, 2001).